Geometallurgy Conference 2025

Future-Ready Geometallurgy: Trusted Data, Advanced Tools, Smarter Decisions

SUPPORTED BY GSSA & MINSA

Proceedings Book

14-15 October 2025

Glenburn Lodge and Spa, Muldersdrift

THE SOUTHERN AFRICAN INSTITUTE OF MINING AND METALLURGY
JOHANNESBURG 2025

Geometallurgy Conference 2025

Future-Ready Geometallurgy: Trusted Data, Advanced Tools, Smarter Decisions

14-15 OCTOBER 2025

Glenburn Lodge and Spa, Muldersdrift

SAIMM PUBLICATIONS

THE MONOGRAPH SERIES

Ml **Lognormal-De Wijsian Geostatistics for Ore Evaluation**
(2nd ed 1981) D.G. Krige

M2 **An Introduction to Geostatistical Methods of Mineral Evaluation**
(2nd ed 1981) J.-M.M. Rendu

M3 **Principles of Flotation**
(1982) (3rd imp. 1986) Edited by R.P. King

M4 **Increased Underground Extraction of Coal**
(1982) Edited by C.J. Fauconnier and R.W.O. Kersten

M5 **Rock Mechanics in Mining Practice**
(1983) (3rd imp. 1986) Edited by S. Budavari

M6 **Assay and Analytical Practice in the South African Mining Industry**
(1986) W.C. Lenahan and R. de L. Murray-Smith

M7 **The Extractive Metallurgy of Gold in South Africa,**
2 volumes (1987) Edited by G.G Stanley

M8 **Mineral and Metal Extraction — An Overview**
(1994) L.C. Woollacott and R.H. Eric

M9 **Rock Fracture and Rockbursts—an illustrative study**
(1997) Edited by W.D. Ortlepp

THE SPECIAL PUBLICATIONS SERIES

SPI **Proceedings, Underground Transport Symposium**
(1986) Edited by R.C.R. Edgar

SP2 **Backfill in South African Mines (1988)**

SP3 **Treatment and Re-use of Water in the Minerals Industry (1989)**

SP4 **COREX Symposium 1990**
(1990) Edited by H.M.W. Delport and P.J. Holaschke

SP5 **Measurement, Control, and Optimization in Mineral Processing**
(1994) Edited by H.W. Glen

SP6 **Handbook on Hard-rock Strata Control**
(1994) A.J.S. Spearing

SP7 **Rock Engineering for underground coal mining**
(2002) J. Nielen van der Merwe and Bernard J. Madden

SP8 **Second Edition: Rock Engineering for underground coal mining**
(2010) J. Nielen van der Merwe and Bernard J. Madden

SP9 **Theoretical Rock Mechanics for Professional Practice**
(2016) M. Handley

SP10 **Johannesburg and its Holey Mining Heritage 2021**
(2021) T.R. Stacey

SP11 **Mineral and Metal Extraction — An Overview**
(2021) L.C. Woollacott and R.H. Eric

SP12 **The Fall of a Giant: The story of the disintegration of the South African Mining Industry**
(2022/2023) Dr I. Robinsoin

SP13 **COMRO's Legacy: Research and Development of Stoping Mining Machinery and Technologies**
(2023) B. Protheroe

SUPPLEMENT TO THE SAIMM JOURNAL

The Metals and Minerals Industry in South Africa - Part 1 (1989)
Edited by H.W. Glen

THE SYMPOSIUM SERIES

S1 **Mathematical Statistics and Computer Applications in Ore Valuation (1966)**

S2 **Planning Open Pit Mines** (1970) (4th imp.)
Edited by P.W.J. van Rensburg

S3 **Application of Computer Methods in the Mineral Industry** (APCOM 1973) Edited by M.D.G. Salamon

S4 **Infacon 1974** Edited by H.W. Glen

S5 **Proceedings of the 12TH CMMI Congress** 2 volumes (1982)
Edited by H.W. Glen

S6 **Rockbursts and Seismicity in Mines** (1984)
Edited by N.C. Gay and E.H. Wainwright

S7 **The Planning and Operation of Open Pit and Strip Mines** (1986) Edited by J.P. Deetlefs

S8 **GOLD 100: Proceedings of the International Conference on Gold (1986)**
Volume 1: Gold Mining Technology
Edited by H. Wagner and R.P. King
Volume 2: Extractive Metallurgy of Gold
Edited by C.E. Fivaz and R.P. King
Volume 3: Industrial Uses of Gold
Edited by G. Gafner and R.P. King

S9 **APCOM 87: Proceedings of the Twentieth International Symposium on the Application of Computers and Mathematics in the Mineral Industries (1987)**
Volume 1: Mining
Edited by L. Wade, R.W.O. Kersten and J.R. Cutland
Volume 2: Metallurgy
Edited by R.P. King and I.J. Barker
Volume 3: Geostatistics
Edited by I.C. Lemmer, H. Schaum and F.A.G.M. Camisani-Calzolari

S10 **International Deep Mining Conference (1990)**
Volume 1: Innovations in Metallurgical Plant
Edited by G.A. Brown and P. Smith
Application of Materials Engineering in the Mining Industry Edited by B. Metcalfe
Volume 2: Technical Challenges in Deep Level Mining
Edited by D.A.J. Ross-Watt and P.D.K. Robinson

S11 **Infacon 6 (Incorporating Incsac) (1992)**
Edited by H.W. Glen

S12 **Massmin 92**
Edited by H.W. Glen (out of print)

S13 **Minefill 93**
Edited by H.W. Glen

S14 **XVTH CMMI Congress Publications (1994)**
Volume 1: Mining
Edited by H.W. Glen
Volume 2: Metals Technology and Extractive Metallurgy (1994) Edited by H.W. Glen

S15 **Surface Mining 1996**
Edited by H.W. Glen

S16 **Hidden Wealth (1996)**
Edited by H.W. Glen

S17 **Heavy Minerals 1997**
Edited by R.E. Robinson

S18 **The 8TH International Platinum Symposium (1998)**

S19 **Mining in Africa '98**

S20 **Extraction Metallurgy Africa '98**

S21 **Sixth International Symposium for Rock Fragmentation by Blasting (1999)**

S22 **Metallurgy Africa '99**

S23 **Heavy Minerals 1999**
Edited by R.G. Stimson

S24 **Tunnels under Pressure**
Technical Editor T.R. Stacey

S25 **Mine Hoisting 2000**

S26 **Coal–The Future (2000)**

S27 **The Fifth International Symposium on Rockburst and Seismicity in Mines (RaSim 5) (2001)**

S28 **6TH International Symposium on Mine Mechanization and Automation (2001)**

S29 **XIV International Coal Preparation Congress and Exhibition**

S30 **Surface Mining 2002—Modern Developments for the New Millennium**

S31 **IFSA 2002, Industrial Fluidization South Africa**

S31a **APCOM 2003—Application of Computers and Operations Research in the Minerals Industries**

S32 **ISSA/Chamber of Mines Conference—Mines and Quarries: Prevention of Occupational Injury and Disease**

S33 **ISRM—Technology Roadmap for Rock Mechanics**

S34 **Heavy Minerals Conference 2003**

S35 **Safety in Mines Research Institutes (2003)**

S36 **VII International Conference on Molten Slags, Fluxes & Salts (2004)**
Tenth International Ferroalloys Congress INFACONX 2004

S37 **Deep and high stress mining 2004**

S38 **'Platinum adding value' 2004**

S39 **Base Metals—Southern Africa's response to changing global base metals market dynamics 2005**

S40 **Strategic *versus* Tactical approaches in mining 2005**

S41 **Best practices in rock engineering SARES 2005**

S42 **IFSA 2005, Industrial Fluidization South Africa**

S43 **Southern African Pyrometallurgy 2006 International Conference**

S44 **Stability of rock slopes in open pit mining and civil engineering situations**

S45 **'Platinum Surges Ahead' 2006**

S46 **Hydraulic Transport of Solids - Hydrotransport 17 (2007)**

S47 **Fourth Southern African Base Metals Conference 'Africa's base metals resurgence'**

S48 **Heavy Minerals Conference, 2007**

S49 **Cave Mining Conference, 2007**

S50 **International Symposium on Lead and Zinc processing – Lead & Zinc 2008**

S51 **Surface Mining 2008**

S52 **Platinum in transformation 2008**

S53 **IFSA 2008, Industrial Fluidization South Africa**

S54 **Hydrometallurgy Conference 2009**

S55 **Shotcrete for Africa 2009**

S56 **Base Metals Conference 2009**

S57 **Heavy Minerals Conference, 2009**

S58 **Hard Rock Safe—Safety Conference 2009**

S59 **Sampling and Blending 2009**

S60 **World Gold 2009 Conference**

S61 **Physical Beneficiation Conference 2010**

S62 **Second Hardrock Safe—Safety Conference 2010**

S63 **Platinum in Transition 'Boom or Bust' 2010**

S64 **South African Pyrometallurgy 2011 International Conference**

S65 **Minefill 2011 (10TH International Symposium on Mining with Backfill)**

S66 **Base Metals Conference 2011**

S67 **MineSafe 2011 Conference**

S68 **Iron Ore and Manganese Ore Metallurgy 2011**

S69 **Percolation leaching: The status globally and in Southern Africa 2011**

S70 **IFSA 2011, Industrial Fluidization South Africa**

S71 **Southern Hemisphere International Rock Michanics Symposium 2012**

S72 **Platinum Conference 'A catalyst for change' 2012**

S73 **Ferrous 2012—Ferrous and Base Metals Development Network Conference**

S74 **Diamonds - Source to use 2013**

S75 **Sampling and analysis: Best-practice in African mining 2013**

S76 **Base Metals Conference 2013**

S77 **Precious Metals 2013 Conference—The Precious Metals Development Network (PMDN)**

S78 **Physical Beneficiation 2013 Conference**

S79 **21st Century challenges to the southern African coal sector 2014**

S80 **Furnace Tapping Conference 2014**

S81 **Platinum Conference 'Platinum—Metal for the Future' 2014**

S82 **IFSA 2014, Industrial Fluidization South Africa**

S83 **Copper Cobalt Africa 2015**

S84 **The Danie Krige Geostatistical Conference 2015 - Vol. 1**
The Danie Krige Geostatistical Conference 2015 - Vol. 2

S85 **World Gold Conference 2015**

S86 **Slope Stability 2015**

S87 **2nd Annual Young Professionals Conference 2015**

S88 **AMI–Nuclear Materials Development Network 2015**

S89 **MPES–23rd International Symposium on Mine Planning & Equipment Selection 2015**

S90 **Diamonds still Sparkling Conference 2016**

S91 **The SAMREC/SAMVAL Companion Volume Conference 2016**

S92 **New Technology and Innovation in the Minerals Industry Colloquium 2016**

S93 **Theoretical Rock Mechanics for Professional Practice** (Special Publications Series 9) by M. Handley - 2016

S94 **Hydrometallurgy Conference 2016**

S95 **10TH Heavy Minerals Conference 2016**

S96 **MineSafe Conference 2016**

S97 **AMI-Ferrous and Base Metals Development Conference 2016**

S98 **3rd Young Professionals Conference 2017**

S99 **Proximity Detection and Collosion Avoidance Systems in Mining Colloquium 2017**

S100 **6TH Sulphur and Sulphuric Acid Conference 2017**

S101 **Mine Planning Colloquium 2017**

S102 **Chrome Colloquium 2017**

S103 **4TH Mineral Project Valuation Colloquium 2017**

S104 **Water Conference 2017**

S105 **Rapid Underground Mine and Civil Access Engineering 2017**

S106 **MineSafe Conference 2017**

S107 **Uranium 2017 International Conference 2017**

S108 **IFSA 2017–Industrial Fluidization Conference 2017**

S109 **AfriRock 2017–ISRM International Symposium 2017**

S110 **AMI Precious Metals 2017–The Precious Metals Development Network (PMDN) Symposium**

S111 **7TH International Platinum Conference 2017**

S112 **Infacon XV: International Ferro-Alloys Conrgress 2018**

S113 **SOMP–Society of Mining Professors 6TH Regional Conference 2018**

S114 **Digitalization in Mining Conference 2018**

S115 **Diamonds – Source to Use 2018 Conference 2018**

S116 **The 9TH Southern African Base Metals Conference 2018**

S117 **Geometallurgy Conference 2018**

S118 **Mine Safe Technical Conference and Industry Day 2018**

S119 **ASM Conference 2018**

S120 **4TH Young Professionals Conference 2018**

S121 **Furnace Tapping 2018 Conference 2018**

S122 **7TH Sulphur and Sulphuric Acid Conference 2019**

S123 **Mine Planner's Colloquium 2019**

S124 **9TH International Conference on Deep & High Stress Mining 2019**

S125 **New Technology Conference and Trade Show 2019**

S126 **Smart Mining Smart Environment Smart Society Conference 2019**

S127 **The Eleventh International Heavy Minerals Conference 2019**

S128 **Surface Mining Masterclass 2019**

S129 **International Mine Health and Safety Conference 2019**

S130 **Tailings Storage Conference 2020**

S131 **IMPC2020 XXX International Mineral Processing Congress**

S132 **Johannesburg and its Holey Mining Heritage**
(Special Publications Series 10) by T.R. Stacey - 2021

S133 **Mineral and Metal Extraction — An Overview**
(Special Publications Series 11) by L.C. Woollacott and R.H. Eric - 2021

S134 **Diamonds - Source to Use - 2021 Online Conference 2021**

S135 **WorldGold Online Conference 2021**

S136 **APCOM 2021 Minerals Industry4.0-The next digital transformation in mining**

S137 **5TH Young Professionals Online Conference 2021**

S138 **Southern African Rare Earths International Online Conference 2021**

S139 **SAMCODES Conference 2021**

S140 **Global Tailings Standards and Opportunities`For the Mine of the Future Conference 2022**

S141 **The Fall of a Giant: The story of the disintegration of the South African Mining Industry**
(Special Publications Series 12) by I. Robinson - 2022/2023

S142 **Battery Materials Conference 2022**

S143 **32ND SOMP Annual Meeting and Conference 2022**

S144 **SDIMI (Sustainable Development in the Minerals Industry) 10TH International Conference 2022**

S145 **THANOS International Conference 2022**

S146 **Mine Impacted Water Online Conference 2022 (Abstract Book Only)**

S147 **8TH International PGM Conference 2022**

S148 **SANCOT Symposium 2022**

S149 **8TH Sulphur and Sulphuric Acid Conference 2023**

S150 **Southern African Hydrogen and Fuel Cell Conference 2023**

S151 **COMRO's Legacy: Research and Development of Stoping Mining Machinery and Technologies**
(Special Publications Series 13) by B. Protheroe - 2023

S152 **Copper Cobalt Africa in Association with The 10TH Southern African Base Metals Conferenc 2023**

S153 **Digital Transformation in Mining Conference 2023**

S154 **Diamonds Source to Use 2023 Online Conference**

S155 **12TH International Heavy Minerals Conference 2023**

S156 **Geometallurgy Conference 2023**

S157 **Next Generation Tailings Opportunitiy or Risk? Conference 2023**

S158 **6TH Young Professionals Conference 2023**

S159 **Southern African Pyrometallurgy 2024 International Conference**

S160 **The 11TH World Conference of Sampling and Blending 2024**

S161 **SANIRE Symposium 2024**
Technical Applications in Rock Engineering

S162 **2ND International Conference 2024 Southern African Rare Earths**

S163 **2ND Battery Materials Conference 2024**

S164 **Hydrometallurgy Conference 2024**

S165 **Environmental Social Governance Sustainability Conference 2024**

S166 **MineSafe Mine Health and Safety Conference 2024**

S167 **Mintek@90 Conference 2024**

S168 **Mine Closure Conference 2025**

S169 **2ND Southern African Hydrogen and Fuel Cell Conference 2025**

S170 **9TH Sulphur and Sulphuric Acid Conference 2025**

S171 **4TH Digital Transformation in Mining Conference 2025**

S172 **AfriRock 2025 Pioneering Progress Conference**

S173 **Thirteen International Heavy Minerals Conference 2025**

S174 **International Mineral Asset Valuation Conference 2025**

Published by The Southern African Institute of Mining and Metallurgy
Minerals Council South Africa, 7th Floor, Rosebank Towers, 19 Biermann Avenue, Rosebank, 2196
Republic of South Africa

ISBN 978-0-6398820-4-8

The papers in this volume have been for the most part prepared from Word documents supplied by the authors, with additional typesetting and formatting by The Southern African Institute of Mining and Metallurgy.

Organising Committee

M. Becker, Conference Chairperson

S. Brand

S. Burness

D. Chetty

A. Johnston

G.T. Nwaila

R. Schouwstra

M. Tadie

SAIMM Conference Secretariat:
G. Charlie
C. Jardine
N. Mamdoo

The Organising Committee would like to thank the reviewers listed below for the efforts in the reviewing process

I. Barton
M. Becker
S. Burness
D. Chetty
J. Gutzmer
A. Johnston
T. Kojovic
T. Louw
M. Manual
B. McFadzean
E. Nienaber
G.T. Nwaila
M. Parian
J. Petersen
R. Schouwstra
A.J.B. Smith
M. Tadie
A. Van der Westhuizen
F. Viljoen
B.P. von der Heyden

Desktop prepared by Camera Press, Johannesburg

FOREWORD

It is with great enthusiasm that the organising committee welcomes you to the third SAIMM Geometallurgy Conference. This year's theme, *Future-Ready Geometallurgy*, explores strategies for generating trustworthy data through the steady application of machine learning, novel sensors, digital twins, and Industry 4.0 technologies in mining. While geometallurgy is now widely recognised as a refined, multidisciplinary approach to enhancing the value of ore deposits, it is critical that practitioners have access to reliable data and innovative tools to enable its success. These empower the industry to make more timely and informed decisions in mine planning and metallurgical plant optimisation.

We are delighted to welcome two keynote presentations by international experts in the field: Wendy Ware (Datarock, Australia) and Adam Johnston (Transmin Metallurgical Consultants, UK). Both will also lead concurrent pre-conference workshops. In addition, we look forward to a diverse range of papers presented by contributors from both academia and industry. These will explore key themes including sampling, standardised reporting methods, geostatistics, data integration, smart workflows, predictive modelling, and a variety of project and operational geometallurgy case studies. The conference programme concludes with a post-conference field trip to Mintek, South Africa's national mineral research and technology organisation. This full-day visit will offer an in-depth look at Mintek's various divisions and facilities that support the mining industry. As the organising committee, we hope this conference provides each of you with a valuable platform for learning, engagement, and networking, and that it sparks innovative research and development in geometallurgy.

We extend our sincere thanks and appreciation to the keynote presenters, authors, reviewers, exhibitors, and sponsors for generously sharing their time, resources, and expertise to make this conference possible. We also gratefully acknowledge the contributions of the Mineralogical Association of South Africa and the Geological Society of South Africa in supporting the organisation and promotion of the event. Special thanks go to Gugu Charlie and her team at the SAIMM for their outstanding coordination and management of the conference.

On behalf of the Organising Committee:
Professor Megan Becker (MSAIMM, FGSSA)
Conference Chair

Contents

The organisers of the conference thanks the following sponsors for their support

CORPORATE SPONSOR

micromine

WORKSHOP SPONSORS

cancha

Datarock

EXHIBITORS

cancha

micromine

SPS
SCIENTIFIC AND PRECISION SOLUTIONS
PREMIUM MICROSCOPY SOLUTIONS

ThermoFisher SCIENTIFIC

wirsam SCIENTIFIC

ZEISS
Seeing beyond

PROMOTIONAL INSERTS

GEO EXPLORE STORE
GEO-EXPLORE STORE (PTY) LTD

SimSAGE PTY LTD

SKEmet
Bringing Balance To Your Process

VBKOM

Reducing processing and cost risks for new processing plants through effective design simulation

S.K. Edwards[1], N.C. Steenkamp[2]

[1]SKEmet (Pty) Ltd, South Africa
[2]Independent Consultant

INTRODUCTION

Most process plants are designed around average process performance parameters, based on an average ore type with characteristics that may not even exist or materialise. This translates into poor economic process plant performance (Ortiz, 2023). This is a consequence of being unaware of variable ores being fed to the plant and thus not being prepared operationally to adjust the plant controls to ensure a positive process response to the changing ore. A combination of a well-designed and executed geometallurgical campaign, utilised as the basis for a production process plant simulation, de-risks the metallurgical operation and can translate into realised process optimisation and operational cost efficiency (Kennedy, 2014; Michaux, 2020). This is on the condition that the process simulation is undertaken during the concept (or early study) phase to identify and optimise aspects related to grind size, flotation reagent consumptions, leach times and ore blending parameters (Kennedy, 2014).

Geometallurgical inputs

An effective geometallurgical program strategically collects data to characterise ore types in relation to process behaviour. Key outcomes—such as ore variability, domain mapping, and ore type definition—directly influence process engineering performance (Dominy & Glass, 2025). These insights also support broader objectives like economic modelling, business development, and mine schedule planning (Ortiz, 2023).

A geometallurgical campaign is most cost-effective when conducted during the project's pre-feasibility study, when it offers the highest leverage of influence relative to cost within the overall mine design cycle. This stage of planning is known as front-end optimisation (Michaux, 2020). A key part of the geometallurgical campaign is the development of the orientation study, which defines representative samples across lithologies and alteration zones (Dominy & Glass, 2025). Geometallurgy connects the results from the orientation study —geological setting, the dominant rock types and mineralisation along with the alteration assemblages —with the metallurgical response in the process plant. The representative sample material is typically sourced from drill core samples, from which composites are created, to accurately represent the entire orebody and ideally processed through the plant over the Life of Mine (LOM) (Dominy & Glass, 2025).

When configuring a geometallurgical campaign for a processing plant, the geometallurgical analyses must focus on mineralogical characteristics that ultimately determine the extent of impact breakage, grinding and mineral recovery. Small-scale proxy tests are conducted to determine whether the mineralogical characteristics can be scaled up and mapped across the deposit (Butcher, *et al.*, 2023). Figure 1 illustrates the types of geometallurgical analyses that are required to characterise mineralogical behaviour. These include mineralogical tests, grain size analysis, hardness indexes, and reagent responsiveness studies (Butcher, *et al.*, 2023).

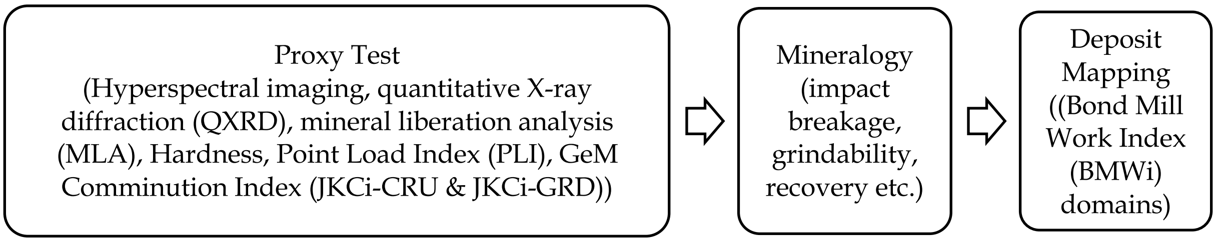

Figure 1: Geometallurgical analyses.

The results from the simple and quick proxy tests determine the reliability of the tests to represent the deposit's mineralogical behaviour or whether more detailed, high-confidence bankable tests are required. The results from the geometallurgical analyses informing the process engineer of the design envelope of the various mineralogical characteristics and the variability within that envelope. Recurring mineralogical characteristics – mineral compositions and grain sizes—that appear across the design envelope assist process engineers to understand the mineral behaviour, during processing, with varying mineral composition. End member ore types displaying similar processing behaviour can be grouped into a single representative ore type. Collectively, this facilitates more informed decisions in circuit design, processing strategy, and predictive modelling (Dominy & Glass, 2025).

METSIM® optimisation

Using the premium simulation software package, METSIM®, the processing challenges with today's complex ores can be effectively modelled (Bartlett, *et al.*, 2014; METSIM® International LLC, 2025). METSIM® predicts the response of a system to a set of conditions and inputs with which it is presented (Kennedy, 2014). The following approach demonstrates how the synergy between predictive analytics and process simulation within METSIM® facilitates a holistic view of mining operations.

METSIM® uses the outputs from the geometallurgical campaign to simulate the ore behaviour through the process flowsheet. Table 1 lists the critical inputs that need to be entered into the METSIM® model to define the BMWi domains—comminution behaviour zones. METSIM® uses the zone categorisation to simulate ore feed, throughput and performance through the process flowsheet.

Table I: Geometallurgical outputs required by METSIM®.

Geometallurgical output	**Purpose in METSIM® simulation**
Mineralogy	Predicts achievable mineral recovery
Grain size distribution	Influences grinding and liberation
Hardness	Determines comminution energy demand
Reagent consumptions	Optimises chemical dosing and recovery
GeM comminution indices	Simulates breakage and grindability
Domain mapping	Links ore types to process behaviour
Deposit model integration	Enables feed sequencing and blending

The proposed process flow sheet is constructed in METSIM® and the drill-core mineralogical and chemical data, and process conditions are entered into the model. The model is set to run, calculating material, discard and vented stream flowrates, achievable recoveries and sizing equipment, as the ore is digitally fed through each section of the flow sheet. The mine block model and the mining sequence are then imported into the METSIM® model and set to re-run, integrating the real mining data to the beneficiation process, shown in Figure 2. Thus, the dynamic nature of the LOM manifests through the process plant producing reliable and accurate results to assist management with making informed decisions (METSIM® International LLC, 2025). Not only does this improve the effectiveness of the mining operation but also promotes sustainable and environmentally conscious mining and processing strategies.

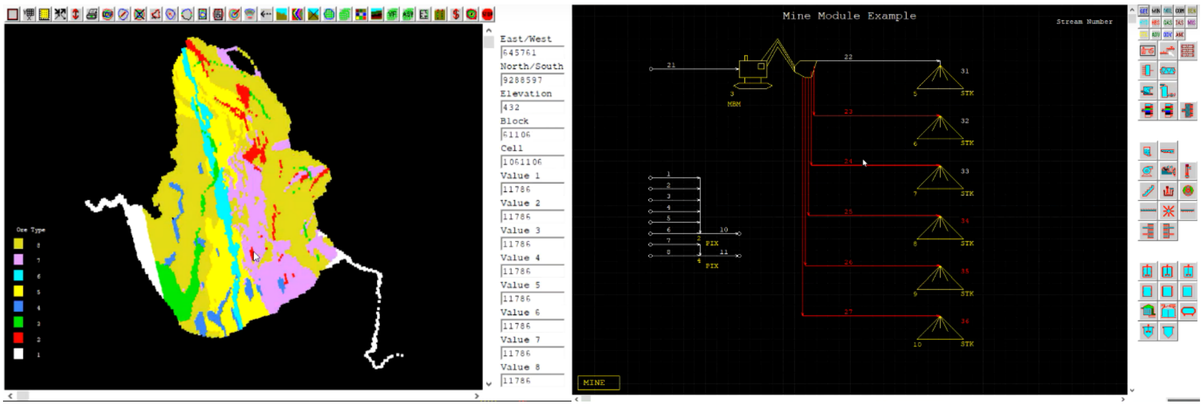

Figure 2: Integration of the Mining Block Model using METSIM®.

SUMMARY

Process plants are often designed around average ore characteristics that may never materialise, leading to poor economic performance and operational inefficiencies. This stems from inadequate anticipation of ore variability and lack of dynamic control strategies. A geometallurgical campaign—executed early in the project lifecycle—provides the mineralogical and metallurgical data needed to simulate realistic ore behaviour. When paired with process simulation tools like METSIM®, this approach de-risks design decisions and enhances operational responsiveness. The outcomes to this approach would expect informed decisions on grind size, reagent dosing, leach times, and blending strategies, enhanced equipment sizing, recovery prediction, and discard stream management, supporting sustainable, cost-efficient, and adaptive processing strategies, aligning technical design with real-world ore variability and operational realities.

REFERENCES

Bartlett, J., Holtzapple, A. & Rempel, C., 2014. A brief overview of the process modeling/simulation and design capabilities of METSIM(R). *Canadian Institute of Mining, Metallurgy and Petroleum.*

Butcher, A., Dehaine, Q., Menzies, A. & Michaux, S., 2023. Characterisation of Ore Properties for Geometallurgy. *Elements,* 19(6), p. pp.352–358.

Dominy, S. & Glass, H., 2025. Geometallurgical Sampling and Testwork for Gold Mineralisation: General Considerations and a Case Study. *Elements,* 15(4), p. p.370.

Kennedy, M., 2014. Metallurgical Plant Optimization Through the Use of Flowsheet Simulation Modelling. *ResearchGate,* January.pp. 367-375.

METSIM® International LLC, 2025. *Comminution & Gravity Separation Module.* [Online] Available at: https://metsim.com/software/comminution-gravity-separation-module/ [Accessed 22 July 2025].

METSIM® International LLC, 2025. *Mine Module.* [Online] Available at: https://metsim.com/software/mine-module/ [Accessed 22 July 2025].

Michaux, S., 2020. *How to Set Up and Develop a Geometallurgical Program.* University of Queensland, Sustainable Minerals Institute.

Ortiz, J. e. a., 2023. Uncertainty and Value: Optimising Geometallurgical Performance Along the Mining Value Chain. *Elements,* 19(6), p. pp.377–383.

Samantha Kay Edwards

Senior Process Engineer
SKEmet Pty Ltd

Samantha is a qualified and experienced process engineer with commissioning, operational and design experience; she has spent the past 20 years as a Process Engineer focussing within the EPCM space. She has recently moved away from EPCMs and now owns her own consulting company, SKEmet (Pty) Ltd, which specialises in Junior mining and process plant optimization utilizing premium simulation software.

SKEmet (Pty) Ltd delivers comprehensive process engineering solutions, including multi-disciplinary detailed plant design, mechanical equipment sizing and procurement, process control, cost estimation, and technical evaluations. Under Samantha's leadership, these services are meticulously tailored to meet each of her client's specific needs, ensuring the delivery of accurate and dependable solutions within tight project timelines. This enables clients to make informed financial decisions with confidence. Samantha leverages the capabilities of METSIM®, a robust process modelling software, to perform accurate mass and energy balances across complex systems, reinforcing the reliability of SKEmet's engineering outcomes.

Furthermore, Samantha holds a Postgraduate Diploma in Business Administration from the WITS Business School, she leverages on the ability to identify her client's needs, engage with technical experts and perform strategic planning according to identified needs. Samantha retains a keen appreciation and understanding of the identification, development and management of business opportunities.

This diversified combination of technical and business dexterity has stood her in good stead as a professional of exceptional value, providing the capability and necessary technical capacity to bid for and deliver on sector specific projects and tender solutions.

Data-Driven delineation of geometallurgical domains in porphyry copper systems

T. Mombe, G.T Nwaila

University of the Witwatersrand, South Africa

INTRODUCTION

Effective mine scheduling, throughput forecasting and metallurgical accounting require partitioning the orebody into geospatially coherent domains whose processing behaviour remains predictable from blast-hole sampling to final concentrate. When domains are defined only by lithology or grade shells, subtle but metallurgically important contrasts remain hidden. Bond Work Index (BWI) is intrinsic to rock type and domain; grade shells can therefore blend materials with different grindability, creating variability that increases mill energy demand and can reduce flotation recovery. In large-tonnage circuits, this variability translates directly into lost revenue. Unsupervised machine learning (ML) techniques have shown promise in revealing these contrasts; however, two persistent limitations curb their wider adoption. First, distance metrics frequently give disproportionate weight to high-variance elements at the expense of lower-variance but behaviour-defining variables. Second, the clusters produced can be challenging for geologists to reconcile with established alteration zonation, thereby undermining confidence in downstream models (Keeney and Walters, 2011; Montoya-Lopera, 2014). This study applies an adaptive weighting and clustering approach to a porphyry copper dataset, aiming to generate geospatially coherent domains that align with classical porphyry alteration zonation while simultaneously explaining observed differences in comminution and flotation response.

Methodology

The study integrates three nested datasets. The base layer comprises assays for 18 major (e.g. Fe, Si, Cu) and trace elements (e.g. Au, Th, U) from 2000 drillcore samples. The comminution subset adds BWI and Drop-Weight Test (DWT) values for 60 intervals; graphite-C first appears in this subset. The flotation subset provides rougher mass pull (Fr), rougher concentrate grade (Xr) and locked-cycle Cu recovery (LCT) for 53 composites. Each variable was standardised and then received a continuous weight whose value was tuned by a Bayesian optimiser to maximise the mean silhouette score. Cu, S and graphite C emerged as the most influential variables, whereas Si and Ca were down-weighted, preventing highly variable but less predictive elements from dominating the distance metric. Weighted pairwise distances were embedded in two dimensions with multidimensional scaling, and K-means clustering was applied to the embedded data. An optimal K = 4, supported by the highest Calinski–Harabasz score and the lowest Davies–Bouldin index, as well as the silhouette peak, proved stable, with fewer than 5% of samples changing label when initial seeds were re-randomised. Finally, principal component analysis within each domain confirmed internal coherence, with the first three components explaining more than 70% of the variance.

RESULTS AND DISCUSSION

The four geological clusters define an outward-to-inward geochemical gradient consistent with the classical mineral zoning of porphyry Cu deposits (Table 1). The propylitic margin shows high Ca + Na

(> 2 wt%) and the lowest Cu (~ 0.3 wt%), a signature typical of chlorite–epidote alteration with minimal metal influx. The argillic–phyllic shell contains > 5 wt% Al and about 0.6 wt% Cu, reflecting alteration that removes Ca–Na plagioclase and introduces sericite-rich clays, while copper increases only to a moderate level. The high-sulfide phyllic core records the peak metal tenor: Cu averages 1.1 wt%, S increases to 0.4 wt%, and Fe rises sharply, reflecting a quartz–sericite–pyrite zone rich in sulfides. Immediately inward, the potassic centre has combined K + Fe > 3 wt% and Cu steadies near 0.7 wt%, matching the expected K-feldspar–biotite assemblage. A graphitic inclusion averages ~ 0.8 wt% Cu, the second-highest copper content after the high-sulfide core, and stands apart from the other clusters because of its elevated graphite-C, denoting local carbonaceous lenses in the deposit. Across all clusters, the inter-quartile Cu spread is < 20% of the deposit-wide range, confirming that the weighting scheme generates internally coherent geochemical groups.

Table 1: Geometallurgical domain delineation for porphyry Cu dataset.

Geomet Domain	Geological Domain	Facies	Cu tenor / Sulfides	Net Processing Behaviour
I – hard / high recovery	Argillic-Phyllic	Sericite–clay halo	Moderate Cu, moderate S	Breakage similar to propylitic rock; acceptable Cu recovery
	Potassic Core	K-silicate inner core	Moderate Cu, high Fe	Hard rock; reliable Cu recovery; useful for blending
	Propylitic	Outer halo / leached cap	Very low Cu, low S	Harder to break; Cu grades too low to influence plant performance
II – soft / low recovery	Graphitic Inclusion	Carbonaceous / skarn lens	Moderate Cu, graphite C	Very soft; carbon can dilute concentrate – best managed separately
	Phyllic Ore	High-sulfide core	Highest Cu & S	Breaks easily but loses copper during cleaning; needs closer monitoring

Comminution data reveal two distinct hardness classes. Propylitic and potassic samples constitute a hard class with an average BWI of 20.6 kWh t^{-1} and a standard deviation (SD) of 2.6, whereas high-sulfide phyllic and graphite-bearing samples form a soft class averaging 19.1 kWh t^{-1} (SD 1.4). A gap of 1.5 kWh t^{-1} corresponds to roughly 10% variation in SAG-mill throughput at constant power, consistent with operational observations (Keeney and Walters, 2011). Flotation results split similarly (Figure 1): samples from the outer and potassic domains achieve an average locked-cycle recovery of 88.7% (SD 4.4%), whereas high-sulfide phyllic and graphite-rich samples recover only 86.3% (SD 6.5%). The latter material also exhibits a higher rougher mass pull (Fr ≈ 26%) with little grade benefit in the initial concentrate (Xr), reflecting entrainment of fine gangue and graphite. At 100 000 t d^{-1} and 0.5% Cu feed, a 2% recovery deficit equates to ~ 10 t Cu lost per day, exceeding US $30 M annually.

The geochemical and test-work results translate into three practical feed categories for planning. First, propylitic and potassic domains form a hard, competent ore that needs more grinding energy yet still yields high Cu recovery once processed. Argillic–phyllic material falls mid-range in both hardness and recovery and is therefore well suited to evening-out daily variations in mill load and metal output (Both and Dimitrakopoulos, 2021). High-S phyllic and graphite-bearing intervals form a soft feed, but their concentrate typically loses about 2% Cu in cleaning because carbonaceous matter and fine clay lower sulfide flotation efficiency. Blending this softer, lower-recovery ore with the harder, higher-recovery feed from the first two categories is a recognised practice for stabilising SAG-mill throughput and sustaining overall copper production (Both and Dimitrakopoulos, 2021; JKTech, 2024).

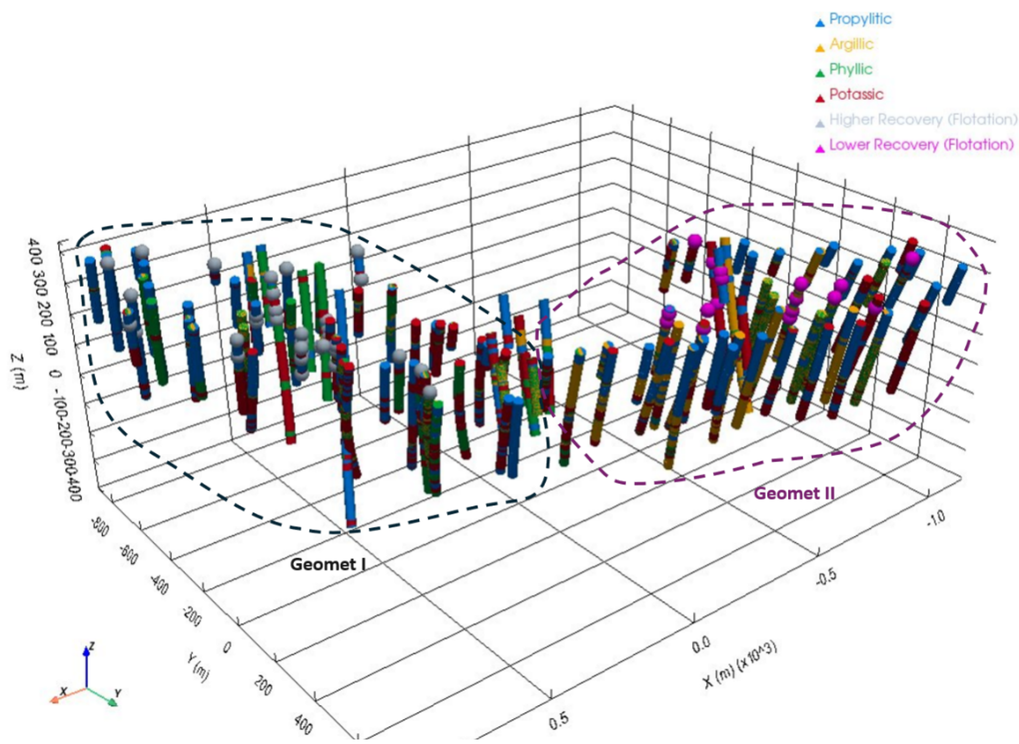

Figure 1: Spatial distribution of geometallurgical domains.

CONCLUSION

An adaptive weighting and clustering workflow generated four geospatially coherent domains in a porphyry copper deposit that align with established alteration zonation and exhibit markedly reduced internal chemical variability. The same domains explain systematic differences in comminution and flotation response, demonstrating a direct link between geology and processing behaviour. Even moderate shifts in hardness (1.5 kWh t^{-1}) or recovery (2%) carry substantial economic consequences, underlining the value of reliable domain definition. The methodology relies on standard assay and metallurgical data, employs open-source software and avoids subjective thresholds, making it readily transferable to other porphyry copper deposits.

REFERENCES

Both, C. and Dimitrakopoulos, R. (2021). Applied machine learning for geometallurgical throughput prediction—a case study using production data at the tropicana gold mining complex. *Minerals*, 11(11), 1-19.

JKTech. (2024). Technical bulletin: the importance of grinding operating stability. JKTech Pty Ltd, Brisbane. https://jktech.com.au/article/2024/08/technical-bulletin-importance-grinding-operating-stability.

Keeney, L. and Walters, S. (2011). A methodology for geometallurgical mapping and orebody modelling. *Proceedings First AusIMM International Geometallurgy Conference*. AusIMM, Brisbane.

Montoya-Lopera, P.A. (2014). Geometallurgical mapping and mine modelling – comminution studies: La Colosa case study, AMIRA P843A. *MSc thesis*, University of Tasmania, Hobart.

Tariro Mombe

PhD Researcher
Wits Mining Institute

Tariro Mombe is a geoscientist and PhD researcher specialising in data-driven mineral resource management. Her expertise spans geometallurgy, resource estimation, and machine learning, with a focus on improving digital workflows that support real-time mine optimisation. She holds a Master of Science (MSc) in Geology from the University of the Witwatersrand, where she applied machine learning techniques to predict in-situ gold grades in the Witwatersrand Basin. She is currently based at the Wits Mining Institute, where her research centres on developing a machine learning–based metal accounting system. This work integrates geological, spatial, and process data to support real-time tracking of material movement and composition – thereby improving how resources, particularly critical raw materials, are monitored, managed, and reconciled. Her broader interests lie in using AI and automation to drive efficiency and sustainability across the mining value chain.

Are variational gaussian processes the missing link in predictive geometallurgy?

G.T. Nwaila[1], Í.G. Gonçalves[2]

[1]University of the Witwatersrand, South Africa
[2]Federal University of Pampa, Brazil

To maximise the value of a mining operation, processes from the ore deposit to the final product and waste streams should be optimised together. Yet mining and metallurgical systems are variable and uncertain because deposits are heterogeneous and process models are incompatible. We present an integrated, uncertainty-aware workflow for the Assen Iron Ore deposit in South Africa in which a multi-output variational Gaussian process (VGP) jointly models lithology, multi-element chemistry and bulk density for a banded iron formation orebody and propagates posterior distributions to blending envelopes and a Bond Ball Work Index (BBWI) meta-model for comminution energy. The main contribution is two-fold: (1) a scalable co-regionalised GP that is computationally tractable at deposit scale while retaining calibrated uncertainty; and (2) an operational coupling that converts model percentiles into decisions for blending, energy sizing and drill targeting. VGP makes deposit-scale multi-output modelling tractable in this study. Importantly, oxide predictions are rendered compositionally coherent through log-ratio transforms, ensuring non-negativity and unit sum. Results identify stationary hematite domains suitable for near-direct sinter blending, silica-rich corridors that govern energy and justify staged grinding with selective reverse flotation, and carbonate lenses best managed via early rejection or dedicated calcination. The approach is generalisable to multi-attribute geometallurgical contexts where decisions must reflect both predictable outcomes and quantified risk.

Keywords: Gaussian Processes; Geometallurgy, Iron Ore, Modelling, Grade, BIF

INTRODUCTION

The goal of geometallurgical programmes is to achieve optimal technical, economic, environmental and social outcomes along the value chain from ore to products and waste. In banded iron formation (BIF) deposits, supergene enrichment, intrusive contacts and deformation impose strong contrasts in ore chemistry, texture and density that propagate to blend stability, comminution energy and specification risk. Predictive geometallurgy requires models that are multi-output, cater for both additive and non-additive variables, uncertainty-aware, and aligned to geological characteristics, with outputs that can be used directly for mine planning and plant optimisation. Gaussian processes provide Bayesian, non-parametric prediction with uncertainty. Classical GP and co-kriging also capture cross-covariance, but training scales as $O(N^3)$ and $O((PN)^3)$, respectively, with the number of joint observations N. With hundreds of intervals and multi-outputs, kernel matrices have on the order of several thousand rows per iteration; deposit-scale block prediction, spatial cross-validation and posterior sampling for decision tools become prohibitive. Variational Gaussian process (VGP) introduces inducing variables and stochastic optimisation, reducing computational costs to $O(NM^2 + M^3)$ with $M \ll N$. We test whether a scalable, compositionally coherent VGP can support blending and energy decisions through posterior block model percentiles rather than point estimates.

DATA AND METHODS

We modelled 807 composited drillhole intervals with assays for FeO total, SiO_2, Al_2O_3, TiO_2, CaO, K_2O, MnO and P_2O_5, and bulk density from the Assen iron ore deposit. Geological mapping delineates three operational domains: hematite-dominant, laminated or cherty BIF, and carbonate-rich lenses. Spatial coordinates and domain indicators are available at interval scale. Oxide vectors are closed to 100% and mapped to the simplex using the isometric log-ratio (ilr) transform. Density is modelled on the positive real intervals. Prediction proceeds in ilr space and is back-transformed to compositions, ensuring non-negativity and unit sum. Uncertainty is propagated by Monte Carlo sampling in ilr space before inverse mapping, yielding credible intervals on the simplex at block scale. A multi-output VGP with a co-regionalised kernel captures cross-attribute covariance among oxides and density. Spatial anisotropy is aligned with the mapped spatial autocorrelation. We use sparse inducing points and stochastic variational inference to optimise the evidence lower bound (Gonçalves *et al*., 2025). Domain-stratified spatial cross-validation evaluates generalisation; calibration is assessed by predictive-interval coverage and accuracy scoring rules.

RESULTS AND DISCUSSIONS

The VGP yields iron-rich central tendencies with low predictive variance in hematite-dominant domains, consistent with high density and supergene silica removal along geological structures (Fig. 1). Laminated and cherty BIF domains show long right tails in SiO_2 and elevated variance near contacts, reflecting band-controlled heterogeneity. Carbonate-rich lenses coincide with CaO spikes and localised variance, consistent with sparser conditioning and textural complexity. Under domain-stratified folds, 90% confidence interval predictive bands achieve coverage close to nominal for major oxides and density, indicating calibrated uncertainty. Outliers, notably in TiO_2 where data are sparse, appear with high posterior variance and are treated as drill targets rather than immediate specification risks. The model's percentile surfaces set lithology-aware blending rules. Hematite-dominant blocks with low SiO_2 P90 and controlled Al_2O_3 P90 support near-direct sinter blending with monitoring of phosphorus. Where the VGP maps high SiO_2 P90 or elevated Al_2O_3 P90 at boundaries, the envelope is tightened, or selective pre-concentration is scheduled. For carbonate lenses, basicity control and loss-on-ignition considerations motivate early mass rejection via density or optical or X-ray sorting, or routing to a dedicated low-temperature calcination stream when economic. The distinction is not generic; it is triggered by posterior quantiles at block or stockpile scale.

Posterior compositions drive a Bond Ball Work Index (BBW) distribution that typically centres near values consistent with hard, but tractable hematite–BIF ore (Fig. 1). Domains with high SiO_2 P90 are those where liberation dominates energy consumption; these justify staged grinding with classification and magnetic cleaning. Because BBWI is available as a distribution, equipment can be sized to a risk percentile rather than a mean, reducing exceedance probability and improving throughput stability. Where magnetic susceptibility is insufficient in high-silica corridors, reverse silica flotation is scheduled for the subset of blocks flagged by SiO_2 risk; this is a targeted action derived from the posterior, not an across-the-board prescription. Blocks that straddle specification thresholds (e.g., Fe near the lower limit with SiO_2 P90 close to the upper limit) and show large predictive variance are deferred or sent for infill drilling. High-confidence hematite zones are advanced to stabilise product quality. This uncertainty-aware scheduling reduces volatility in blend chemistry and moderates' energy excursions. Classical methods such as co-kriging would require repeated factorisations of dense kernels with thousands of rows. The VGP framework retains GP uncertainty but replaces the bottleneck with inducing-point inference, enabling deposit-scale modelling, cross-validation and repeated sampling for blending and energy tools. The gain is therefore scalability with maintained calibration, not a different notion of uncertainty. Without transformation, predicted oxides can be negative or fail to sum to one, invalidating downstream slag and blend calculations. The ilr transform and inverse mapping guarantee physically admissible predictions on the simplex, so that both expected values and quantiles are internally consistent. This addresses a frequent source of bias in geometallurgical block models and is integral to the workflow.

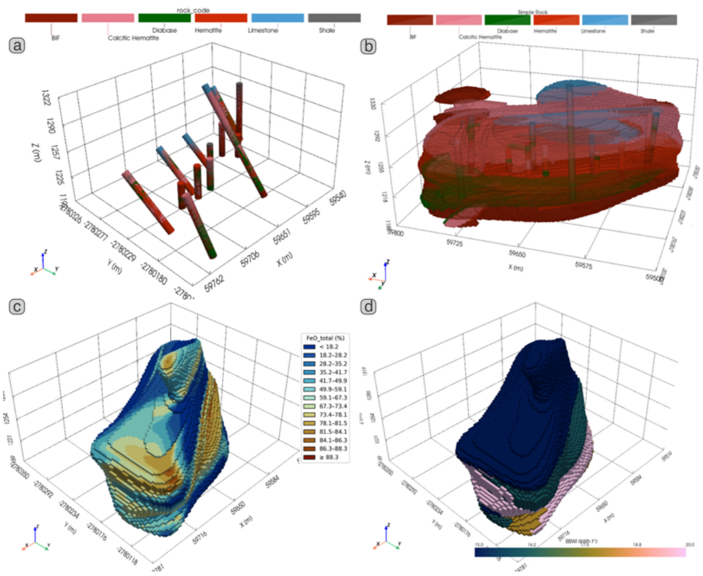

Figure 1: Integrated 3D geometallurgical visualisation of the Assen deposit: (a) borehole lithologies, (b) implicit geological block model, (c) Fe total (%) voxel block, and (d) BBWI voxel block model.

CONCLUSION

We presented a structured and decision-oriented application of VGPs for predictive geometallurgy. The main contribution is an integrated workflow that combines a scalable co-regionalised GP with compositionally constrained multi-output predictions and direct propagation of uncertainty to blending and energy decisions. In the study orebody, the model distinguishes: (i) hematite domains suitable for near-direct sinter blending with attention to aluminium and phosphorus; (ii) silica-rich BIF domains where staged grinding, classification, magnetic cleaning and, where required, reverse silica flotation are justified; and (iii) carbonate lenses that are best managed by early rejection or dedicated calcination. The choice of VGP over classical GP or co-kriging is justified by computational scalability at deposit scale with maintained uncertainty calibration, which is necessary for spatial cross-validation and repeated posterior sampling. The framework generalises to other multi-attribute systems in which composition, texture and density co-vary and where decisions must reflect expected outcomes and quantified risk.

REFERENCES

Gonçalves, Í.G., Wellmann, F., 2025. Uncertainty Propagation in Deep Gaussian Process Networks. *Math Geosci* (2025).

Glen Nwaila
Associate Professor and Deputy Head of the School of Geosciences,
University of the Witwatersrand

Glen Nwaila is an Associate Professor and Deputy Head of the School of Geosciences at the University of the Witwatersrand. He is also the Director of the African Research Centre for Ore Systems Science (CORES) and former Director of the Wits Mining Institute. Glen holds a PhD (University of Würzburg) and an MSc in Chemical Engineering (University of Cape Town) and is a Fellow of the Geological Society of South Africa (FGSSA). His work integrates geometallurgy, geostatistics and machine learning. He leads multi-partner collaborations with academia, government and industry.

Mineralogy as a predictor of comminution behaviour for Merensky Reef low-grade Ores

V. Notole[1], G.T. Nwaila[1], M. Safari[1,2], S. Ndlovu[3]

[1]University of the Witwatersrand, South Africa
[2]Mintek, South Africa
[3]The University of Arizona, USA

INTRODUCTION

Modern mining increasingly targets complex, low-grade deposits, requiring efficient and integrated processing strategies. Geometallurgy addresses this challenge by integrating geological, mineralogical and metallurgical data to optimise the value chain, from resource estimation to recovery through predictive modelling (Frenzel *et al*., 2023; Tusa *et al*., 2025). This is important for ore bodies like the Merensky Reef in Bushveld Complex, where mineralogical variability (including sulfides, oxides, silicates, and alteration phases like serpentine and talc) affects both comminution and downstream recovery. Comminution, typically consuming up to 50% of the total energy used in mineral processing plants, is sensitive to ore mineralogy (Napier-Munn, 2015; Daniel, 2016; Jeswiet and Szekeres, 2016). Traditional optimisation methods rely on bulk assays and mechanical testing, which often fail to capture the spatial and textural variations. The Tescan Integrated Mineral Analyser (TESCAN TIMA) now allows detailed quantification of mineral phases, grain size, and liberation at the micron scale, but correlating this data to comminution performance remains challenging. The Bond Work Index (BWI) provides a standardised measure of ore grindability but does not account for mineralogical factors like phase hardness or textural complexity (Chandar *et al*., 2016; Nikolić *et al*., 2024). Machine learning (ML) provides a solution by identifying non-linear relationships between mineralogy and processing behaviour. Techniques such as convolutional neural networks (CNNs), combined with image processing methods such as Local Binary Patterns (LBP) and K-means clustering, enable automated, scalable analysis of ore textures. Generative Adversarial Networks (GANs) can augment limited datasets, improving model robustness and generalisation. This study investigates how mineralogical and textural features influence the comminution response of two low-grade PGE ores and evaluates the potential of ML algorithms to predict grinding behaviour from microstructural data.

Methodology

Two Merensky Reef ores (Ore A and Ore B) were selected for their contrasting mineralogy and flotation behaviour. Both samples were crushed, homogenised, and wet-milled under controlled conditions to reach target grind sizes (P_{40}, P_{68}, and $P_{80} \approx -75$ µm). Subsamples were characterised using TIMA, and backscattered electron images were processed using LBP to extract texture descriptors. These were clustered with K-means (K = 2) to identify dominant PGE-hosting textures. Image enhancement (histogram equalisation and Gaussian filtering) improved pattern recognition. A CNN was trained on classified textures, with synthetic training data generated using GANs. Model performance was evaluated via the Silhouette Score. BWI tests were conducted using a standard rod mill, with feed and product sizes set at F_{80} = 212 µm and P_{80} = 75 µm. Cumulative revolutions, grams per revolution, and energy-based work indices (Wi) were determined over five grinding cycles. Subsequently, Monte Carlo simulations (n = 1000) were conducted to quantify the impact of feed size variability (F_{80}), product fineness (P_{80}) and grindability on energy-liberation-recovery relationships under different mineralogical characteristics. Specific grinding energy (E) was calculated using Bond's equation:

$$E = Wi.\left(\frac{1}{\sqrt{p_{80}}} - \frac{1}{\sqrt{F_{80}}}\right) \tag{1}$$

Where Wi represents the BWI and F_{80} and P_{80} are the feed and product 80% passing sizes in mm. Mineral liberation (L) of sulfides was modelled using a logistic function:

$$L(P_{80}) = \frac{1}{(1 + exp[k(P_{80} - P_{50})])} \tag{2}$$

Where P_{50} is the product grind size at 50% liberation and k is the curve steepness parameter. Metallurgical recovery (R) was modelled as a linear function of liberation:

$$R(P_{80}) = \alpha \cdot L(P_{80}) \tag{3}$$

Where α representing flotation efficiency losses. Experimental data were used to parameterise the model variables as normal distributions. The BWI (W_i), representing the energy required for grinding, was modelled as $W_i \sim N(20;1.0^2)$ kWh/t and $\sim N(18;1.0^2)$ kWh/t for Ore A and Ore B, respectively. The 80% passing feed size (F_{80}) and 50% passing product size (P_{50}) were defined as $F_{80} \sim N(0.0750;\ 0.002^2)$ *mm*; $P_{50} \sim N(20;\ 2^2)\ \mu m$ for Ore A and $P_{50} \sim N(25;\ 2^2)\ \mu m$ for Ore B, respectively. The grindability, expressed as the breakage rate constant (k), was set as $k \sim N(0.2;\ 0.02^2)\ \mu m^{-1}$ for Ore A and 0.25 μm^{-1} for Ore B. Simulations were performed in Python and outputs were visualised as (1) Specific Energy vs Product Size (P_{80}), (2) Liberation vs Product Size (P_{80}), and (3) Recovery vs Specific Energy (E), with 95% confidence intervals to represent uncertainty in the system.

RESULTS AND DISCUSSION

Results confirm that the two ore types are mineralogically different. Ore A is dominated by coarse-grained silicates with lower sulphide content, while Ore B contains a higher abundance of fine-grained sulfides and secondary alteration minerals. Ore B shown superior comminution efficiency compared to Ore A under the same wet-milling conditions. Ore B have finer grain sizes, higher sulphide content (pentlandite, pyrrhotite, chalcopyrite and pyrite), and abundance of soft alteration phases (serpentine, chlorite, talc) contributed to lower grindability energy requirements. Ore A, by contrast, showed increased resistance to grinding due to its coarser grain size and dominance of harder silicate phases, especially plagioclase and pyroxene. The distinct plagioclase–pyroxene ratios (1:2.44 for Ore A and 1:1.68 for Ore B, Fig. 1a) and varying grain-boundary textures significantly influenced fracture behaviour and hardness. Liberation trends showed a strong dependence on mineral grain size and textural complexity. A novel image-based textural analysis pipeline, including LBP, contrast enhancement and K-means clustering, identified two dominant textural clusters (K = 2) among PGE host minerals (isoferroplatinum and pyrrhotite) (Fig.1b–e). These were validated via LBP-intensity scatter plots and frequency distributions. The integration of GANs to augment training data enabled the development of a robust CNN model capable of classifying mineral textures with >90% accuracy, even with limited training samples, showing the potential of ML for automated texture recognition in mineralogical studies (Fig. 1e). BWI predictions and simulations showed that Ore A required ~44 kWh/t to achieve at least 50% particle size reduction at a grind size of P_{80} = 30 µm, while Ore B needed only 40 kWh/t under the same conditions (Fig. 1F). Monte Carlo simulations (n = 1000) accounted for feed size (F_{80}), median size (P_{50}) and grindability variability, confirming that energy demand increased non-linearly beyond P_{80} = 20 µm with increasing liberation returns.

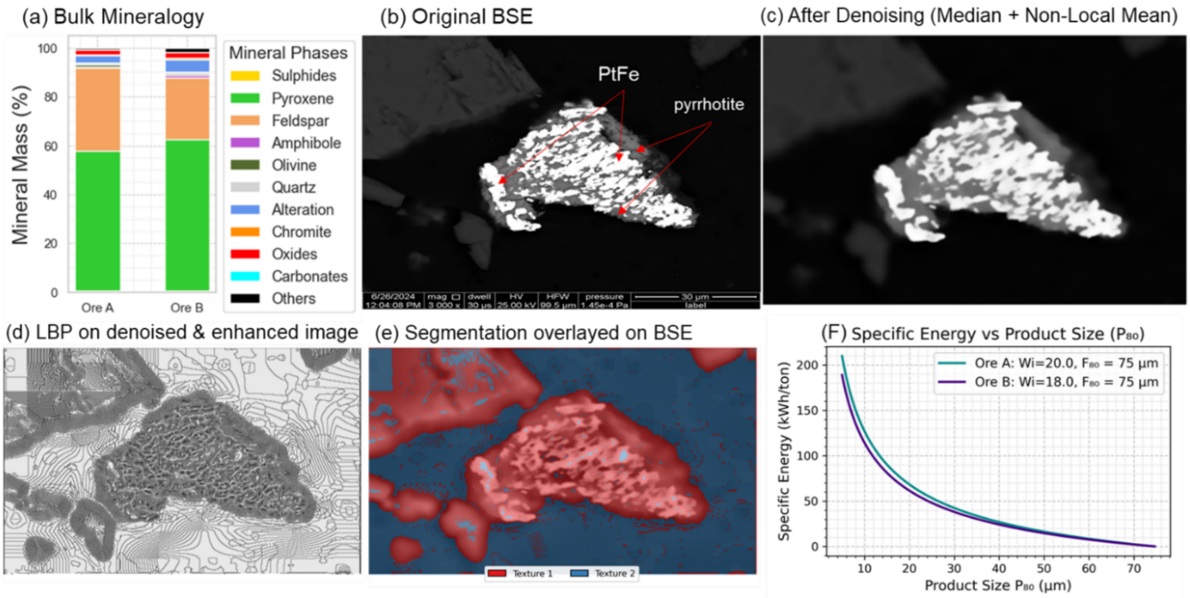

Figure 1: *Summary of mineralogical characterisation and comminution prediction/analysis: (a) stacked bar graph showing bulk mineralogy; (b) original BSE image from TIMA showing textural relationships between PtFe and pyrrhotite; (c) ML denoised image to reduce noise while preserving textural features; (d) LBP transformation on the denoised and enhanced image to peak textural differences; (e) segmented image overlaid on the BSE image, identifying two dominant mineralogical textures; (f) comminution-specific energy versus particle size distribution showing the relationship between grinding energy and particle size.*

CONCLUSION

The integration of quantitative mineralogical analysis, image-based textural metrics and ML provides a robust predictive framework for understanding ore-specific comminution behaviour. These results support the development of geometallurgical models that correlate mineral textures to energy consumption and liberation efficiency, offering actionable discernments for optimising mine-to-mill strategies in complex, low-grade PGE ore systems.

REFERENCES

Chandar, K.R., Deo, S.N. and Baliga, A.J., 2016. Prediction of Bond's work index from field measurable rock properties. International Journal of Mineral Processing, 157, pp.134-144.

Daniel, M.J., 2016. Energy use in comminution in a global context. In Sustainability in the Mineral and Energy Sectors (pp. 51-72). CRC Press.

Frenzel, M., Baumgartner, R., Tolosana-Delgado, R. and Gutzmer, J., 2023. Geometallurgy: present and future. Elements, 19(6), pp.345-351.

Jeswiet, J. and Szekeres, A., 2016. Energy consumption in mining comminution. Procedia CIRP, 48, pp.140-145.

Napier-Munn, T., 2015. Is progress in energy-efficient comminution doomed?. Minerals Engineering, 73, pp.1-6.

Nikolić, V., Ferradal, P.S., Medina Pierres, J., Menéndez-Aguado, J.M. and Trumić, M., 2024. Methods for estimating the bond work index for ball mills. Minerals, 14(12), p.1264.

Smith, A.J.B., 2013. The Geometallurgical Characterization of the Merensky Reef at Bafokeng Rasimone Platinum Mine, South Africa. University of Johannesburg (South Africa).

Tusa, L., Frenzel, M., Pereira, L., Thiele, S., Tolosana-Delgado, R. and Gutzmer, J., 2025. Geometallurgy: Future Directions. SEG Discovery, (140), pp.27-39.

Viwe Notole

PhD Candidate
University of the Witwatersrand

Viwe is a geoscientist with special interest in geometallurgy and geodata analysis, with two years of hands-on professional experience in mineral characterisation, mineral processing, geohydrology, database management, and geological data analysis. He has worked as a consultant junior geologist, conducting fieldwork that involved geological mapping, collection of geological and hydrogeological data, as well as overseeing borehole drilling and test-pumping activities. He served as intern mineralogist at Mintek, geohydrologist at Umvoto Africa, and a geologist at A&B Global Mining.

Viwe holds a B.Sc. in Geology and Chemistry, a B.Sc. Hons. in Geology, and an M.Sc. in Economic Geology (GeoMetallurgy) from the University of the Witwatersrand. He is currently completing his Ph.D. at the same university, with a focus on metal accounting, mineral processing, and machine learning.

Assessing lateral variability in ore hardness and geochemistry at the Namakwa Sands deposit

S. Mgoduka[1], A. van der Westhuizen[1], C. Philander[2], M Becker[1]

[1]University of Cape Town, South Africa
[2]Tronox Mineral Sands, South Africa

INTRODUCTION

The Namakwa Sands deposit, a world-class mineral sands deposit located on South Africa's west coast, presents a unique scenario in the heavy mineral sands sector, where unconsolidated mineral sands are interspersed with cemented hard layers (CHL). These layers differ in composition and hardness, significantly impacting mining and mineral processing. While vertical variations in hardness and composition have previously been described (Philander & Rozendaal, 2011; Sikushumane *et al.*, submitted), attention is also being given to lateral variability across the deposit. This paper focuses on the lateral distribution of key geochemical and mechanical properties across the deposit, using three datasets – sampled in 2017, 2022 and 2024. The objective of this paper is to explore the variability in chemistry, mineralogy and surface hardness across these datasets – focusing on west-east variability across the four mining pits (West, Centre, East, Far East), and north-south variability across the three datasets. The study will also test and revise existing models developed by Sikushumane *et al.*, (submitted) to quantify hardness (A*b).

Methodology

A total of 86 samples will be analysed for this study: 19 samples from an in-house Namakwa database from 2017 (database 1), 43 samples from the study of (Sikushumane, *et al.*, submitted) (database 2) and 24 samples from a recent 2024 sampling campaign (database 3). Samples for databases 1 and 3 were obtained through bulk sampling, whereas database 2 used individual CHL specimen selection. All three databases consist of major element oxides determined using X-ray fluorescence spectrometry, Leeb surface hardness determined with an Equotip device (S-type probe; referred to HLS), mineralogical analyses (X-ray diffraction and QEMSCAN), and A*b hardness measurements determined using the HIT (hardness index tester; Kojovic, 2023) (selected 2017 samples, 2022 samples, 2024 results pending). The 2024 samples also have accompanying BWI and UCS measurements. Five rocks from each sample location were selected by the laboratory and drilled into cores (H/D ratio of 2.0-2.7 with diameters 35-75 mm) for UCS and the fragments for BWI. A closing screen size of 300 µm for the BWI test was selected as it reflects the known soft grinding behaviour of the cemented matrix whilst liberating valuable minerals without breakage.

SUMMARY OF RESULTS

Consistent with literature in the concrete domain (Moutassem & Chidiac, 2013; Buertey, *et al*., 2018), the study of Sikushumane *et al.*, (Submitted) posed that impact hardness has a direct relationship with matrix minerals. CHL with a greater proportion of matrix minerals are expected to be harder (c.f. higher proportion of cement compared with aggregate in concrete). They identified HLS, MgO and loss on ignition (LOI) as having statistically significant negative correlations with A*b, thus making the ore harder, and SiO_2 as having a statistically significant positive correlation, making the ore softer. The MgO and LOI are considered to represent the matrix minerals sepiolite, as well as calcite, whereas SiO_2 mostly represents granular quartz. It is these components that are explored in more detail in Figure 1.

MgO and LOI exhibit a decreasing trend from north to south along the orebody (Figure 1), alongside rebound hardness (HLS), further supporting the hypothesis that a reduction in MgO and LOI-bearing matrix minerals corresponds to a 'softer' ore. In contrast, SiO_2 — identified as the coarser 'aggregate' — shows an opposite trend and maintains a negative correlation with surface hardness, as previously established for impact hardness. Across the west–east axis of the four mining pits, the variability in these four features is less pronounced. Only MgO and HLS display slight decreasing trends, particularly in the more recent datasets, DB2 and DB3, from the western to the far eastern pits.

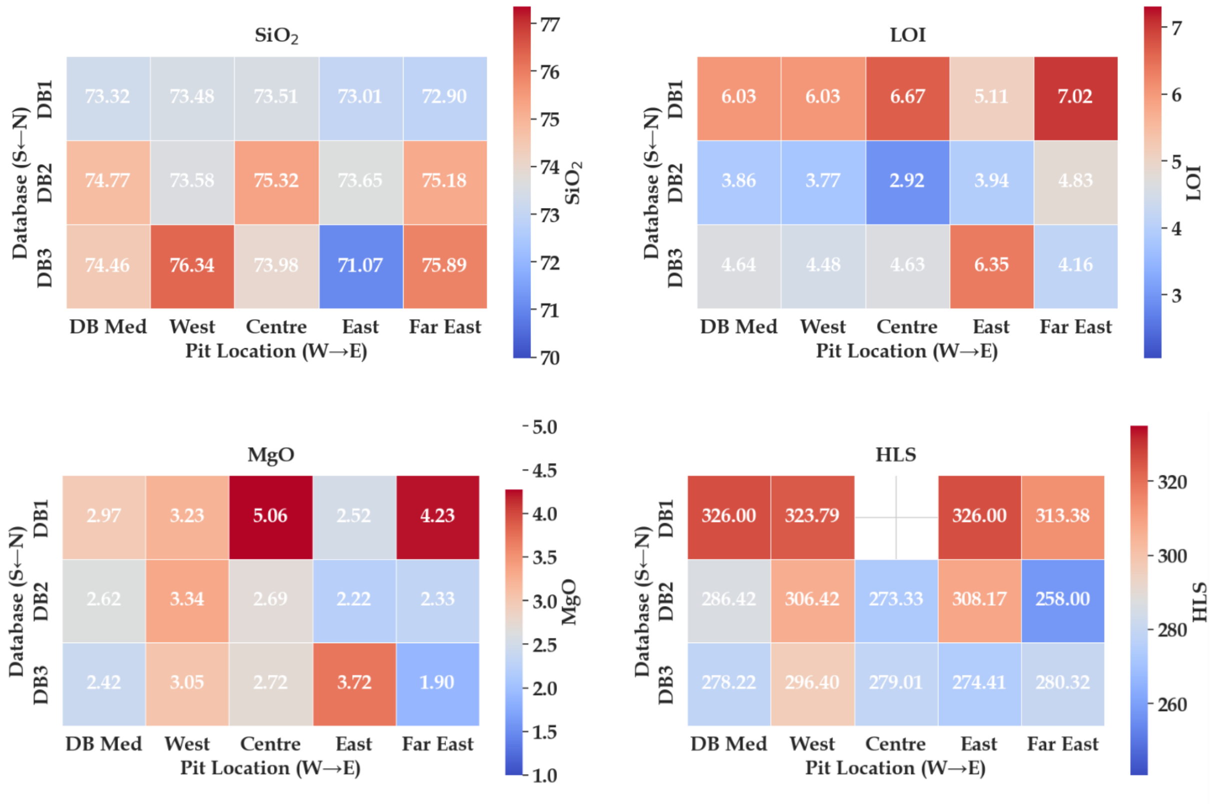

Figure 1: Heatmaps showing median geochemical and rebound hardness (HLS) values across the three different databases from north to south, and pit location from west to east of the mine. 'DB Med' is the median value for each database (DB1, DB2 and DB3) combined.

A major objective considered when designing the sampling strategy for the 2024 dataset (database 3) was to generate sufficient sample mass so that larger-scale geometallurgical tests could be commissioned (note that the CHL are too friable to generate drill core, requiring bulk sampling with an excavator). These larger sample masses allowed for UCS and BWI to be determined, measurements that ultimately have a stronger relationship to mining excavation rates and grindability. The correlation matrix in Figure 2 shows the relationship between the selected oxides and hardness indicators (HLS, UCS and BWI) for the 2024 dataset. Statistically significant relationships ($|R| > 0.4$, for $n = 24$) are primarily between LOI and MgO ($R = 0.72$) and HLS and BWI ($R = 0.63$). The positive relationship between HLS and BWI implies that as surface hardness increases (reflected in HLS), more energy is needed to grind it (higher BWI), aligning with geometallurgical expectations. Conversely, LOI and SiO_2 are strongly negatively correlated ($R = -0.85$), meaning that higher LOI values correspond to rocks with lower quartz content, as per the concrete analogy. Other variable pairs show weaker insignificant correlations. For example, UCS shows no significant correlations, potentially reflecting inconsistencies in sampling, variability in testing, or that different rock hardness measurements are affected differently.

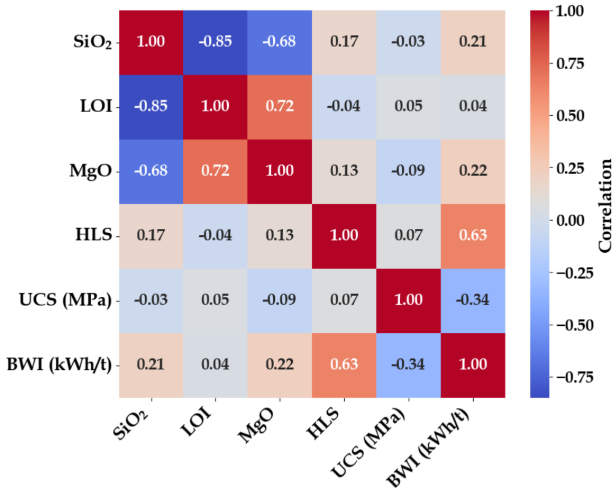

Figure 2: Correlation matrix for the 2024 dataset showing the relationships between selected geochemical oxides (SiO_2, LOI, MgO) and different hardness indicators (HLS, UCS, and BWI). Note that |R| values greater than 0.40 for n=24 are considered statistically significant at the 95% confidence level.

PRELIMINARY FINDINGS

This paper contributes to the study on ore hardness at Namakwa and presents the following findings:

- Initial inspections across the three datasets indicate significant correlations identified in earlier studies remain valid, suggesting geometallurgical consistency across time and sampling campaigns.
- Hardness variability appears more pronounced along the north-south direction than west-east.
- A strong relationship between comminution hardness, in this case, BWI, and HLS has been reaffirmed in 2024 data.

The 2024 dataset offers improved coverage through the inclusion of complementary geochemical and mechanical variables, making it a critical bridge between historical and future test work. Upon receipt of the 2024 A*b results, detailed regression and machine learning models will be developed.

REFERENCES

Buertey, J. I. T., Offei, S. W., Kumi, T. A. & Astrim, F., 2018. Effect of aggregates mineralogy on the strength of concrete: Case study of three selected quarry products in Ghana. *Academic Journals,* 9(1), pp. 1-10.

Kojovic, T. & Bucknell, C., 2024. *Application of HIT in Orebody Hardness Domanining Using Exploration Samples.* International Mineral Processing Congress, Washington DC.

Moutassem, F. & Chidiac, S. E., 2013. Assessment of concrete compressive strength prediction. *Korean Society of Civil Engineers,* pp. 1-16.

Philander, C. & Rozendaal, A., 2011. The contributions of geometallurgy to the recovery of lithified heavy. *Minerals Engineering, ScienceDirect,* Volume 24, pp. 1357-1364.

Sikushumane, M., van der Westhuizen, A., Philander, C. & Becker, M., submitted. Development of preliminary geometallurgical proxies to predict the hardness of the cemented hard layers in a mineral sands deposit. *Natural Resources Research, Submitted.*

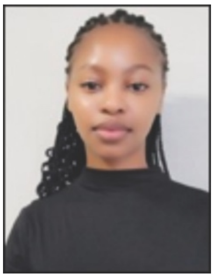

Sibulele Mgoduka

University of Cape Town

Sibulele Mgoduka is a Master of Science candidate in Geometallurgy at the University of Cape Town and holds a Bachelor of Science in Chemical Engineering, completed with First-Class Honours. Her research focuses on understanding ore hardness variability and developing predictive approaches to improve ore characterization and process performance, while her broader interests include tackling complex challenges, sustainability projects, and process optimization.

Addressing the elephant in the room: Integrating diamond breakage into Kimberlite geometallurgy

S. Burness, S. Bremner, M. Becker, G.H. Howarth, A.N. Mainza

University of Cape Town, South Africa

INTRODUCTION

Published accounts of existing geometallurgy programs for kimberlites largely focus on the effects of ore variability on throughput, equipment performance, power and water consumption, and diamond yield (% recovery to XRT or DMS concentrates) (e.g., Zhang *et al.,* 2012; van Niekerk *et al.*, 2016; Lechuti-Tlhalerwa *et al.*, 2019; Gilika & van der Westhuyzen, 2023; Lang *et al.*, 2025). But the value of kimberlite ore lies not in the host rock itself but in the discrete diamonds it contains. Since the central aim of geometallurgy is to anticipate and manage risks linked to ore variability, this raises an important question: why has relatively little emphasis been placed on factors unique to kimberlites? These include the role of indicator minerals (e.g., Hoal *et al.*, 2008) in predicting grade, the diverse characteristics of diamonds that influence recovery, and the significant risks associated with diamond breakage during processing. To some extent, this has been driven by the proprietary practices within the industry.

Approach

The geometallurgical approach aims to develop a spatially informed understanding of the ore body to manage operational risk by integrating geological, mineralogical, and geochemical input data with response variables such as metallurgical performance and physical properties. At UCT, this framework is applied to the study of diamond breakage using two complementary methods: detailed mineralogical characterisation of diamond parcels (Burness *et al.*, 2024), and controlled laboratory experiments involving synthetic diamond simulants embedded in kimberlite analogues (Chele, 2021). While natural geological breakage is unavoidable and often influenced by features such as inclusions, cleavage along (111) planes, and twin plane inversions (Figure 1a), mechanical processing can further exacerbate breakage (Burness *et al.*, 2024). Surface wear through abrasion and attrition (shear forces) can produce features such as tram-line pits and chatter marks, while internal micro-fractures, commonly located around inclusions, may propagate under stress (Figure 1b), particularly along natural cleavage planes. Excessive or improperly applied impact or compressional forces during comminution can initiate new fractures, increasing the risk of significant breakage.

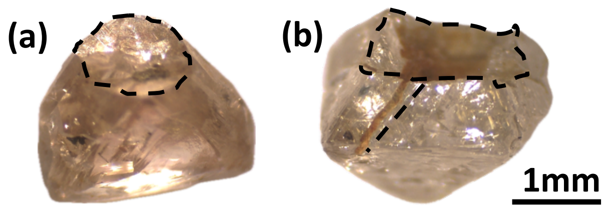

Figure 1: (a) Macle diamond showing a breakage zone aligned with the twin plane inflection. (b) Octahedral diamond exhibiting breakage due to fracture propagation around an inclusion; an extended abrasion pit is also visible.

Understanding the energies required to break diamonds is the first step to mitigating breakage in the comminution circuit. In particular, understanding how unliberated and partially liberated diamonds respond to impact forces within the processing circuit is essential for identifying conditions that lead to product loss. To investigate this, controlled ore characterisation tests were designed to define energy thresholds beyond which diamonds are likely to fracture during liberation. Due to the high value and handling restrictions of natural diamond ore, ceramic simulants were embedded in synthetic concrete matrices of differing strength to act as proxies (Chele, 2021). These were subjected to drop-weight impact testing, replicating the forces encountered in a typical comminution circuit.

The comminution tests revealed four distinct outcomes based on simulant and host matrix behaviour: full liberation with broken simulants (Figure 2a), full liberation with intact simulants (Figure 2b), partial liberation (Figure 2c), and complete retention within the host matrix (Figure 2d). Results demonstrate that excessive impact energy leads to simultaneous breakage of both the simulant and host matrix, representing poor processing conditions with high risk to the diamond product. Conversely, optimal energy levels result in host rock fragmentation while preserving the simulant, indicating favourable conditions for diamond liberation with minimal breakage.

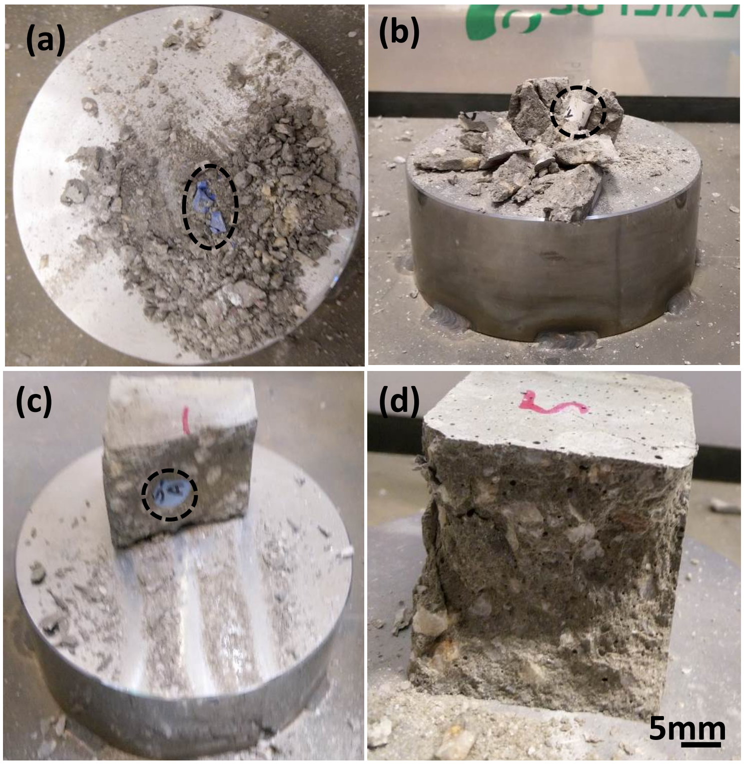

Figure 2: Results from drop-weight impact tests showing four possible outcomes for simulant liberation and breakage: (a) liberated simulant that is broken, (b) liberated simulant that remains intact, (c) partially liberated simulant, and (d) simulant retained within a partially broken host matrix.

Inadequate impact energy produced partial or no liberation, resulting in ore that would be recirculated back through the circuit. This repeated exposure to impact forces increases the likelihood of diamond damage over time and reduces overall throughput efficiency. The findings from these tests establish critical energy thresholds that define the operating window for comminution devices, based on the mechanical properties of the host material. These thresholds support informed decisions for process design and optimisation, with the dual aim of protecting the integrity of the diamond product and improving circuit performance through reduced recirculation load and improved liberation efficiency.

Preliminary insights

- Traditional kimberlite geometallurgy primarily addresses ore variability impacts on throughput, equipment performance, power and water consumption, and diamond yield (percent recovery to XRT or DMS concentrates). However, to more accurately assess and manage value-based risk, diamond breakage must be incorporated as a fundamental input within the geometallurgical model. This involves a detailed understanding of the crystallographic mechanisms of diamond breakage and identifying which processing circuit components contribute most to breakage.
- Analysis of diamond parcels processed through a traditional kimberlite processing circuit reveals distinct breakage patterns. These breakage types can be linked to specific forces such as impact, compression (including chipping and severe fragmentation), and shear (attrition and abrasion), which upon further investigation could be linked to specific equipment in the comminution circuit.
- The drop-weight tests demonstrate a clear relationship between impact energy, host rock strength, and diamond breakage. Four distinct liberation outcomes were observed, indicating that both excessive and insufficient energy result in suboptimal performance—either through diamond breakage or poor liberation causing unwanted load recirculation. Defining and controlling this 'safe window' of comminution energy is therefore vital for optimising recovery and preserving value.
- Assigning distinct diamond types or properties to specific kimberlite zones can significantly improve our understanding of the spatial variability within the orebody and its impact on breakage risk. Variations in inclusions and crystal structure affect diamond breakage during processing. Integrating this variability into geometallurgical models enables more targeted, adaptive strategies that enhance recovery and preserve value.

REFERENCES

Zhang, J., Kouznetsov, D.L., Yu, M., Rylatt, M. and Yoon, R.H., 2012. Improving the separation of diamond from gangue minerals. *Minerals Engineering, 36*, pp.168-171.

Van Niekerk, L.M., Olivier, A., Armstrong, J. and Sikwa, N.A., 2016. Pioneering large diamond recovery at Karowe diamond mine. *Journal of the Southern African Institute of Mining and Metallurgy, 116(8)*, pp.709-714.

Lechuti-Tlhalerwa, R., Coward, S. and Field, M., 2019. Embracing step-changes in geoscientific information for effective implementation of geometallurgy. *Journal of the Southern African Institute of Mining and Metallurgy, 119(4)*, pp.355-360.

Gilika, O. and van der Westhuyzen, P., Application and integration of a geometallurgical model and integration thereof, with quantitative simulation at Orapa Mine. *Geometallurgy Conference*, 2023. Available at: https://www.saimm.co.za/Conferences/files/geomet-2023/04_563-Gilika.pdf.

Lang, Z., Alam, S., Hunt, L., Di Feo, A., Robben, C., Kinakin, Y. and Tjossem, R., 2025. Comparative Evaluation of X-Ray Transmission and X-Ray Luminescence Sorting Technologies for Fine Diamond Recovery. *Minerals*, *15*(8), p.773.

Hoal, K., Botha, P.W.S.K., Forsyth, A., Butcher, A. and Palmer, C., 2008, October. Mineral characterization and geometallurgy of diamond deposits and mantle materials Using QEMSCAN® Techniques. In *International Kimberlite Conference: Extended Abstracts* (Vol. 9).

Burness, S., Becker, M., Howarth, GH., Mainza, A., 2024. Characterising diamond breakage from the processing of Kimberlite Ore: A Case Study. *In Proceedings of the XXXI International Mineral Processing Congress.* National Harbor, Washington, DC.

Sara Burness

Lecturer
University of Cape Town

Dr. Sara Burness is a lecturer in the Department of Chemical Engineering at the University of Cape Town and is affiliated with the Centre for Minerals Research. Her research focuses on process mineralogy and geometallurgy across a variety of ore deposit types, with particular emphasis on diamond breakage and xenolith studies. She teaches applied mineralogy to undergraduates and process mineralogy and geometallurgy to fourth-year students. Sara holds a unique crossover position funded by the South African Minerals Qualification Authority, designed to bridge Chemical Engineering and Geological Sciences and promote interdisciplinary collaboration. She completed her PhD at the University of the Witwatersrand, investigating sulphur mobility and metallogeny in eclogite xenoliths associated with kimberlite volcanism.

Advancing geometallurgical modelling with machine learning: Recovery and comminution hardness estimation at Mogalakwena Platinum Mine

C.N. Govender[1], T. Scott[2]

[1]Valterra Platinum, South Africa
[2]Anglo American, South Africa

INTRODUCTION

A key challenge in the integration of geometallurgical data into resource model estimation is often the limited availability of high-resolution datasets. This limitation is primarily driven by the high cost and large sample mass requirements associated with conventional metallurgical testing methods. Consequently, datasets generated through these methods are often sparse, restricting the resolution and reliability of spatial estimates. Additionally, when working with sparse and heterogenous datasets conventional interpolation methods often struggle to capture the complex, non-linear relationships between primary geological attributes and metallurgical responses (Sepulveda *et al*., 2017). To address this challenge, machine learning (ML) is a tool that has increasingly been adopted within modern estimation workflows, demonstrating its ability in predicting geometallurgical properties by leveraging the correlations which exist between sparsely sampled geometallurgical variables and more densely sampled geological data such as primary metal assays, mineralogy, and oxides (Deutsch *et al*., 2023; Mu and Salas., 2023).

This paper demonstrates the application of ML to predict plant recovery and comminution hardness parameters - the Bond Ball Work Index (BWi) and Drop Weight Index (DWi) - from densely sampled geological assay and mineralogy data. The aim of the application is to improve the spatial resolution and confidence of geometallurgical models and enable more dynamic, data-driven decision-making at Mogalakwena PGE Mine, located in the Northern Limb of the Bushveld Complex, some 40 km north-west of the town of Mokopane in the Limpopo Province of South Africa.

Methodology

A supervised decision tree-based ML framework using extreme gradient boosting (XGBoost) was developed using BWi, DWi and flotation recovery data with collocated bulk modal mineralogy and major element oxide chemistry data. The workflow starts with exploratory data analysis, followed by multivariate data imputation using Gaussian Mixture Models (Silva and Deutsch, 2018). Imputation is required for projection pursuit multivariate transformation and the subsequent independent simulation of predictor variables (including major element geochemistry and mineralogy). The imputed results then provide an isotopic dataset to be used during ML model training. Predictor optimisation was performed by the iterative removal of low-importance predictor variables. Hyperparameters were optimized across a range of tree depths, number of tree estimators, learning rates and subsample sizes, to find the combination that produced the highest-performing model. Alternative methods, random forest and stochastic gradient boost, were also evaluated for comparison. However, the XGBoost method outperformed the others in terms of both accuracy and generalization. The findings here were consistent with similar studies where gradient boosting methods have demonstrated strong performance in capturing complex, non-linear relationships between geological and metallurgical variables (Dimitrakopoulos & Both, 2021).

The resultant models were assessed using K-fold cross validation, a common technique used for evaluating ML model error, particularly when using sparse and heterogenous datasets. Five-fold cross validation was adopted where 20% of the data was withheld in each iteration to monitor overfitting and validate model robustness. However, due to the relative sparsity of collocated metallurgical and mineralogical data the final model was trained on the full dataset. The trained models were then applied to each simulated realisation of the predictor variables to generate high-resolution geometallurgical predictions.

RESULTS

Both DWi and BWi models were trained on similar dataset sizes (1044 and 1061 samples respectively) and both models achieved strong predictive performance with a correlation coefficient (R^2) of 0.747 and root mean square error (RMSE) of 0.839 on the full dataset for DWi (Figure 1 – left graph) and an R^2 of 0.803 and RMSE of 0.928 (Figure 2 – left graph) on the full dataset for BWi. The K-fold validation test results, shown on the right, are expected to show poorer performance due to the withholding of test data. However, both plots show similar statistics and overall scatter plot trends, indicating a robust ML model that is not susceptible to over fitting. Analysing feature importance analysis highlighted the strong influence of mineralogical variables such as serpentine, chlorite, amphibole, and clinopyroxene on hardness variability.

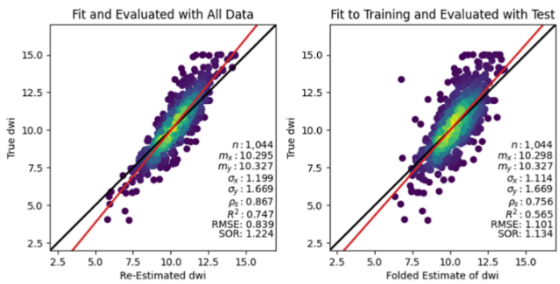

Figure 1: Machine Learning models for DWi.

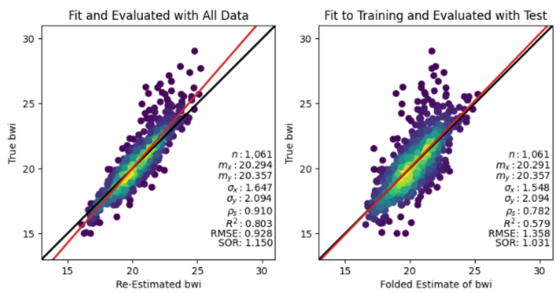

Figure 2: Machine learning models for BWi.

Recovery data, generated from bench-scale flotation tests, was only assessed for one specific pit of the mine, resulting in a relatively small training dataset of 183 samples. However, owing to the strong relationship between mineralogy and recovery, the final models performed reasonably well considering the low sample numbers. Models were developed for Pt, Pd, Cu, and Ni recovery; this paper presents results for the combined Pt and Pd (2E) model (Figure 3). The models showed strong performance when fit to all data (R^2 = 0.835, RMSE = 2.488), while validation using the test data yielded an R^2 of 0.558 and RMSE of 4.314, indicating moderate generalisation capability with possible overfitting. To mitigate overfitting additional training data is required. Feature importance analysis identified SiO_2, orthopyroxene, serpentine and amphibole as the most influential predictors, highlighting the significance of mineralogical composition in flotation. Selected ML algorithms for the BWi, DWi and metal recoveries were then applied to each cell of the block model which contains spatial estimates of the individual predictor variables, yielding estimates of those metallurgical values in the resource block model.

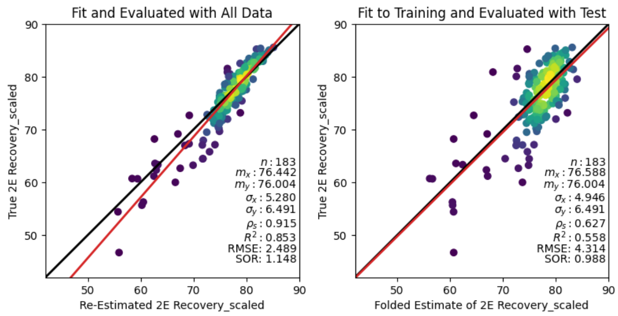

Figure 1: Machine learning models for combined Pt and Pd (2E) recovery.

CONCLUSION

This paper demonstrates the suitability of ML applications in resource estimation to incorporate sparse geometallurgical data into spatial models. In orebodies exhibiting complex and variable mineralogical and geometallurgical characteristics—such as the Platreef at Mogalakwena—spatial geometallurgical modelling plays a critical role in optimising mine planning, ore control, and metallurgical forecasting. Whilst still in the early stages of implementation, the geometallurgical models developed for Mogalakwena mine, enabled by advanced ore characterisation, rapid resource estimation techniques, and machine learning tools, have already contributed towards delivering actionable insights and measurable value to the business.

REFERENCES

Deutsch, J.L, Barnett, R.M., Deutsch, C.V. (2023). Integrating supervised machine learning and geostatistics for enhanced geometallurgical models. The Southern African Institute of Mining and Metallurgy, *Geometallurgy Conference 2023.*

Sepulveda, E., Dowd, P.A., Xu, C. (2017). Multivariate Modelling of Geometallurgical Variables by Projection Pursuit. *Math Geosciences* 49, 121–143

Mu, Y.; Salas, J.C. (2023). Data-Driven Synthesis of a Geometallurgical Model for a Copper Deposit. *Processes 2023,* 11, 1775. https://doi.org/10.3390/pr11061775.

Caillan Nicholas Govender

Specialist Geometallurgist
Valterra Platinum

I am a Geologist with over a decade of diverse experience spanning mine geology, minerals processing, and geometallurgy, across both underground and open-pit mining operations. I currently serve as a Specialist for Geometallurgical Modelling at Valterra Platinum, where I bring a multidisciplinary approach to ore characterisation, resource development and operational optimization. My expertise lies in enhancing ore control and metallurgical practices through the development of innovative rock characterization workflows and their integration into spatial models using rapid resource modelling techniques. These workflows are designed to improve value-based ore control, optimize mine planning and processing strategies, and support the assessment and implementation of emerging technologies in mining and processing environments.

I am passionate about leveraging geoscientific data to drive strategic decision-making, and I thrive in collaborative environments where technical excellence and innovation are key to unlocking resource value.

Differentiation of iron oxides using modern automated scanning electron microscopy

K. Youlton[1], L. Vonopartis[2], S. Poelinca[1], R. Harrison[1]

[1]SGS, South Africa
[2]University of the Witwatersrand, South Africa

INTRODUCTION

Differentiating hematite from magnetite is critical for interpreting redox conditions, alteration processes, and ore-forming environments. However, their similar chemistry and BSE response complicate identification using Automated SEM (AutoSEM) (Figueroa *et al*., 2012). Previous studies using MLA, QEMSCAN, and TIMA have highlighted these challenges and proposed improved workflows (Shaffer, 2009; Grant *et al*., 2018; Honeyands *et al*., 2019). These works highlight the limitations of traditional segmentation and calibration approaches and underscore the need for refined workflows tailored to iron oxide discrimination. This paper presents a refined AutoSEM-based approach for reliable phase discrimination and iron oxide ratio determination to support geological modelling and metallurgical planning.

Methodology
This study utilised the TIMA-X AutoSEM platform (TESCAN) to differentiate hematite and magnetite across a suite of commercial samples. Calibration on reference materials established Fe/O thresholds and BSE brightness criteria, forming the basis for classification subsequently applied to complex assemblages. In cases where elemental impurities (Ti, V, Al, Si) exceeded 1%, adjustments were made, though a bimodal Fe/O distribution generally allowed effective phase separation. High-resolution mapping was performed at 1.5 µm pixel spacing with 1500 X-ray counts per point, enabling accurate mineralogical mapping and textural analysis. Mineral maps provided bulk modal and spatial data, validated against X-ray diffraction (XRD) and optical microscopy.

XRD analysis was conducted on pulverised material using a Panalytical Empyrean diffractometer with Fe-filtered Co-Kα radiation. Diffraction data were processed in HighScore Plus, and quantitative phase analysis employed the Rietveld refinement method with the PanICSD database.

RESULTS

The AutoSEM methodology applied using the TIMA-X platform, enabled consistent differentiation between hematite and magnetite across a range of commercial samples. Two representative case studies are presented and illustrate the effectiveness of this approach.

In the first case, three heavy mineral sand samples were analysed to quantify bulk modal mineralogy. The bulk modal mineralogy (Table 1) showed hematite contents ranging from 38.4% to 46.2% and magnetite from 0.78% to 16.6%. These values were validated against XRD data (Table 1), which reported hematite between 31.7% and 42.5% and magnetite between 2.0% and 11.9%. While the two methods show broadly comparable trends, some variation is evident, likely reflecting differences in sample preparation, detection limits, and phase quantification approaches.

Table 1. A comparison of TIMA and QXRD bulk modal mineralogy for Fe oxide phases. Values given in weight percent (w.t.%)

TIMA Abundance			
Mineral	**Sample 1**	**Sample 2**	**Sample 3**
Ilmenite	30.0	51.4	43.1
Hematite	**38.5**	**46.2**	**38.4**
Magnetite	**16.6**	**0.8**	**4.8**
Quartz	4.5	0.4	3.2
Titanomagnetite	0.4	0.2	7.4
Chlorite	3.1	0.6	2.0
Apatite	4.9	0.0	0.0
Garnet	1.1	0.2	0.4
Other	0.4	0.4	0.5
Feldspar	0.4	0.0	0.0
Ulvospinel	0.2	0.0	0.2
XRD Abundance			
Hematite	**31.7**	**42.3**	**42.5**
Magnetite	**11.9**	**2.0**	**3.6**

In the second case study, polished sections of banded iron formation (BIF) samples were mapped at high-spatial resolution (Figure 1). The TIMA-X analysis revealed fine-scale layering and complex intergrowths of hematite and magnetite. Notably, hematite was observed replacing magnetite in late-stage oxidised zones, consistent with paragenetic interpretations.

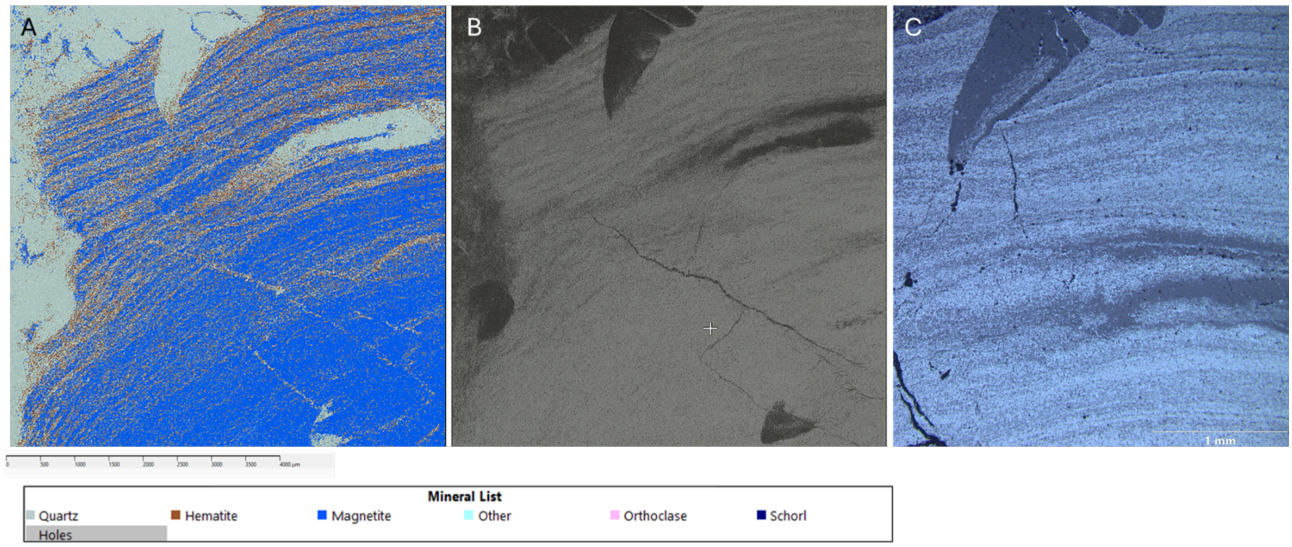

Figure 1: TIMA-X results of the fine banded iron formation (BIF) analysis. (a) Mineral map. (b) Backscattered electron map and (c)Reflected light optical petrograph, the magnification for which is finer to allow for better visual discrimination of hematite and magnetite.

DISCUSSION AND CONCLUSION

In this study, we demonstrate a consistent, reliable, and flexible workflow for SEM-based differentiation between hematite and magnetite. This is accomplished by using a basic workflow that requires minor adaptation of classification schemes and calibration of mineral definitions to account for subtle yet significant chemical differences exhibited between deposits. The methodology includes adjusting elemental thresholds and subsequent elemental signatures to reflect fine-scale variations in Fe/O ratios and trace element incorporation, which influences phase discrimination. The improved phase resolution enables better interpretation of paragenesis, as hematite commonly replaces magnetite in late-stage oxidised conditions.

The ability to resolve iron oxide phases at scale provides an important tool for bulk commodity mineralogy and timely results for mineral processing applications. Additionally, the ability to differentiate hematite from magnetite was found to be a reliable indicator of supergene versus hypogene mineralisation within a deposit. This distinction has direct implications for expected recovery through flotation, as mineralisation in oxide zones is often locked in non-sulphide phases, making conventional flotation techniques ineffective. The integration of phase differentiation with mineral deportment data was shown to be highly valuable for long-term mine planning, informing both metallurgical strategy and resource evaluation. The spatial resolution of the AutoSEM allowed for detailed textural analysis, supporting the interpretation of redox evolution and mineralisation processes.

We demonstrate that the refined TIMA-X workflow provides both accurate bulk mineral quantification and high-resolution textural insight, enabling robust interpretation of iron oxide mineralogy in diverse geological settings.

REFERENCES

Figueroa, German, Kurt Moeller, Michael Buhot, Gerda Gloy, and David Haberla. "Advanced discrimination of hematite and magnetite by automated mineralogy." In Proceedings of the 10th International Congress for Applied Mineralogy (ICAM), pp. 197-204. Berlin, Heidelberg: Springer Berlin Heidelberg, 2012.

Grant, D.C., Goudie, D.J., Voisey, C., Shaffer, M. and Sylvester, P., 2018. Discriminating hematite and magnetite via Scanning Electron Microscope–Mineral Liberation Analyzer in the− 200 mesh size fraction of iron ores. Applied Earth Science, 127(1), pp.30-37.

Honeyands, T., Manuel, J., Matthews, L., O'Dea, D., Pinson, D., Leedham, J., Zhang, G., Li, H., Monaghan, B., Liu, X. and Donskoi, E., 2019. Comparison of the mineralogy of iron ore sinters using a range of techniques. *Minerals*, *9*(6), p.333.

Shaffer, M., 2009. Discriminating hematite and magnetite and quantifying their associations using the JKTech Mineral Liberation Analyzer™. In The 48th Annual Conference of Metallurgists, Laurentian University, Sudbury, Ontario (Vol. 73).

Kirsten Leigh Youlton

HOD Mineralogy
SGS

Dr Kirsten Youlton is a process mineralogist with over five years of experience in mineralogical investigations, project management, and cross-disciplinary collaboration in the mining and metals industry. She holds a PhD in Geosciences from the University of the Witwatersrand, with a focus on economic geology and metallurgy. Her expertise spans a wide range of commodities—including gold, copper, PGEs, and industrial materials—and she is proficient in advanced mineralogical techniques such as TIMA/QEMSCAN, XRD, SEM-EDS, and optical microscopy. Dr Youlton has held senior roles at SGS and Mintek, where she led high-value technical projects, managed mineralogical instrumentation, and mentored junior staff. She is a published geoscientist with a strong interest in data-driven process optimisation and interdisciplinary problem-solving within the mining sector.

The role of mineralogy in geometallurgy

M. Becker

University of Cape Town, South Africa

INTRODUCTION

Although the contribution of mineralogy to mining, mineral processing, and environmental management has been recognised for several decades, formal integration of these activities into a discipline (geometallurgy) focused on managing risk only came about in the late 1990s and early 2000s. In their seminal paper, Williams and Richardson (2004) explicitly mention mineralogy as one of the key disciplines contributing to ore characterisation in geometallurgy. Walters' (2008) overview of the AMIRA Geometallurgical Mapping and Mine Modelling (GEM) project importantly introduced the concept of the geometallurgical framework, a useful construct for representing the interplay between sample size, number of samples, simplicity of testwork and scale-up. Because geometallurgy requires abundant data that reflects ore variability, the initial emphasis of the GEM project was on the development of predictive geometallurgical indices. These indices, more commonly known as proxy data, were designed to be simple, inexpensive, quick and easy to implement. Many of these indices were centred on mineralogy.

The Global Mining Guidelines (GMG) group recently published a geometallurgy White Paper (GMG, 2025) that also recognises mineralogy as an important contributor to geometallurgy. The White Paper highlights that the current operating context has changed since earlier publications – now with greater focus on (i) data-driven technologies; (ii) ore characterisation for future resources; (iii) waste management for closure planning; and (iv) reconciliation.

Having recognised the importance of mineralogy in geometallurgical programmes, one must now ask where mineralogy fits into geometallurgical programmes. Lishchuk *et al.*, (2015) proposed three different approaches: (i) traditional approach – response of an ore is predicted based on a model linking metallurgical response with feed chemical assay data; (ii) proxies approach – response of an ore is inferred from small scale 'proxy' tests; and (iii) mineralogical approach – response of an ore is predicted based on mechanistic or empirical models using mineralogy. To apply the mineralogical approach, we should first pose the theory statement as follows: *Mineralogy is the blueprint that encapsulates all the properties of a rock (primary variables), carrying signatures of the ore-forming and subsequent alteration processes. These ultimately define the response to an applied process (response variables).*

Application of the theory statement

To apply our theory statement, we should first describe the mineralogy – this can be done using both the mineral composition triad and mineral texture. The mineral composition triad uses the interrelationship between bulk chemistry, mineral chemistry, and mineral grades (x) defined by Equation 1:

$$b_i = \sum(A_{ij} \times x_j) \qquad \text{Equation 1}$$

Where: b_i is the bulk chemistry of element i; A_{ij} is the proportion of element i in mineral j; and x_j is the grade of mineral j in the bulk. The mineral composition triad underpins the calculation of quantitative element distribution (both valuable and deleterious, e.g., Fig. 1a); provides the means to back calculate elemental assays from measured mineral grades data thus increasing confidence in our analysis (which should be standard use for all auto-SEM-EDS measurements, e.g., Fig. 1b); and is the basis of calculating mineral grades from chemical assay data, also known as element to mineral conversion (EMC; Whiten, 2008). EMC has been used in various geometallurgical studies, and its key advantage is that it provides a methodology to turn abundant chemistry datasets into comprehensive mineralogy datasets (generally, the number of mineralogy datasets is several orders of magnitude lower due to the costly and time-consuming nature of acquiring this data). The widespread availability of certified reference materials for elemental assays in accredited analytical laboratories contributes to a greater level of confidence. Machine learning algorithms using input data from the mineral composition triad are also increasingly being used in geometallurgy to predict mineral grades e.g., Cupido *et al.,* (Submitted).

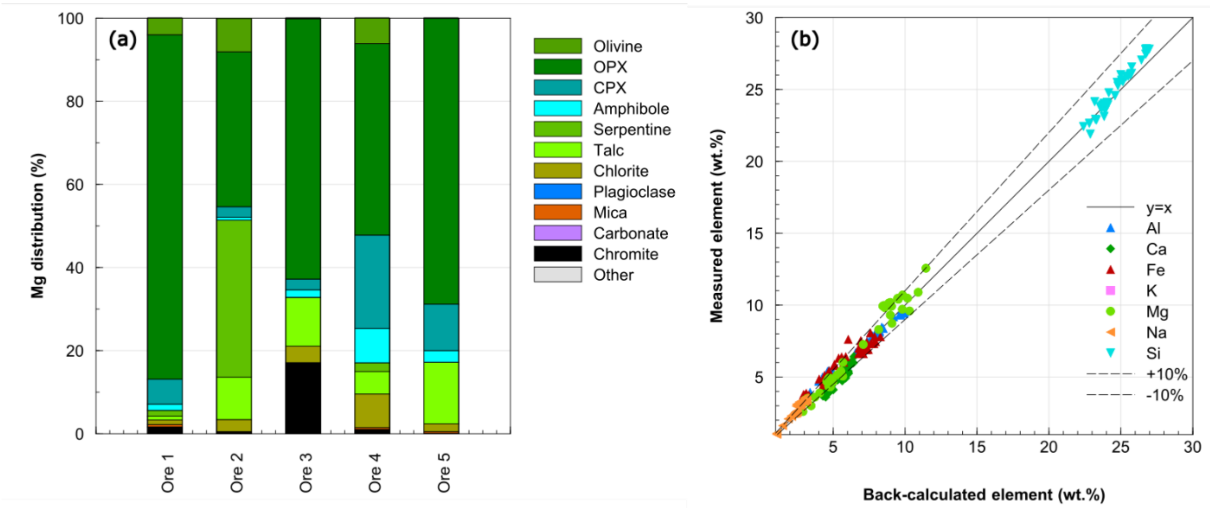

Figure 1: Application of the mineral composition triad to (a) calculate element distribution of Mg in 5 different platinum ores; and (b) compare Auto-SEM-EDS derived back-calculated elemental assays with measured elemental assays to increase confidence in mineralogy data.

Secondly, we can describe mineralogy through mineral texture that defines the interrelationship between mineral grains. For unbroken rocks and particles, one is interested in defining grain size distributions, grain shape distributions, porosity, and mineral association. But we can also describe mineral texture attributes as a consequence of an applied process. For example, defining the liberation after grinding (be it for the bulk sample or discrete size fractions). Measuring quantitative mineral texture information is generally the costliest analysis and is often more readily incorporated into process mineralogical studies.

Inevitably, we also ask if there is a linkage between the mineral composition triad and mineral texture. For example, it has been an inherent rule of thumb on many flotation concentrators that higher grade ores give better recovery, but why is this so? Due to the nature of mineralisation, higher grade ores often have coarser grain size distributions of valuable sulfide minerals, which means they are more likely to be liberated at a coarser grind, creating particles that have a greater potential for flotation recovery. Jameson (2012) showed that equivalent sized particles have a higher flotation rate constant when they are more liberated. Although von der Heyden *et al*., (2024) also presented a relationship between the mineral composition triad and mineral texture for manganese ores, the lack of studies on this topic suggests these relationships may be more readily applicable to high-grade and bulk commodities. Further investigating and articulating the relationship between the mineral composition triad and mineral texture across a range of commodities ranging from precious metals, base metals to bulk commodities through different ore forming processes is an area of study that will deliver valuable heuristics that can be further explored in geometallurgical modelling.

Before we apply our theory statement, we should consider (i) what we should measure and (ii) what happens if we cannot prove our theory statement. In an ideal situation, one would measure every parameter on every sample, but this is not practical. Therefore, the answer to both questions considers both sampling as well as the types of mineralogical measurements. These two questions will be further discussed in the paper, using case study examples, and will conclude by reflecting on the role of mineralogy for 'future-ready' geometallurgy. Having the ability to generate trusted data and using advanced tools, allows for smarter decision-making as geometallurgy enters a new era. Here, data-driven models will find increasing prevalence in characterising the complex and sometimes unconventional ores needed to generate the metals our future society demands.

REFERENCES

Cupido, I., Burness, S., Becker, M. & Nwaila, G. (Submitted) Predictive modelling of lithium mineral grades using data analytics and chemical assay data. *Minerals Engineering*.

Global Mining Guidelines Group (2025) *Introduction to Geometallurgy. White Paper*

Jameson, G. J. (2012) The effect of surface liberation and particle size on flotation rate constants. *Minerals Engineering*, 38, 132-137.

Lishchuk, V., Koch, P. H., Lund, C. & Lamberg, P. (2015) The geometallurgical framework: Malmberget and Mikheevskoya case studies. *Mining Science*, 22, 57-66.

von der Heyden, B., Mathebula, I. P., van Eeden, L., Tadie, M., Louw, T. & Katsumbe, T. (2024) Quantifying chemistry-mineralogy-texture inter-relationships to predict manganese ore comminution response. *Proceedings of MEI Process Mineralogy*. Cape Town.

Walters, S. G. (2008) An overview of new integrated geometallurgical research, *9th International Congress for Applied Mineralogy*. Brisbane: AusIMM, 79-82.

Whiten, B. (2008) Calculation of mineral composition from chemical assays. *Mineral Processing and Extractive Metallurgy Review*, 29, 83-97.

Williams, S. R. & Richardson, J. M. (2004) Geometallurgical mapping: a new approach that reduces technical risk geometallurgical mapping, *Proceedings of the 34th Annual Canadian Mineral Processors Meeting*. Ottawa, Canada.

Megan Becker

Researcher
University of Cape Town

Professor Megan Becker is a researcher at the Centre for Minerals Research within the Department of Chemical Engineering at the University of Cape Town (UCT). She holds degrees in Geological Sciences (UCT) and Metallurgical Engineering (UP). Her research focuses on using mineralogical insights to better understand, optimize, and predict key processes in the mining industry—considering both technical and environmental factors.

To date, she has supervised nearly 50 postgraduate students and published over 100 peer-reviewed papers. Professor Becker is a fellow of the Geological Society of South Africa and a member of the South African Institute for Mining and Metallurgy. She currently serves as the Chairperson of the committee organising of the SAIMM Geometallurgy Conference, and is a member of the technical committee organising the next International Mineral Processing Conference taking place in Cape Town in Sept 2026, as well as a consultant for the Minerals Engineering International Process Mineralogy Conference series

Is it time to rethink gold tailings characterisation using real-time portable and automated technologies?

X.C. Simelane[1], S. Ndlovu[1,2], G.T. Nwaila[1]

[1]University of the Witwatersrand, South Africa
[2]University of Arizona, USA

INTRODUCTION

Sustained gold production over time serves as a testament to the historical significance and enduring legacy of gold mining in South Africa. Estimated to have started in the 1800s, gold mining has been the leading influence on the country's strong economy and sustained Global Domestic Product (Durand, 2012). With this remarkable golden history however, mining activities have left significant marks on the country's landscape; evident in the large number of tailing dumps in Gauteng. The Witwatersrand goldfields have produced approximately 53 000 metric tons of gold and about a third of all gold ever mined historically (Frimmel, 2014; WGC, 2018; Nwaila *et al.*, 2019). The total number of waste dumps generated in Gauteng is estimated to be about 500 tailings dumps (Rensburg, 2016). Tailings are residue material that remain after the processing or extraction of valuable metals and minerals, and the production of mine tailings is ongoing for as long as the primary resources exist (Schoenberger, 2016). Composition of Witwatersrand auriferous primary ores are predominantly known to be associated with sulphide minerals such pyrite, arsenopyrite and chalcopyrite. Legacy tailings contain valuable trace metal and precious metals that were not properly extracted due to ineffective and underdeveloped extraction processes. Particularly in legacy tailings, low technology efficiencies could have been the cause of elevated grades in tailings (Nwaila *et al.*, 2021). This has resulted in a re-emerged view on the circular economy within the industry, shifting waste from being worthless, discarded material to a valuable resource. The current gold market price, low cost of reprocessing and minimum effort in comminution has made reprocessing of tailing economical. The resurgence of interest in gold tailings dumps as a secondary resource further creates a gap for better understanding of the complexities associated with the mining of the Witwatersrand gold tailings. This paper frames a different view on valorisation of tailings dumps by using portable and automated technologies for a more effective strategy of characterising these secondary resources.

Materials and methods

At the Far West Rand (Driefontein), near Carletonville and the East Rand tailing processing project sites, five samples were taken in a 50 m grid spacing. The West Rand region sampling campaign was conducted alongside a 40 metre bore drilling campaign. Both hand grab and borehole drill samples were pulverised, homogenised and once prepared by employing the developed integrated characterisation framework, were analysed using the quantitative X-ray diffraction (QXRD), portable X-ray fluorescence (pXRF) and tescan integrated mineral analysed (TIMA). A total of 99 borehole samples (West Rand) and 10 hand grab samples (West and East Rand) were analysed. Lab based XRF was conducted to determine the degree of error of the XRF analysis, to benchmark and determine any correlations of the results.

RESULTS AND DISCUSSION

The paper developed an integrated characterisation framework that incorporates as shown in in Figure 1a, inclusive of use of technologies such as pXRF, QXRD and TIMA. Portable and automated technologies used in this paper were beneficial in that the result provided a wider spectrum of elements in near real time. This type of comprehensive reporting produced by the pXRF can only be achieved by employing a suite of lab-based technologies i.e., XRF, ICP-MS and Leco technologies; highlighting the advantages of pXRF, i.e., cost saving and efficient turnaround time. The tool identified gold proxies in the Witwatersrand tailings inclusive of Fe (15,68 %), and As (135,33 ppm) associated with arsenian pyrite, Ni (0,026 %) and Co(5.00 ppm) indicative of Ni-Co pyrite phases, and U(34.00 ppm), Mo (15.00 ppm), Cu (288.00 ppm), Zn (4061.00 ppm) and REE (e.g. Ce (10.00 ppm), La (182.00 ppm), Nd (440.50 ppm)) linked to uraniferous zones and heavy mineral bands. Figure 1a. shows a comparative plot of elements detected with pXRF and lab-based XRF (comparing borehole sample D6501 and hand grab sample), and the concentration obtained by both technologies, i.e., for silica concentration that showed 20% variation.

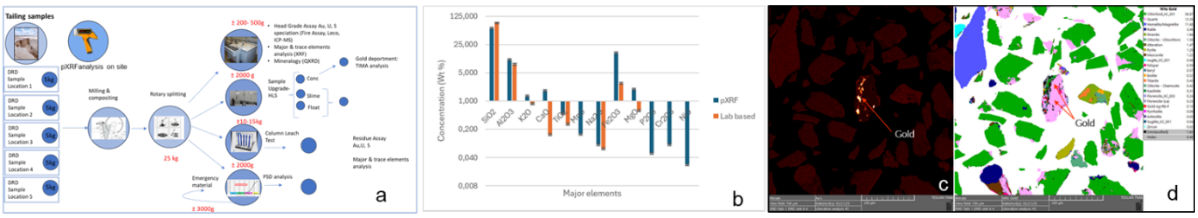

Figure 1: (a) Elemental composition plot of West Rand tailings sample comparing pXRF and lab-based XRF results; (b) BSE images heat maps showing gold grain locations of West Rand concentrate sample; c. False colour images showing mineral phases of the West Rand sample.

Sample preparation had to be included within the hybrid workflow developed for this paper (Figure 1a), to overcome the shortcomings of the effect of water on the results. Pinto, (2018), identified moisture as one of the major sources of error when analysing soil sample with pXRF. QXRD determined a mineralogy synonymous with the Witwatersrand Basin ores, including minerals such as silicates, sulphides with unusual elevation of oxides and hydroxides. The TIMA results corresponded with both techniques by reporting bulk composition of minerals such as quartz (83.62 %), feldspar (6,93 %), chlorite (2.42 %), muscovite (2.31 %), with low concentration of minerals such as hematite (0.21 %), florencite (0.18 %) and zircon (0.02 %). The TIMA analysis confirmed the association of residual gold with silicates (reporting quartz (42.46 %), feldspar 6.77 %) and phosphate mineral phases (florencite (50.72 %), to a lesser extent with refractory pyrite), often below the detection limit of bulk assays, however with recoverable potential under alternative flowsheet design. Dump 5 reported mineral liberation of 59.84 % while dump 3 was 100 % locked. Figure 1b shows the typical locked gold grain and host mineral within the West Rand TSF. These results from research work done on neighbouring TSF (Dump 5) had significant variation to current TSF (Dump 3), indicative of the heterogeneity of the Wits gold tailings (Simelane, 2022). In Dump 5 gold was associated with mineral quartz (24.51 %), florencite (4.89 %), and hematite (4.73 %). These outcomes reveal the potential challenges that will be encountered during processing i.e., encapsulation of gold in dissolution due to the complex mineralogy and geochemistry of the tailings. The proactive identification of the potential challenges during processing will permit and promote the development of a geometallurgical flowsheet to render the ore amenable to processing and ensure efficient gold recoveries. The presence of certain silicates and phyllosilicates are known to be associated with preg-robbing (such muscovite, chlorite etc.) or the absence of copper rich mineral (cyanide consumers) with the tailings (Coetzee, 2011).

CONCLUSION

The complexity and heterogeneity of the Witwatersrand gold tailings call for an independent characterisation of each mined TSF using recently improved automated technologies for further improved gold recovery. The paper reveals and affirms the reliability of these technologies, and their potential use. Our findings suggest that the integration of portable and automated characterisation tools offers not merely an operational upgrade but a conceptual rethinking of how we engage with TSFs as urban mineral systems.

REFERENCE

1. Coetzee, L.L.,Theron, S. J., Martin, G. J., Van Der Merwe, J. D. and Stanek, T. A . 2011. Modern gold deportments and its application to industry. Mineral Engineering 24, pp. 565-575.
2. Durand J.F. (2012). The impact of gold mining on the Witwatersrand on the rivers and karst system of Gauteng and Northwest Province, South Africa. Journal of African Earth Sciences 24-43pp.
3. Frimmel, H.E. (2014). A giant Mesoarchaean crustal gold-enrichment episode: Possible causes and consequences for exploration. Society of Economic Geologist Special Reviews, 180, 148-158.
4. WGC (World Gold Council). (2018) Gold demand and suppy. http://www.gold.org/about-gold. Accessed 20 August 2023.
5. Nwaila, G.T., Ghorbani, Y., Becker M., Frimmel, H.E., Petersen, J., & Zhang, S. (2019). Geometallurgical Approach for Implications of Ore Blending on Cyanide Leaching and Adsorption Behaviour of Witwatersrand Gold Ores, South Africa. Natural Research Resource. http://link.springer.com/article/10.1007/s11053-019-09522-4
6. Schoenberger E. 2016. Environmentally sustainable mining: The case of tailings storage facilities. Resources Policy. 112-128pp
7. Nwaila, G. T., Ghorbani, Y., Zhang, S. E., Frimmel, E., Tolmay, L. C. K., Rose, D. H., Nwaila, P. C., & Bourdeau, J. E. (2021). Valorisation of mine waste– Part 1; Characterisation of, and sampling methodology for, consolidated mineralized tailing by using Witwatersrand gold mine (South Africa) as an example. Journal of Environmental Management, 295.
8. Musingwini, C. (2014). Introduction of specialisation in Mine planning and Optimisation within the Master degree (MSc) program. Sun City, s.n.
9. Simelane, X.C., (2022). Recovery of gold from mine tailing dumps of the Witwatersrand goldfields using cyanide-free reagents. MSc Thesis. University of Johannesburg. Available at: https://ujcontent.uj.ac.za/esploro/outputs/graduate/Recovery-of-gold-from-mine-tailing/9915704207691. Accessed: 06 March 2024.

Xolile Carol Simelane

Postgraduate Student
University of the Witwatersrand

Ms. Simelane is a geoscientist who passionately specializes in economic geology and geometallurgy. She is currently pursuing a PhD degree in Geology at the university of the Witwatersrand. She holds a MSc in geology from the university of Johannesburg and a BSc Hons in geology from the university of KwaZulu-Natal (South Africa). She has extensive work experience in mining geology and geometallurgy within the gold mining industry with ambitions to expand this experience into other commodities (i.e. platinum, coal etc.) within the mining and metals industry. She has a keen interest in economic geology, process engineering, geometallurgy and environmental conservation. Her PhD project focuses on the valorisation of mine waste from the Witwatersrand goldfields using an approach that incorporates predictive geometallurgy and the application of alternative or eco-friendly reagents in gold recovery.

Maximising throughput of ore characterisation by means of automated mineralogy

M. Dosbaba

TESCAN Group, Czech Republic

INTRODUCTION

Automated Mineralogy (AM) is an established technology used in modern mineral processing and metallurgy, enabling high-resolution, quantitative characterisation of ore mineralogy and microtextures. Based on scanning electron microscopy (SEM) with energy-dispersive X-ray spectroscopy (EDS) and image analysis, AM provides data on mineral associations, liberation, and grain size distribution, supporting exploration, process optimisation, and resource modelling.

Despite its robustness, throughput remains a critical challenge, as geometallurgical characterisation typically requires processing a significant number of samples. Efficiency can be improved by adaptive measurement protocols, spectral summing, and software automation for segmentation and phase identification.

Materials and Methods

Samples of REE-bearing apatite ore are used as an example of an ore bearing only small amounts of the target elements which is more challenging from a throughput perspective. Two types of apatite were present with the average difference in the sum of La, Ce, Nd reaching 2.46 wt.%. Experiments with optimisation of AM data acquisition were performed using a TESCAN Integrated Mineral Analyser (TIMA) configured on a MIRA FEG-SEM platform. Data acquisition combined backscattered electron (BSE) imaging and energy-dispersive X-ray spectroscopy (EDS) collected using 25 kV and beam current of 10 nA and various number of counts (10,000; 1,000 and 100 counts per pixel). Various analytical modes with varying numbers of counts per pixel were used (point spectrometry, line mapping and dot mapping [1]). Various BSE acquisition speeds were also tested to provide a means of data quality improvement. Individual measurement points were grouped using a similarity search algorithm, and coherent BSE–EDS data were merged into segments corresponding to mineral grains. Spectra from all points within a segment were summed to allow more straightforward phase identification, and the resulting datasets were compared against a mineral classification scheme.

SUMMARY OF RESULTS

The aim of the study was to establish an optimised analytical workflow yielding maximum throughput on apatite REE ore. Virtually every mineral in the ore can host REEs and contribute to its overall balance. Detailed quantification of both apatite types allows estimation of the total recoverable REE content. Ten thousand counts per pixel delivered highly reliable results even with segmentation turned off (each pixel processed and identified individually). Practical applicability due to extensive duration is limited, however. One thousand counts per pixel is the default value used in TIMA. With these settings the differences between REE-rich and REE-poor apatite grains are too subtle for correct recognition on a pixel-by-pixel basis. With the segmentation turned on it was possible to produce segment spectra (sum spectra) containing a sufficient number of counts. The success rate was dependent on the total number of counts in each segment.

Large homogeneous grains were correctly identified. Boundaries between the two apatite varieties were not correctly identified with the default segmentation settings. The same applies to 100 counts per pixel data. Data over-segmentation introduced by stricter segmentation parameters proved to work as a kind of binning. None of the newly created segments corresponded to actual grain boundaries; however, this approach allowed spectra from a sufficient number of pixels to be summed for correct phase identification.

Both types of apatite grains show slightly different BSE intensity values (0.3% on the 100% scale from black to white). Correct identification would not be possible on the pixel by pixel basis due to the noise in the BSE image. Segmentation, however, reduced the impact of noise in a way similar to extended dwell time. Apatite was used as a model case but the approach can be applicable to other similar phases varying just by minor differences in chemistry such as for example magnetite - hematite.

Apart from the above-mentioned optimisations, there is much more room for improvement, particularly in the choice of analytical mode. Since different modes provide different kinds of information, the choice must always be driven by the purpose of the analysis.

The overall efficiency of the AM has to be judged in the context of the entire geometallurgical characterisation workflow since this technique is rarely used on its own. Other techniques such as laser ablation or electron microprobe can be optimised by more efficient sample navigation (grain coordinate transfer) and also by reducing the number of analytical points based on the AM input. Techniques such as core scanners or computed tomography (CT) can both precede or follow AM analysis. Both are typically used to select the right sampling position for AM. On the other hand, AM data are often fed back into these systems to improve interpretation.

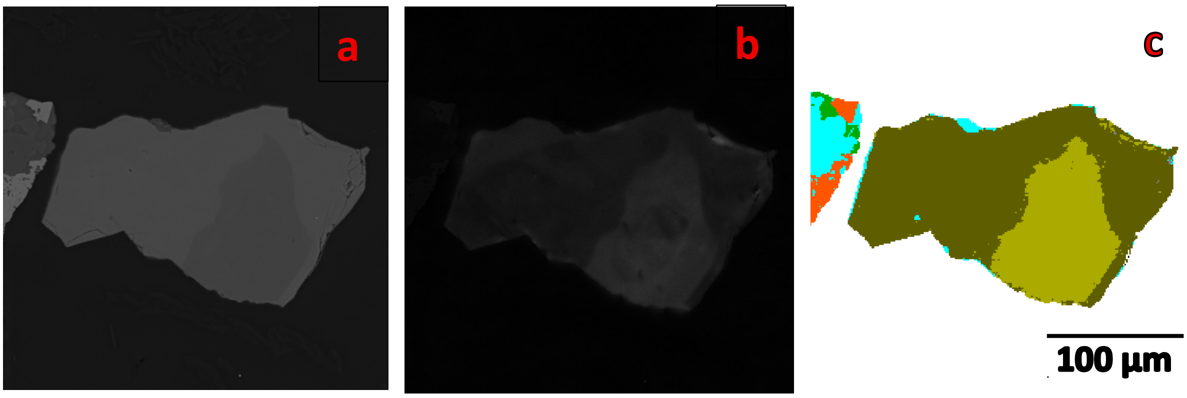

Figure 1: BSE image of apatite particle (a) formed by REE-rich (bright) and REE-poor apatite (dark), apatite particle as imaged by CL detector (b) and corresponding phase map after optimisation (c): REE-rich (dark green), REE-poor (light green), silicates (blue), sulfides (orange), carbonates (grass green).

REFERENCES

[1]Hrstka, T., Gottlieb, P., Skála, R., Breiter, K., Motl, D. (2018). Automated mineralogy and petrology – applications of TESCAN Integrated Mineral Analyzer (TIMA). *Journal of Geosciences*, 63 (1), 47–63. DOI: 10.3190/jgeosci.250.

Marek Dosbaba

Automated mineralogy specialist
TESCAN GROUP, a.s.

Marek Dosbaba has over 20 years of experience in applied geology, mineral characterization, and microanalytical instrumentation. After earning a master's from Masaryk University (Brno, Czech Republic), he held roles in surveying, exploration, and microanalysis, progressing to senior technical and leadership positions in industry. Since 2013, he has worked at TESCAN, where he is Product Marketing Manager for Microanalysis. His focus is on integrating automated mineralogy into analytical workflows, optimizing throughput, and enhancing usability. Marek has contributed to publications and conferences, especially in process mineralogy, rare-metal deposits, and SEM-based analytics. His fieldwork spans Central Asia and the Balkans, and he collaborates closely with R&D and TIMA development teams to align the tool with real-world ore characterization needs.

Communicating uncertainty in geometallurgical models

A. Johnston

Transmin Metallurgical Consultants, Peru

INTRODUCTION

Geometallurgical modelling is entering a new phase in the mining industry, where the limitations of traditional deterministic models are becoming increasingly apparent. While these models strive for the 'best fit' and deliver single-value predictions for each ore block, they often mask the underlying uncertainties inherent to complex ore bodies. This extended abstract demonstrates how effective communication of geometallurgical uncertainty not only enhances technical understanding but is vital for risk management and value generation throughout the mining value chain.

Why Focus on Uncertainty?

Risk is a central concern for mining projects. Other domains, such as medicine and aviation, routinely communicate uncertainty—stating the odds of complications or the frequency of rare events—so that practitioners and stakeholders can make informed decisions. The mining industry already has precedent for this in resource classification (measured, indicated, inferred categories) and capex estimation, but metallurgical predictions still rely heavily on single, 'precise' values. This can mislead stakeholders about the confidence level of predictions, amplify project risk, and result in inappropriate design, investment, and operational choices.

Deterministic vs. Stochastic Approaches

Deterministic models typically deliver a single output for outcomes such as metal recovery; assuming that all inputs are either known or have insignificant variation. These models can provide misleading precision—offering numbers that appear rigorous but ignore the true range of outcomes.

Stochastic simulation methods, by contrast, explicitly generate probability distributions for metallurgical responses and other key outcomes. This probabilistic modelling allows engineers and decision-makers to visualise and quantify the range and likelihood of possible results, moving from the comfort of apparent certainty to more robust risk characterisation.

Case studies and experience indicate that relatively simple models, when paired with well-defined uncertainty bounds, frequently offer greater practical value than highly complex models that hide their assumptions. In highly variable or data-deficient contexts, simple, explainable models with clear confidence intervals are preferable: they are transparent, easier to validate, and less likely to mislead—especially when used for risk-based decision-making.

Practical Communication and Decision Integration

Uncertainty management is not only about the numbers but about how they are communicated and actioned across teams. The pitfalls of geometallurgical modelling—complexity, poor-quality data, or siloed communication—are all 'risk amplifiers.' By contrast, risk can be reduced through:

- Thorough, fit-for-purpose data collection and modelling
- Integrated communication across mining, geology, and processing teams
- Simple, actionable, and transparent model outputs.

Graphical tools such as tornado diagrams, box plots, and heat maps play an essential role in communicating uncertainty visually. Moreover, matching the communication style to the team's sophistication—using box plots and confidence intervals for less experienced teams, and more advanced simulation results for expert groups—improves risk understanding and buy-in.

Clear explanation matters: narrative-first approaches enhance trust and transferability and facilitate troubleshooting when unexpected outcomes arise. Ultimately, the goal is to use models to enable better, more robust decisions—not to chase technical perfection at the cost of transparency.

Case Study Examples
Several operational scenarios illustrate the benefit of this approach:

- 'Calm Waters': For simple, low-variability ore bodies and well-proven plants, minimal geometallurgical modelling is required; simple confidence intervals suffice for planning.

- 'Chaotic Disorder': In highly variable deposits, complexity should be tempered. Rather than attempting to force precision, broad-domain stochastic predictions help communicate a realistic range of risks and frame conservative design choices.

- 'Mapped Drivers': Where mineralogical or metallurgical variability is well understood, targeted data collection and scenario-focused modelling allow for blending strategies and process adjustment plans, reducing both technical and financial risks.

Quantifying and Reducing Risk
The ultimate aim is to improve project outcomes—better mine plans, more realistic forecasts, and smarter capital allocation—by quantifying the probability and impact of uncertainty. For example, if a model yields a copper recovery estimate of 87% ± 5%, and the NPV impact per 1% recovery is USD $100M, the risk envelope associated with model uncertainty is USD $500M. Recognising rather than ignoring this uncertainty compels more robust planning.

Risk reduction comes from both technical steps—better data, fit-for-purpose modelling, and ongoing validation—and cultural shifts toward integrated, transparent risk communication.

RECOMMENDATIONS

- Add confidence intervals or probability ranges to all future metallurgical predictions.

- Prioritise model explainability over spurious precision, and focus technical investigations on understanding and communicating the true drivers of uncertainty.

- Tailor communication tools to audience sophistication and decision context.

- Integrate data and insights across all domains and foster regular dialogue between teams.

- Document and communicate limitations, to prevent overconfidence and misclassification of risk.

CONCLUSION

Uncertainty in geometallurgical modelling is not the core problem; rather, the challenge is in how it is recognised, communicated, and acted upon. The transparent quantification and communication of uncertainty empower better decisions, foster realistic expectations, and promote genuine project robustness—making geometallurgy future-ready, trusted, and aligned with the needs of a dynamic mining industry.

Deportment of gold in historical Witwatersrand tailings: Implications for geometallurgy

S. Chingwaru, B.P. von der Heyden, M.Tadie
Stellenbosch University, South Africa

INTRODUCTION

The Witwatersrand Basin, discovered in 1884, is the world's largest gold-producing region, yielding around 53,000 tons of gold. Despite over a century of mining, the origin of its gold remains debated, with competing models—placer, modified placer, and epigenetic—proposing different metallogenic processes (Frimmel *et al.*, 1993; Robb and Meyer 1995; Tucker *et al.*, 2016). Following the modified placer model, gold and other detrital minerals such as pyrite, uraninite, and oxides likely originated from an Archean granite-greenstone hinterland. Remnant vestiges of these greenstone belts (e.g., Barberton, Kraaipan greenstone belts (Pearton and Viljoen 2017) contain significant 'invisible' or refractory gold within sulfides, notably pyrite, arsenopyrite, and arsenian pyrite. Comparable mineralisation occurs in the Kalgold deposit of the Kraaipan Greenstone Belt, where fine-grained sulfides host micron-scale gold. These analogies imply that many detrital sulfides in the Witwatersrand quartz pebble conglomerates may also contain gold, supported by analyses showing detrital pyrite with gold contents up to 1400 ppm (da Costa *et al.,* 2020).

Historically, standard milling and cyanidation processes in the Witwatersrand achieved about 95% recovery (Vaughan 2004), leaving an estimated 2650 tons of unrecovered gold in tailings. Secondary reprocessing of these dumps operates at only 30–50% efficiency, leaving another 1325–1855 tons unextracted. This inefficiency is likely due to the presence of refractory or 'invisible' gold bound within sulfide minerals, which conventional cyanidation cannot liberate. Better understanding the ultimate deportment of the unextracted gold has implications for its geometallurgy, future value realisation, and environmental stewardship.

Methodology

Duplicates of 150 kg tailings samples were collected from four Witwatersrand Basin goldfields: Evander, Carletonville, Central Rand, and Klerksdorp. After homogenisation, ~1 kg subsamples underwent pre-concentration involving desliming, superpanning, and two-stage heavy liquid separation using tetrabromoethane (2.95 g/cm^3) and lithium metatungstate (2.71 g/cm^3). This produced three density fractions: slimes (< 25 µm), light (< 2.95 g/cm^3), and heavy (> 2.95 g/cm^3). Representative 0.3 g aliquots from each fraction were embedded in epoxy and polished for analysis.

Analytical work included aqua regia digestion and ICP-MS to quantify trace elements (As, Au, Co, Cu, Hg, Ni, Pb, Sb, Se, Zn, U) from duplicates of bulk and density-separated samples, along with blanks, performed at the Central Analytical Facilities (CAF), Stellenbosch University. Petrographic and textural analyses were completed using optical microscopy, SEM, and QEMSCAN (University of Cape Town). QEMSCAN determined mineral abundances in heavy fractions, validating chemical assays and aiding mass balance calculations. False-colour mineral maps were also produced to identify visible gold, potential Au-bearing phases, and candidate grains for laser analysis.

Laser ablation ICP-MS (LA ICP-MS) was performed on 800 oxide (hematite, goethite/limonite, rutile) and sulfide (pyrite, arsenopyrite, galena, sphalerite, chalcopyrite, pentlandite, pyrrhotite) grains from heavy fractions using a 193 nm excimer laser coupled to an Agilent 7700 Q ICP-MS at CAF. This provided in situ trace element concentrations (Co, Ni, Cu, Zn, As, Se, Ag, Sb, Te, Au, Hg, Pb, Bi) within each mineral phase. Resulting data were processed using LADR software from Norris Scientific.

Results and Discussion

Gold deportment in mineralogical and operational fractions

The identification of the principal gold-hosting phases within the Witwatersrand tailings began by assessing which operationally defined size–density fractions contained the highest gold concentrations. Across all four investigated goldfields the heavy mineral fraction consistently hosted the greatest proportion of gold, with aqua regia-determined grades ranging from 0.71 to 10.12 ppm, representing 0.89–13.23% of the total gold mass. In contrast, the light mineral (density < 2.95 g/cm^3; 15–75 µm) and slimes (< 10 µm) fractions exhibited much lower concentrations (0.05–0.22 ppm and 0.17–0.76 ppm, respectively). This preferential gold enrichment in the heavy fraction may reflect either the presence of nano-particulate native gold or chemical association with dense gangue minerals, particularly sulfides and oxides (Goodall 2008; Coetzee *et al.*, 2011; Goodall and Butcher 2012).

QEMSCAN imaging, combined with optical and SEM microscopy, revealed that the heavy mineral fraction is dominated by sulfides (35–76%), followed by silicates (13–44%), oxides (9–20%), and minor carbonates and phosphates (0.01–0.34%). No native or 'free' gold was observed. Pyrite is the predominant sulfide, occurring in distinct textural forms identifiable under microscopy. Guided by QEMSCAN maps, LA ICP-MS analyses quantified gold distribution among mineral phases, confirming that pyrite and arsenian pyrite are the dominant hosts. These two minerals contain approximately 65% of gold in Klerksdorp, 78% in Carletonville, and 85% in Evander samples. Other minerals, including goethite/limonite, hematite, and pyrrhotite, contribute minimally (~1–6% of total gold), with average concentrations of 0.78 ppm, 0.64 ppm, and 0.34 ppm, respectively.

Textural analysis further revealed that rounded pyrite grains—interpreted as detrital due to fluvial transport and sedimentary rounding—host the highest gold contents, with mean spot values of 21.36 ppm and maxima reaching 2700 ppm. These findings highlight detrital pyrite as the key refractory gold carrier in Witwatersrand tailings.

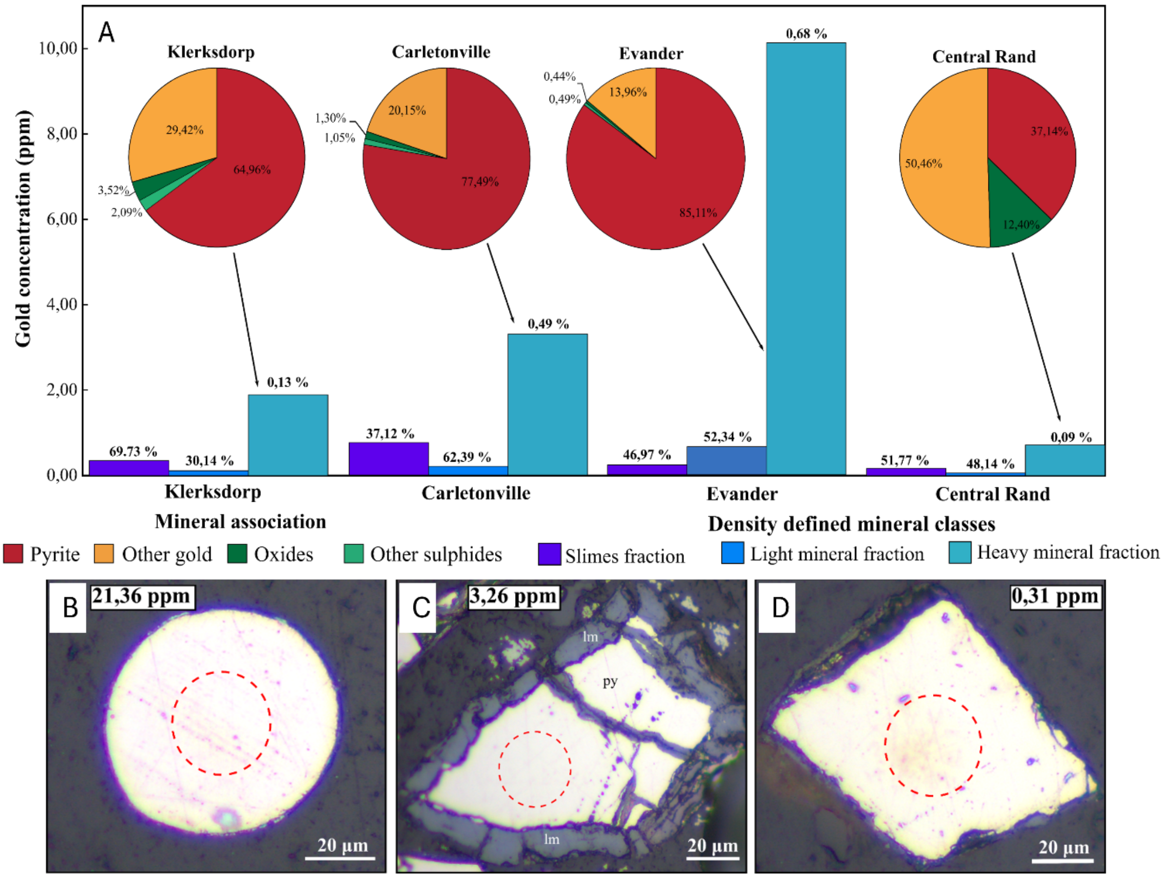

Figure 1 a. Gold distributions summarised per operational definition and per individual mineral phase. b-d. Example spot loci in various pyrite morphological types (b: rounded/detrital pyrite, c: oxide rim pyrite, and d: euhedral pyrite classes respectively). Figures adapted from Chingwaru et al.*, 2023.*

Pyrite chemistry: implications for economic extraction and the environment
The discovery of auriferous sulfides within surface tailings across the Witwatersrand has significant economic and environmental implications. Traditional and secondary mining operations have primarily targeted native gold, neglecting the 'invisible' gold hosted within pyrite, which cannot be recovered through conventional cyanidation (e.g., Coetzee *et al*., 2011). This refractory gold likely contributes to the 50–70% recovery inefficiency of current tailings reprocessing. Economically, auriferous pyrite in tailings presents a low-cost resource: it occurs near the surface and is already finely milled, reducing both comminution and mining costs.

Environmentally, re-mining the sulfide-rich fraction would not only enable recovery of residual gold but also mitigate acid mine drainage by removing sulfide minerals that host most environmentally harmful elements. Mass balance results show that the sulfide fraction contains up to 95% of Zn, Cu, As, and Pb; 55–97% of Ni; 64–99% of Co; 77–99% of Se; and 84–99% of Sb. Moreover, recovery of valuable by-products—Co (~9755 ppm), Cu (~8771 ppm), and Ni (~9822 ppm)—could further enhance the economic viability of reprocessing these tailings.

CONCLUSIONS

The results of this study indicate that the proportion of gold remaining inaccessible to conventional processing technologies within the Witwatersrand tailings is largely attributable to the presence of 'invisible' gold, predominantly hosted within arsenian pyrite and pyrite. Rounded detrital pyrite grains preserved within the tailings material display the highest gold concentrations, with maximum values comparable to those of auriferous pyrite from known granite–greenstone belt deposits. These residual sulfides within the tailings therefore represent a substantial, yet under-exploited, economic resource, estimated at up to 420 tons of gold. Implementation of appropriate pre-treatment beneficiation techniques could enhance overall gold recovery by approximately 22% during secondary reprocessing. In addition to improving metal recovery, the selective re-mining of the sulfide fraction would mitigate the impacts of acid mine drainage and reduce effluent contamination by deleterious elements in the Witwatersrand mining district, while enabling recovery of valuable by-product metals of growing economic importance.

REFERENCES

Chingwaru, S.J., Von der Heyden, B. and Tadie, M., 2023. An underexploited invisible gold resource in the Archean sulphides of the Witwatersrand tailings dumps. Scientific Reports, 13(1), p.3086.

Coetzee, L.L., Theron, S.J., Martin, G.J., Merwe, J.D. Van Der & Stanek, T.A. 2011. Modern gold deportments and its application to industry. Minerals Engineering. 24(6):565–575.

da Costa, G., Hofmann, A. & Agangi, A. 2020. A revised classification scheme of pyrite in the Witwatersrand Basin and application to placer gold deposits. Earth-Science Reviews. 201.

Frimmel, H.E., Le Roex, A.P., Knight, J. & Minter, W.E.L. 1993. A case study of the postdepositional alteration of the Witwatersrand Basal reef gold placer. Economic Geology 88(2):249–265.

Goodall, W.R. 2008. Characterisation of mineralogy and gold deportment for complex tailings deposits using QEMSCAN®. Minerals Engineering. 21(6):518–523.

Goodall, W.R. & Butcher, A.R. 2012. The use of QEMSCAN in practical gold deportment studies. In Vol. 121 Transactions of the Institutions of Mining and Metallurgy, Section C: Mineral Processing and Extractive Metallurgy. 199–204.

Pearton, T. & Viljoen, M. 2017. Gold on the Kaapvaal Craton, outside the Witwatersrand Basin, South Africa. South African Journal of Geology. 120:101–132.

Robb, L.J. & Meyer, F.M. 1995. The Witwatersrand Basin, South Africa: Geological framework and mineralization processes. Ore Geology Reviews 10(2):67–94.

Tucker, R.F., Viljoen, R.P. & Viljoen, M.J. 2016. A Review of the Witwatersrand Basin - The World's Greatest Goldfield. Episodes. 39(2):105–133.

Vaughan, J.P. 2004. The process mineralogy of gold: The classification of ore types. JOM: The Journal of The Minerals, Metals & Materials Society (TMS). 56(7):46–48.

Bjorn von der Heyden

Associate Professor: Economic Geology
Stellenbosch University

Dr Bjorn von der Heyden completed his Ph.D. in geology at Stellenbosch University in 2013 and subsequently spent two years working as a geologist in the South African minerals sector for Exxaro Resources Ltd. He gained excellent exposures and experiences at Arnot underground coal mine, Grootegeluk open cast coal mine, the Research and Development Unit (Mineralogy section), and the Mayoko iron ore exploration project in the Republic of Congo.

In 2015, he returned to academia appointed as a lecturer in Economic Geology at Stellenbosch University (SU). He has worked on a number of research projects, both nationally and internationally (Namibia, Malawi, Tanzania), and has published on a wide variety of ore commodities including gold, diamonds, copper, cobalt, zinc, manganese, iron, and lithium-bearing pegmatites. He has developed fluid-inclusion microthermometry capabilities and hyperspectral core scanning facilities, bth currently housed at the Department of Earth Sciences at Stellenbosch University.

In 2020 he was promoted to Senior Lecturer, and then in 2025 to Associate Professor in Economic Geology. Dr von der Heyden was elected as a fellow of the Society of Economic Geologists in 2021 and starting from 2022 he fulfilled a position of co-Chair for the African Rainbow Minerals Chair in Geometallurgy. In this role, he places equal emphasis on generating and publishing exciting new science, and on providing high-quality education to the next generation of African earth scientists and geometallurgists.

His research interests include understanding the processes of ore mineralisation in hydrothermal, magmatic and chemical sedimentary sub-classes, and modelling the detailed geometallurgical characterisation of these deposits to facilitate enhanced efficiencies in downstream mining and processing of ore bodies. Bjorn has published 44 peer-reviewed research articles and will have graduated 55 post-graduate research students at the end of 2025. Many of these students have received national and international awards and recognition for their research endeavours. He sits on a number of committees and conference organising panels and has received several accolades for his efforts in teaching and learning.

Upgrading of low-grade manganese ores by hydrogen-rich reduction for the ferroalloy industry

D.A. Barrett[1], M. Tadie[1], B.P. von der Heyden[1], R. Cromarty[2]

[1]Stellenbosch University, South Africa
[2]University of Pretoria, South Africa

BACKGROUND

Manganese is a key global resource used in the steel industry for ferroalloy production. South Africa has the world's largest manganese reserve, found in the Kalahari Manganese Field. Fines (D_{50} = 193 µm) from the Nchwaning mine, previously considered subeconomic, contain recoverable manganese but are penalised by elevated and complex iron content. The material contains 44 wt. % Mn and has a Mn/Fe ratio of 2.6 (wt. %/wt. %). To be used as high-quality ferroalloy feedstock, iron needs to be separated and removed to achieve a target grade of 44 wt. % Mn and a Mn/Fe ratio of 7.5 (Elliot and Barati, 2020). Therefore, the manganese content is acceptable, but the iron content poses the primary challenge. There is a high degree of mineralogical variability found in the fines. Iron is present both as discrete hematite and in solid solution in manganese minerals such as bixbyite, braunite, and braunite II.

The mineralogical distribution influences process response during beneficiation. The solid solution of Fe in Mn minerals, in particular, complicates separation, as it has been shown to lead to the formation of mixed (Mn, Fe)O phases during conventional carbothermic roasting (Matabadal, 2022). Addressing this required an integrated approach by way of process mineralogy and metallurgy to develop a process that could separate the iron, regardless of its host phase. This study employed reductive roasting in a hydrogen-rich atmosphere, followed by magnetic separation. Hydrogen can have a low carbon footprint and is sufficiently reducing to produce metallic iron that can be separated magnetically. Lime and silica additives were investigated to determine their influence on Fe reduction kinetics and globule formation, which impacts the separability of Fe and Mn.

EXPERIMENTAL PROCEDURE

The process followed in this research is summarised in Figure 1.

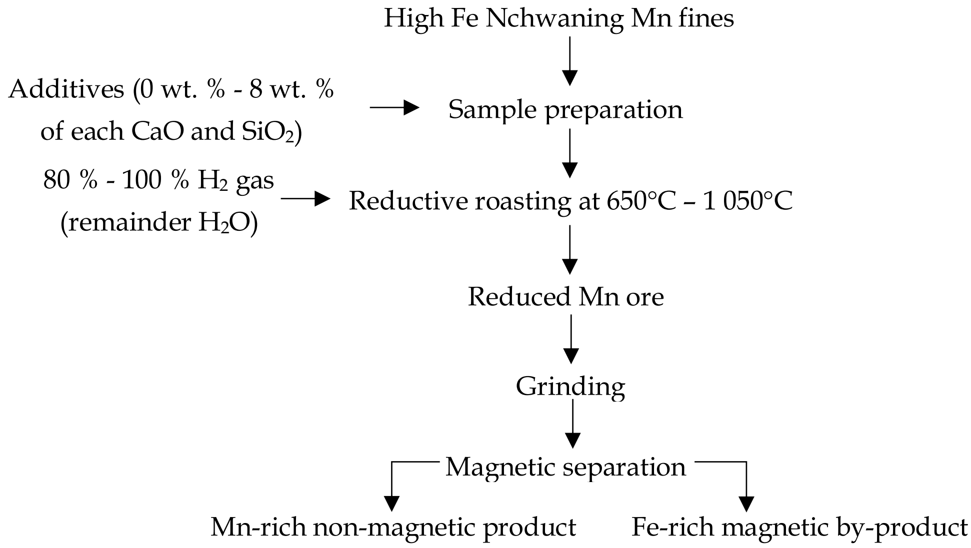

A central composite design was employed in laboratory-scale experiments to optimise key response variables such as Mn grade, Mn/Fe ratio, and Mn recovery while minimising the number of experimental runs (Montgomery, 2013). A triplicate of the centre point runs was performed to ensure the repeatability of the testwork. The fines were pressed into briquettes before undergoing isothermal reduction in a controlled atmosphere retort for two hours. Following reduction, the briquettes were crushed to liberate the metallic Fe with the crushed material having a D_{50} of 43.7 µm. The sample was then separated into a magnetic and non-magnetic fraction using a Davis tube. The reduced pellets were mounted, then analysed using scanning electron microscopy (SEM), while the magnetic and non-magnetic fractions were characterised using X-ray fluorescence (XRF) and statistical analysis performed using Statistica. The range of reducing conditions was chosen so that the Fe oxides present in the starting material would be reduced to metallic Fe. The formation of metallic Fe was verified using SEM.

RESULTS

The results of the XRF analysis of the magnetic and non-magnetic fractions were used to calculate the Mn/Fe ratio, Mn grade and Mn recovery to the non-magnetic stream. The highest Mn/Fe ratio achieved was 4.52 for an experimental run where all operating conditions were at their low level. This test run also resulted in a Mn grade of 57.4 wt. % and an 85.5 wt. % recovery of Mn.

Statistical analysis was used to isolate the influence of each factor on the response variables. Second-order models were regressed for each response using response surface methodology. The models yielded R^2 values of 0.89, 0.91, and 0.92 for the Mn/Fe ratio, Mn grade, and Mn recovery, respectively. Therefore, the model provides a good fit for the responses of the experimental factors. Temperature was found to yield lower Mn/Fe ratios as it increased. A similar response in Mn/Fe was observed for variations in H_2 enrichment, indicating that stronger reducing conditions result in a lower Mn/Fe ratio. This behaviour is better understood when considered alongside microscopy. The SiO_2 dosage had a substantial influence on the Mn grade, with higher dosages resulting in a lower grade. This behaviour is not a result of SiO_2 influencing reduction but rather due to minimal silica reporting to the magnetic stream and therefore diluting the Mn content of the non-magnetic fraction.

Optical microscopy and SEM analysis of the reduced material revealed distinct metallurgical behaviour between metallic iron formed from hematite—forming larger globules (50-600 µm)—and iron reduced from Mn-hosted phases, forming smaller Fe flecks (0.1–2 µm). The hematite is found to be fully reduced at reduction temperatures of 750°C and higher (agrees with observations made by Sarkar, 2024).

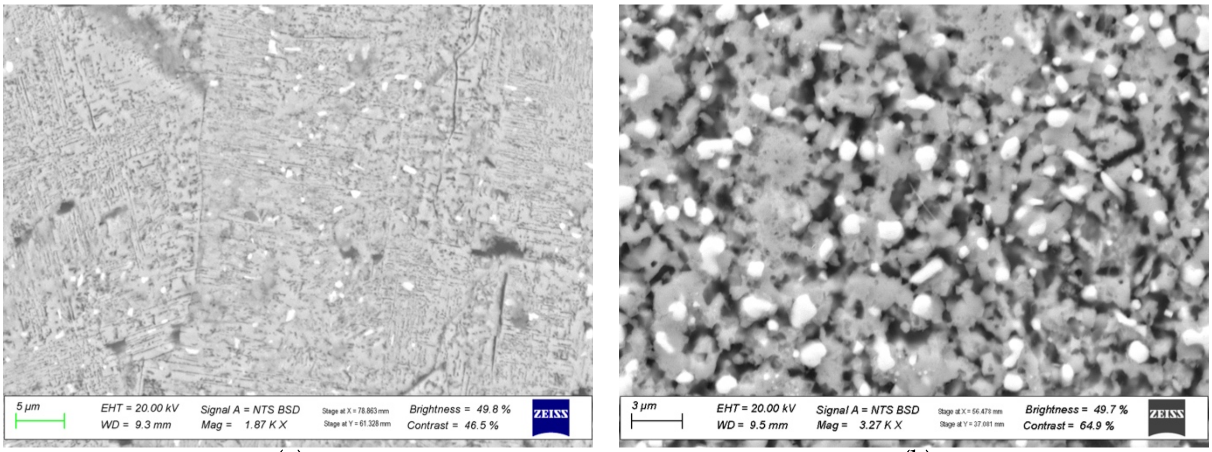

(a) (b)

Figure 2: Backscattered electron SEM images of Fe globules in manganosite (ex-bixbyite) reduced at: (a) 750 ℃ in 85 vol. % H_2, (b) 850 ℃ in 90 % vol. % H_2.

Two reduced samples with contrasting reducing conditions are shown in Figure 2. The best separation between Mn and Fe was found in tests with milder reducing conditions (750°C or 850°C with low H_2). At these weaker conditions, the hematite was fully reduced and likely well liberated once crushed to be separated magnetically. While the Fe present in the Mn-hosted phases has not yet been fully reduced, with only small flecks being formed, if any, as seen in Figure 2 (a), with most of the Fe in solid solution. At stronger reducing conditions (≥ 850°C and ≥ 85% H_2), the Fe flecks formed are three times larger by area and contain purer Fe (as seen in Figure 2 (b)) which makes them more magnetically susceptible. However, these flecks are still too small to be well liberated after crushing so will cause some Mn associated with these flecks to report to the magnetic stream, resulting in a lower Mn/Fe ratio in the non-magnetics. The area, size, and Fe content of the flecks shown in Figure 2 are compared in Table 1.

Table 1: Comparison between Fe flecks formed at different reducing conditions

Reducing conditions	Median fleck area (μm^2)	Median fleck ferret diameter (µm)	Iron content of flecks
750°C; 85% H_2	0.099	0.571	± 50 wt. %
850°C; 90% H_2	0.313	0.82	> 80 wt. %

CONCLUSIONS

Hydrogen-rich reduction of Nchwaning tailings was investigated under isothermal conditions from 650°C to 1 050°C at a fixed reduction time of 2 h. CaO and SiO_2 additives were not found to have a significant influence on the reduction behaviour; however, both additives diluted the non-magnetic product stream, decreasing the Mn grade and the Mn/Fe ratio. Mild reducing conditions maximised the Mn/Fe ratio due to a combination of two key factors. Firstly, the atmosphere was sufficiently reduced pure hematite grains into metallic Fe, which reported to the magnetic stream. Secondly, the conditions were not strongly reducing enough to reduce Fe oxides present in solid solution with Mn-bearing minerals. This prevented the formation of dispersed metallic Fe globules within the Mn-rich phases, thereby reducing the likelihood of Mn reporting incorrectly to the magnetic stream.

The investigated process upgrades the tailings to 57 wt. %,which is well beyond the 44 wt. % Mn target; however, it falls short of the Mn/Fe target of 7.5, with a maximum Mn/Fe ratio of 4.52 achieved. However, the Mn grade is high enough that the target specifications can be met by blending the product stream with other low-grade ores that lack Mn but also contain minimal Fe.

This approach provides a mineralogy-informed carbon-friendly beneficiation route that improves tailings recovery and supports the full orebody utilisation. Ferruginous manganese ores of various ore types can be upgraded using the investigated process then blended with carbonate-rich Mn ores to deliver a metallurgical-grade Mn ore for ferroalloy production. The process can form part of a larger geometallurgical solution to beneficiate parts of the orebody that are identified to have low Mn/Fe.

Recommended future work includes investigating the grind size of reduced material and the magnetic intensity used in the magnetic separation step. The addition of CaO and SiO_2 can be excluded in any future work, as this hinders the upgrading process.

REFERENCES

Eilliot, R. and Barati, M. (2020). A review of the beneficiation of low-grade manganese ores by magnetic separation. *Canadian Metallurgical Quarterly*, 22 (1), 1-16.

Matabadal, Y. (2022). Evaluation of the Reduction Roast-Magnetic Separation Process to Upgrade Low-Grade Ferruginous Manganese Ore Fines. *MEng*. University of Pretoria, South Africa.

Sarkar, A., Schanche, T. L., Wallin, M., and Safarian J. (2024). Evaluating the Reaction Kinetics on the H_2 Reduction of a Manganese Ore at Elevated Temperatures. *Journal of Sustainable Metallurgy. 10(4), 2085-2103*

Montgomery, D.C. (2013). *Design and Analysis of Experiments*, 8th edition, John Wiley & Sons.

Daniel Anthony Barrett

MEng (Chem) Candidate
Stellenbosch University

Daniel Barrett is currently pursuing a master's degree in chemical engineering, specialising in pyrometallurgy and extractive metallurgy. He graduated with a bachelor's degree in chemical engineering from Stellenbosch University in 2023, where he was awarded the SAiChE Silver Medal for best final-year student in the Department of Chemical Engineering. Daniel's ongoing project focuses on the green beneficiation of ferruginous manganese tailings from the Kalahari Manganese deposit.

Hydrometallurgical pretreatments for the enhancement of magnetic separation of ferruginous manganese tailings

E. Olivier, M. Tadie, B.P. von der Heyden, P. van Wyk

Stellenbosch University, South Africa

INTRODUCTION

While local hydrothermal alteration has significantly enriched regions of the Kalahari Manganese Deposit (KMD) in manganese (Mn), it has also enriched the iron (Fe) concentration, resulting in ore that cannot be used to produce ferromanganese due to a low Mn/Fe ratio (< 3). The high-iron material associated with the alteration can be blended with the low-Mn and low-Fe sedimentary ore from unaltered zones to achieve the desired Mn/Fe ratio of 7.5 (Olsen *et al.,* 2007), but this may result in inadequate manganese grade (<44%, (Olsen *et al.,* 2007)) for smelting. Hence, material with low Mn/Fe is often categorised as waste rock during geological modelling of orebodies despite Mn grades above 44%, resulting in significant manganese tonnages remaining unmined. While the Mn/Fe ratio can be improved using magnetic separation, the overlap between the magnetic susceptibilities of iron and manganese-bearing minerals unique to the KMD presents a challenge Roasting to liberate iron from hematite is often recommended as a pretreatment step, though this is associated with carbon emissions and high energy. Thus, further research on alternative beneficiation methods such as hydrometallurgy is beneficial to potentially unlock value from this deposit by redefining the ferruginous material as ore requiring upgrading and not simply waste.

This study aims to adopt a mineralogical approach comparing two hydrometallurgy-based pretreatment methods for enhancing the magnetic separation of ferruginous manganese tailings and to suggest a flowsheet for effective resource utilisation that minimises waste. The first method, proposed by Singh & Biswas (2017) for the beneficiation of pyrolusite-hematite rich ore, utilises a two-stage process using oxalic acid to selectively leach iron and form humboldtine (FeC2O4•2H2O) on the surface of iron-bearing minerals in the first stage, followed by roasting to convert the humboldtine to highly ferromagnetic magnetite (Fe_3O_4). The second method, proposed by Zhou et al (2023) for the iron removal from high-iron red mud, involves the reaction of tailings in an alkaline medium containing ferrous (Fe^{2+}) ions that attach to trivalent iron oxides at the particle surfaces to form magnetite directly. The preferential formation of magnetite on iron mineral surfaces allows for magnetic separation at a lower field strength, thus reducing the loss of manganese to the magnetic fraction.

Methods and materials

Ferruginous tailings samples were obtained from N'Cwhaning II mine in the KMD. The bulk rock chemistry and mineralogy were investigated using X-ray Fluorescence (XRF) and Diffraction (XRD). Bench-scale aqueous experiments were performed on the tailings, and the solid residues from the treatments were filtered and dried overnight in the case of samples that underwent alkaline treatment or roasted in a muffle furnace for 4 hours at 350°C for samples that underwent treatment in oxalic acid. During scoping experiments, the treatments from literature were applied using the optimum conditions reported by the respective authors. Alkali treatment was performed for 10 minutes at 80°C in 0.2M oxalic acid with 6mM FeSO4·7H2O and a solid to liquid ratio (S:L) of 200g/L. Acidic treatment was performed for 2 hours at 90°C in 0.5M oxalic acid S:L of 100g/L. Treated samples then underwent dry magnetic separation via the Franz Isodynamic Separator (Model L-1).

Note, recovery to magnetics was defined as the percentage of the feed material to the separation unit that reported to the magnetic fraction on a mass basis and that the current supplied to the separator is recorded instead of a fixed magnetic field strength as the field strength varied over the length of the Frantz separator. The solid products were then digested in aqua regia to allow for chemical analysis via ICP-OES to determine their Mn/Fe ratio. Following the scoping experiments, key process parameters were identified, and further experiments were performed using a 3-factor 2-level central composite design (CCD) to determine the relationship between the selected parameters and magnetic separation efficacy, with parameters as described in the table below.

Table 1: Parameters for CCD experiments for acid (top) and base (bottom) treatment

Acid treatment					
Parameter	-α	-1	0	+1	+α
Temperature (°C)	70	75	83	90	95
Duration (minutes)	70	90	120	150	170
Oxalic acid concentration (M)	0.08	0.25	0.50	0.75	0.92
Base treatment					
Parameter	-α	-1	0	+1	+α
Temperature (°C)	72	75	80	85	88
Duration (minutes)	2	5	10	15	18
$FeSO_4$ concentration (mM)	3	4	6	8	9

RESULTS AND DISCUSSION

The tailings had a high manganese content of 44.5 wt.% but an average Mn/Fe ratio of 2.6, with the manganese predominantly being present as trivalent manganese in braunite (61.1 wt.%) and manganite (7.9 wt.%), while the iron presented mainly as hematite (23.2 wt.%). As such, blending the tailings with lower-grade ore to improve the Mn/Fe ratio would result in inadequate Mn grade. Using the average chemical composition per mineral reported by Chetty (2008), the iron deportment was estimated as ~90% being present as hematite, with the remainder being present as substitutional impurities in the manganese minerals. Ultimately, selective removal of hematite could theoretically be utilised to improve the overall Mn/Fe ratio. However, the effectiveness of magnetic separation of hematite and braunite is limited by the high overlap in magnetic susceptibility between the two mineral forms. In dry magnetic separation experiments from literature, braunite was noted as a significant limitation due to its paramagnetic nature (Peterson *et al*., 2023). Correspondingly, the range of magnetic field strength settings that maximises hematite recovery to the magnetic fraction (0.025-0.5A) overlaps completely with that of braunite (0.025-0.5A), as reported by Rosenblum and Brownfields (2000). Figure 1 shows the magnetic recovery vs current supplied to the Franz separator for acid and alkaline-treated and untreated samples.

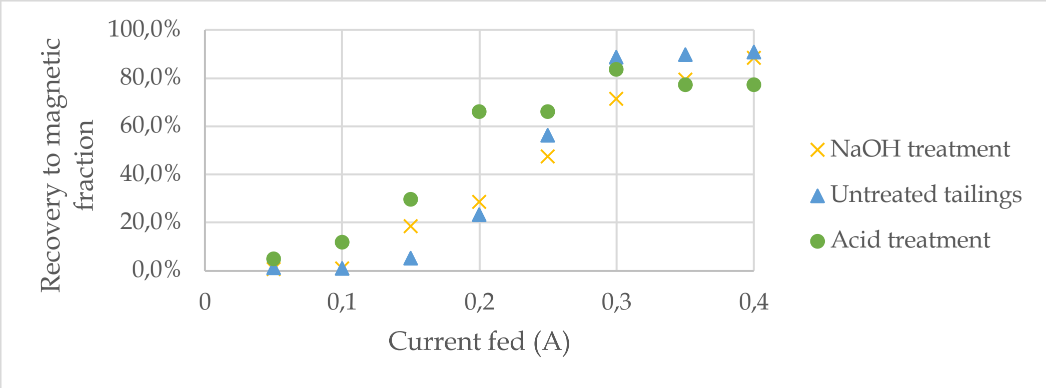

Figure 1: Recovery to magnetic stream vs current to Frantz separator for treated and untreated samples.

The acid-treated samples showed higher recovery at lower current settings compared to the untreated material, suggesting that highly magnetic material had been formed, as reported in literature (Singh and Biswas, 2017). However, the fraction that was not magnetic at >0.3A increased after treatment. This may be due to liberation of silica from braunite, as quartz would be non-magnetic at field strengths lower than 1.7A (Rosenblum and Brownfield, 2000). Ultimately, the acid scoping experiments achieved a maximum Mn/Fe ratio of 3.35 at a Mn grade of ~48% which was improved to 3.65 Mn/Fe at ~50%Mn in CCD experiments. Similarly, the NaOH-treated samples showed higher recovery at current settings lower than 0.25A, suggesting the partial conversion of hematite to magnetite, with the presence of magnetite being confirmed via XRD analysis. Despite the successful formation of magnetite, the treatment did not achieve the desired increase in Mn/Fe in the non-magnetic fraction as it only achieved a maximum Mn/Fe in of 2.74. However,

Multivariate regression was used to relate the recovery of material to the magnetic fraction to the variables that were selected for the CCD (Table 1 and 2). For oxalic acid treatment, concentration of oxalic acid proved a significant (P=0.002) predictor of the overall recovery to magnetics, while the significance of temperature and reaction time could not be concluded. Similarly, the concentration of Fe^{2+} appeared to have the largest effect on magnetic recovery. Both CCDs showed a positive relationship between reagent concentration and overall recovery to the magnetic fraction, suggesting that more iron-bearing particles could be magnetised at higher reagent concentrations. This may be due to the manganese minerals interacting with reagent resulting in lower availability of aqueous species to react with the hematite. Thus, the concentration parameters for both treatment methods must be scaled with respect to variability in manganese and iron mineralogy and not solely on iron content from chemical assays. The manganese deportation to each valence state (2+, 3+, and 4+) in manganese oxides must be assessed via mineralogical assay to estimate the amount of additional reagent that is needed to compensate for the interaction between solid Mn and aqueous species, with divalent and trivalent manganese minerals (hausmannite, bixbyite, and braunite). These minerals require significantly higher reagent concentrations when compared to the relatively inert tetravalent manganese oxide, pyrolusite.

CONCLUSIONS

Both pretreatments showed some promise in increasing the magnetic susceptibility of iron minerals in ferruginous manganese tailings. The lower iron concentration, in turn, allows for more freedom to blend the tailings with other ore types to achieve the desired Mn/Fe ratio for smelting. However, the unique mineralogy of the KMD necessitates tailoring the processes to the deposit. The presence of trivalent manganese cations results in significant interaction between the manganese minerals and the chemical reagents, resulting in increased reagent consumption and further process implications. In the case of the acid treatment, the lower valence resulted in significant manganese co-leaching, which limited the use of leaching as a method of selective iron removal. During base treatment, unliberated hematite limited the effectiveness of the treatment despite successful magnetite conversion. As such, both beneficiation processes have the potential to unlock low grade domains with high Mn/Fe ratios, yet their effectiveness is limited by mineralogy and texture. This highlights the necessity of understanding the geology of natural deposits when applying metallurgical processes.

REFERENCES

Cairncross, B. and Beukes, N.J. (2013). *The Kalahari Manganese Field*, Random House Struik Publishers, Cape Town.

Chetty, D. (2008). A geometallurgical evaluation of the ores of the northern Kalahari Manganese Deposit, South Africa. *PhD Thesis*, University of Johannesburg, Johannesburg.

Olsen, S.E., Tangstad, M., Lindstad, T. (2007). *Production of Manganese Ferroalloys*. Tapir Academic Press, Trondheim.

Peterson, M.J., Karadkal, R., Nunna, V., Hapugoda, S., Austin, P. (2023). Demonstration of dry magnetic separation to upgrade the Mn:Fe ratio of a ferromanganese ore sample. *Mineral Processing and Extractive Metallurgy* 132, 156–171.

Rosenblum, S., Brownfield, I. (2000). Magnetic susceptibilities of minerals. Open-File Report 99-259. US Department of the Interior, Denver, CO.

Singh, V., Biswas, A. (2017) Physicochemical processing of low grade ferruginous manganese ores. *International Journal of Mineral Processing* 158, 35–44.

Zhou, X., Liu, G., Qi, T., Zhao, J., Peng, Z., Wang, Y., Shen, L. (2023). Increasing Iron Recovery from High-Iron Red Mud by Surface Magnetization. *Journal of Sustainable Metallurgy*, 9, 795–805.

Edwin Olivier

Postgraduate Student (M.Eng Chemical)
Stellenbosch University

Edwin Olivier is currently pursuing a Master's Degree in Chemical Engineering, specialising in Hydrometallurgy and Extractive Metallurgy. He graduated with a Bachelor's Degree in Chemical Engineering from Stellenbosch University in 2023, where he was awarded the SAIMM prize for best mineral processing student in his third year. His master's project focuses on comparing two innovative hydrometallurgical methods to enhance the magnetic separability of iron from ferruginous tailings of the Kalahari Manganese deposit. His research seeks to unlock additional value from manganese deposits and enable more efficient utilisation of ore bodies.

Geometallurgy in the Kalahari Copper Belt, Ngami district Botswana

J. K. Mangwiro[1], A. Bayani[2], K. Kgotlele[2], R. Situmorang[2], G. Mosanga[2], M. Babusi[2]

[1]Fluor, South Africa
[2]MMG Khoemacau, Botswana

INTRODUCTION

The Zone 5 deposit, located in the Kalahari Copperbelt, was developed as the primary feed source for the Boseto processing plant. Metallurgical testwork, including mineralogical characterisation, comminution testing, and flotation, was undertaken to support the plant expansion from 3.0 to 3.65 Mtpa. The deposit hosts variable copper sulfide mineralogy dominated by bornite, chalcopyrite and chalcocite, with minor deleterious arsenic and antimony minerals. Bond Ball Work Index (BBWi) correlated strongly with the alteration index (Alti = %Ca/(%Si+%Ca+%Al)), by linking ore hardness to gangue mineralogy. High quartz content was associated with elevated BBWi and reduced sulfide liberation, whereas calcite-rich ores displayed lower BBWi and improved flotation response. Recovery algorithms were developed using Cu:S ratios and validated against plant performance, giving average copper and silver recoveries of 87.5% and 84% respectively, with prediction accuracy within ±5%. The study highlights the value of integrating mineralogy and comminution parameters into geometallurgical models for reliable recovery forecasting in the Kalahari Copperbelt.

The mineralogy of the 46 selected samples from Zone 5 varied widely in bornite, chalcopyrite and chalcocite contents with average depicted in Figure 1. The orebody also contains arsenic and antimony bearing tennantite/enargite and tetrahedrite respectively. Minor galena, sphalerite, molybdenite, arsenopyrite and silver were also observed. The main gangue minerals are calcite and silicate minerals, primarily quartz, feldspars, muscovite and chlorite.

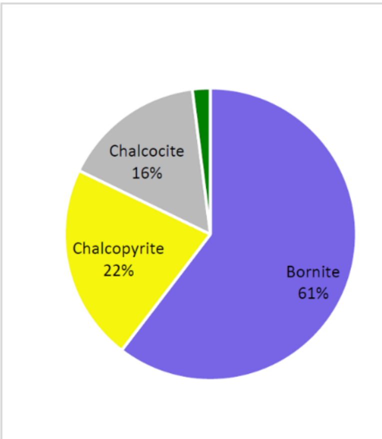

Figure 1: Average sulfide mineralogy of Zone5.

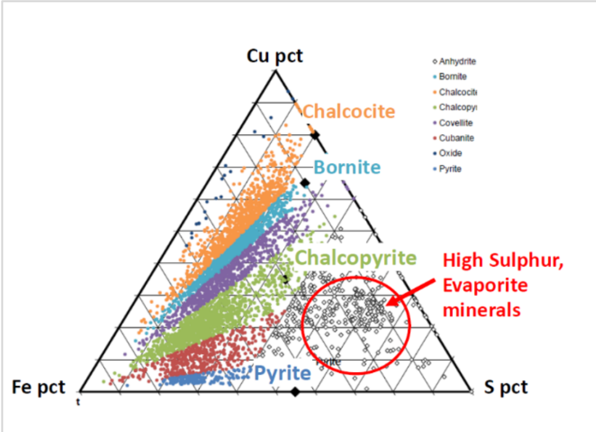

Figure 2: Zone 5 ternary diagram (Credit Suisse, 2023).

The evaluation of the deposit was conducted by developing recovery and concentrate algorithms using sulfide mineralogy (Credit Suisse, 2023; Mangwiro, 2018, 2020). A multiple linear regression analysis was used to develop the correlation between the copper recovery and sulfide mineralogy based on Cu:S ratios and 46 flotation testwork results. The recovery equations were extended to the resource model by correlating copper recovery to the dominant sulfide mineralogy as determined by the molar copper to sulfur ratio shown in *Table 1* and confirmed using the copper sulfide minerals domains in the Cu, Fe, S ternary diagram in Figure 2. The recovery values were discounted by the proportion of oxide when the acid soluble copper to total copper content (AsCu/TCu) was greater than 10%.

Table 1: Metallurgical Recoveries for Cu and Ag based on Predominant Mineral Domain (Mangwiro, 2020).

Cu:S Ratio Range	Dominant Mineralogy	Copper Recovery Formula (2020)	Silver Recovery (2020)
0.01 – 0.75	Chalcopyrite	86.12 + 0.56 × %Cu	83.3%
0.75 – 1.5	Bornite	86.42 + 0.56 × %Cu	83.1%
1.5 – 99	Chalcocite	88.85 + 0.56 × %Cu	87.1%

*where %Cu in the recovery formulas is the TCu

Table 2: concentrate recovery equations

Cu:S ratio		Copper concentrate grade formula (2020)
From	To	
0.1	1	(49.0 * Cu:S) - (5.2 * %Cu)
1	2	(23.0 * Cu:S) + (4.8 * %Cu)

*where %Cu in the recovery formulas is the TCu

Silver recovery followed the Cu:S domains as it hosted within the copper sulfides. The recoveries were estimated initially using a global Cu recovery of 85% and Ag recovery of 79% across the sulfide portion of the deposit before the metallurgical testwork (Credit Suisse, 2023). The resulting equations in Tables 1 and 2 were incorporated into the Zone 5 resource model, allowing short interval prediction of Cu and Ag recoveries. The updated recoveries, based on mineralogy and grade were estimated at 87.5% and 84% copper and silver recoveries respectively. The copper recovery equation exhibited a high correlation against copper to sulfur molar ratio with a coefficient of 0.97 and a standard error of 3.3%. The silver recovery at silver feed grade greater than 10g/t Ag showed a high correlation coefficient of 0.96 despite the high standard error of 5.1% due to the lower assay precision at lower feed grades. There is good agreement between predicted copper and actual recoveries from plant operational data which showed standard error of ±5% as shown in Table 3.

Table 3. Comparison of Actual and Predicted Recovery and Concentrate grades (Situmorang, 2024)

Samples Number	**Cu:S ratio**	**Actual Cu recovery (%)**	**Predicted Cu Recovery (%)**	**Residual (%) (Actual - Predicted)**	**Standard error of estimate (%)**
485	0 to 0.75	86.2	86.9	-0.7	5.1
1359	0.75 to 1.5	88.3	87.4	0.9	4.2
20	>1.5	88	90	-2	4.1

Samples Number	**Cu:S ratio**	**Actual Cu Concentrate Grade (%)**	**Predicted Cu Concentrate Grade (%)**	**Residual (%) (Actual - Predicted)**	**Standard error of estimate (%)**
1407	0 to 1.0	31.1	34.3	-3.1	7
420	>1	34	36.6	-2.7	6.4

The concentrate grade prediction algorithms shown in Table were developed in a similar manner to recovery equations. The copper concentrate grades were predominantly influenced by the copper sulfide mineralogy, non- sulfide gangue as well as the relative concentrations of lead to copper (Pb:Cu) and zinc to copper (Zn:Cu) and rougher concentrate liberation. The latter is influenced by the Cu:S ratio and regrind mill performance. A regrind mill is included in the circuit to improve liberation and the concentrate grade by lowering the silica levels to mitigate the effect of ore hardness variability.

The gangue mineralogy influences liberation as dictated by ore competency through the Bond Ball Work Index (BBWi). The BBWi correlated well with the alteration index 2 (Alti [2]) which is defined by (%Ca/(%Si+%Ca+%Al)). Ores with higher quartz content and low alteration index are associated with higher BBWi and poor sulfide liberation while ores with higher calcite content (higher Alti [2]) are softer and had favourable sulfide liberation. The BBWi correlationship was later improved by the use of elements as dictated by the correlation matrix in Table 4 (Mosanga, *et al.*, 2025).

Table 2: BBWi Correlations with gangue chemistry and alteration indices (Mosanga, *et al.*, 2025)

	Chemistry			**Alteration Index**				**BBWi (kW/t)**
	Al (%)	**Ca (%)**	**Si (%)**	**Alti [1]**	**Alti [2]**	**Alti [3]**	**Alti [4]**	
Al (%)	1.00							
Ca (%)	-0.53	1.00						
Si (%)	0.40	-0.93	1.00					
Alti [1]	-0.82	0.80	-0.68	1.00				
Alti [2]	-0.57	0.99	-0.95	0.83	1.00			
Alti [3]	-0.42	0.96	-0.93	0.65	0.95	1.00		
Alti [4]	-0.50	0.99	-0.96	0.80	1.00	0.95	1.00	
BBWi (kW/t)	0.188	-0.747	0.790	-0.469	-0.742	-0.762	-0.763	1.00

Alteration indices definition: Alti [1] = %Ca/(%Ca+%Al), Alti [2] = %Ca/(%Si+%Ca+%Al), Alti [3] = %Ca/%Si, and Alti [4] = %Ca/(%Ca + %Si).

The BBWi correlations were validated with additional data which showed strong correlationship with the Zone 5 lithology as shown in Figure 3. Production data trends of recovery, Cu:S ratio and Alti (3) showed the influence of both gangue and sulfide mineralogy on concentrate grade and metal recoveries.

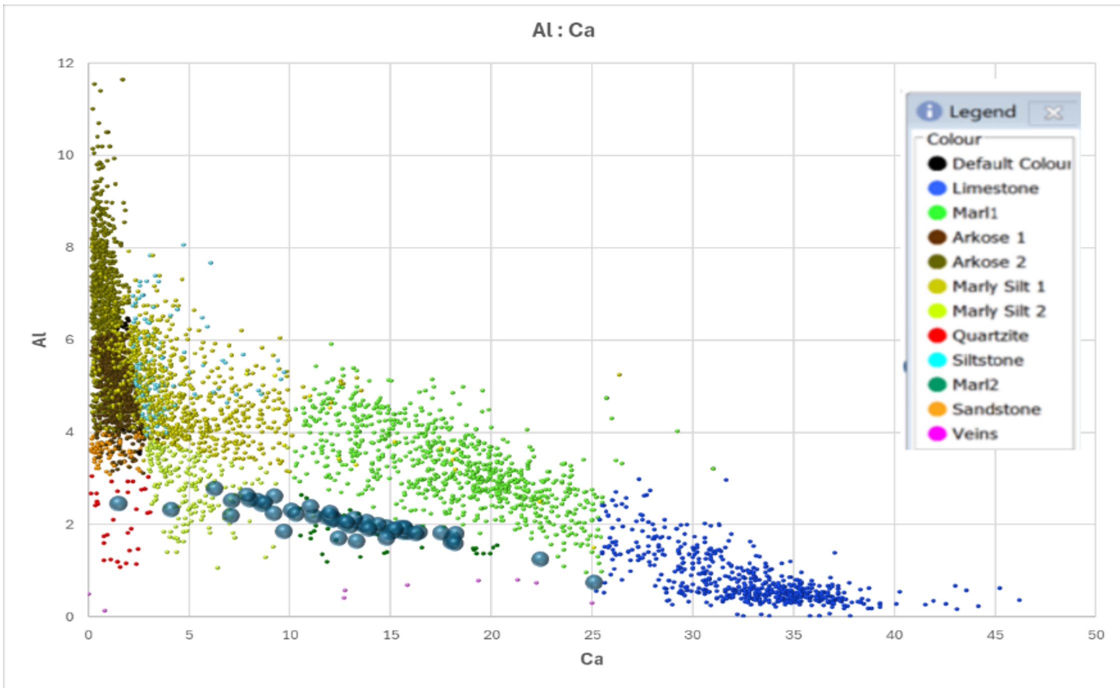

Figure 3: BBWi relation with lithology based on Al and Ca.

There is scope to improve recovery and concentrate prediction accuracy by incorporating multivariate correlationships and accounting for the impact of gangue mineralogy effect of lead and zinc into the algorithms.

REFERENCES

Credit Suisse, 2023. Khoemacau Copper Mine - Project Leopard, s.l.: s.n.

Dlame, M., 2023. Recovery optimisation and detailed concentrate for Khoemacau's Zone 5 quartely feed material for the first three years of life of mine, s.l.: s.n.

Fluor, 2020. Optimisation of the recovery and grade prediction of Zone 5 based on mineralogical, s.l.: s.n.

Mangwiro, J., 2018. Metallurgical optimisation test programme for Zone 5 effect of mineralogy on recovery. Report No. K1OE-6000-25-RP-016., s.l.: s.n.

Mangwiro, J., 2020. Optimisation of the recovery and grade prediction of Zone 5 based on mineralogical domains, Copper & Silver Feed Grades And Alteration Index By Regression Analysis. Report No. K1OE-6000-25-RP-037., s.l.: s.n.

Mangwiro, J., 2020. Recovery and grade prediction update of Zone 5 based on mineralogical domains, Copper& Silver Feed Grades And Alteration Index By Regression Analysis. Report No. K1OE-6000-25-RP-035., s.l.: s.n.

Mosanga, G., Mangwiro, J., Kgotlele, K. & Situmorang, R., 2025. Technical Note for the Record – Ore hardness consideration - BBWi prediction model., s.l.: s.n.

Situmorang, R. M. G. M. J. K. K., 2024. Recovery model review, s.l.: s.n.

John Mangwiro

Principal Engineer
Flour

John has over 30 years of experience in the mining industry with major and junior mining houses which include Anglo American; Rio Tinto, Blue Ridge, MMG and Umbono Capital. John has assumed executive and leadership roles in his career in the operation of plants; in conducting prefeasibility and feasibility studies; in the commissioning and startup of green and brown field operations in Africa. John worked at Palabora Copper (PC) for over 7 years with the first 4 years in the smelter for the upgrade study and the last 3 years in the concentrator where he led the underground transition study from 100,000 tpd to 60,000 tpd.

John has been involved in the design and optimisation of PGM concentrators on the Bushveld and Great Dyke complexes. He ws involved in the design and operation of the Blue Ridge concentrator and the Feasibililty of the Sheba Ridge where HPGR technology was evaluated. John has been involved in the recovery optimisation of Great Dyke PGM ores using high intensity shear conditioning (HIC). Johh worked as an owner metallurgist on the Lesego Platinum and Khoemacau project.

John has extensive base metal concentrator experience. John was the Lead process engineer on the Khoemacau Copper and Silver Project where he evaluated fine grinding, filtration, online analysers and fine floatation technology. He was responsible for the metallurgical testwork, plant design, commissioning, rampup and optimisation. He was involved is colloboration with MMG in the development of the geometallurgical model using multiple linear regression analysis, its validation and fine-tuning tuning during the operation.

John has extensive knowledge of coarse and fine particle floatation technologies which involve the hydrofloat and Jameson circuits for base and PGM concentrators. John is currently the lead processing engineer for the backfill project at Khoemacau. John is providing technical support for geometallurgy during the ramp up. John was the lead process engineer for the Khoemacau expansion project. He is geometallurgical consultant for the expansion deposit the MMG.

John worked on the feasibility of the copper, lead and zinc ore project South Africa where he was involved in the floatation testwork, plant design, evaluation of the DMS and provided input for CAPEX and OPEX during fund raising.

John commissioned Kolomela process plant and the automated laboratory successfully with characterisation of products. He has extensive experience in metallurgical processing of copper and associated by products (PGM); gold; Iron; PGM; Chrome; Manganese; Coal; Phosphate; Lead & Zinc; Magnetite; Uranium, Zirconia; Nickel. John participated in the development and assessment of tehcnology for fine chrome recovery and its economic assessment.

Linking mineralogy to comminution behaviour in the Kalahari manganese field

M. Tadie, B.P. von der Heyden, P. Mathebula, L. van Eeden

Stellenbosch University, South Africa

INTRODUCTION

The geometallurgical characterisation of manganese ores in the Kalahari Manganese Field (KMF) has progressed from traditional chemical classifications to more informative mineralogical frameworks. Chetty (2008) demonstrated the value of quantitative X-ray diffraction (XRD) in identifying both manganese-bearing and gangue minerals, offering a more predictive basis for processing. More recently, von der Heyden et al. (2024) highlighted the importance of ore texture, showing that combining mineralogical and textural data with machine learning can improve the prediction of comminution behaviour.

As the exploitation of lower-grade, texturally variable manganese ores becomes more critical, understanding how mineralogical and structural variability affects processing response is essential. While high-grade ores typically undergo minimal beneficiation, complex ores demand deeper insight into their breakage characteristics. This study investigates whether mineralogical composition can be used not only to classify ore types but also to predict their comminution performance, thereby advancing geometallurgical modelling capabilities for manganese ore deposits.

Methodology

This study investigated the relationship between mineralogy and comminution behaviour across four manganese ore types from the northern Kalahari Manganese Field namely: **Gloria high grade ore (GL-HG)** – a medium-grade carbonate-rich ore; **HG (High Grade ore)** – a high-manganese ore , **Mn-2 (Nchwaning ore)** – a lesser-mined ore associated with the upper Seam 2 mining horizon and **Gloria low grade (GL-LG)** – a low grade Mn lutite ore that is carbonate rich. Representative bulk samples for each ore type were subjected to mineralogical characterisation using quantitative X-ray diffraction (QXRD) to determine modal mineralogy. Comminution behaviour was assessed using three indices: uniaxial compressive strength (UCS), crushability index (CI), and Bond ball mill work index (BWI). The Bond ball mill work index (BWI) was estimated using a proxy method based on comparative grinding energy, calibrated against a reference ore with known BWI under controlled conditions. These tests served as proxies for breakage resistance under compressive and grinding conditions. Furthermore, within each ore type, internal variability was utilised to determine whether fundamental correlations exist between specific mineral phases and breakage parameters. This was accomplished using statistical techniques, including the application of machine learning algorithms, to model and interpret the relationships between modal mineralogy and the measured comminution indices.

RESULTS AND DISCUSSION

X-ray diffraction analysis revealed distinct differences in modal mineralogy across the four manganese ore types investigated (Figure 1). The GL-LG ore showed elevated levels of kutnohorite and rhodochrosite, indicative of a carbonate-rich mineralogy. HG ore, in contrast, was dominated by manganese minerals such as braunite and hausmannite.

These mineralogical distinctions are consistent with the geological origin of the ores. The GL ore types are more closely related to the Mamatwan-type ores, which are fine-grained and gangue-rich (Steenkamp et al., 2020), while the HG and Mn-2 ores represent Wessels-type material, often coarse-grained and manganese-rich (Gutzmer and Beukes, 1996; Steenkamp et al., 2020).

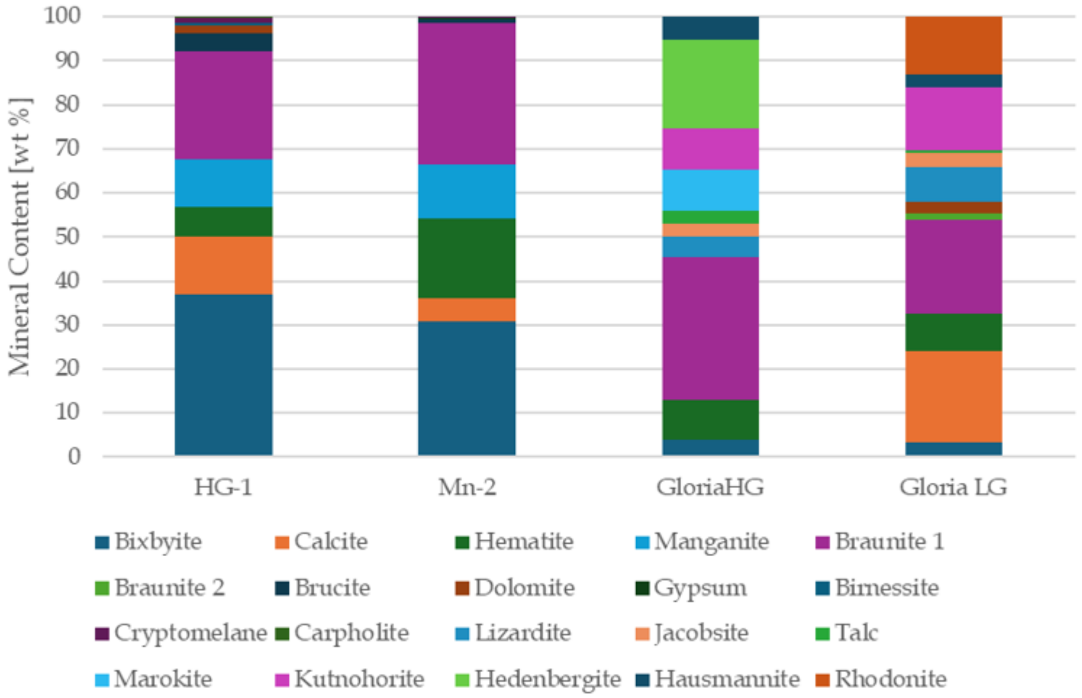

Figure 1. Modal mineralogy (wt.%) by ore type as determined by quantitative XRD (left) and Mn- and Gangue mineral content (right)

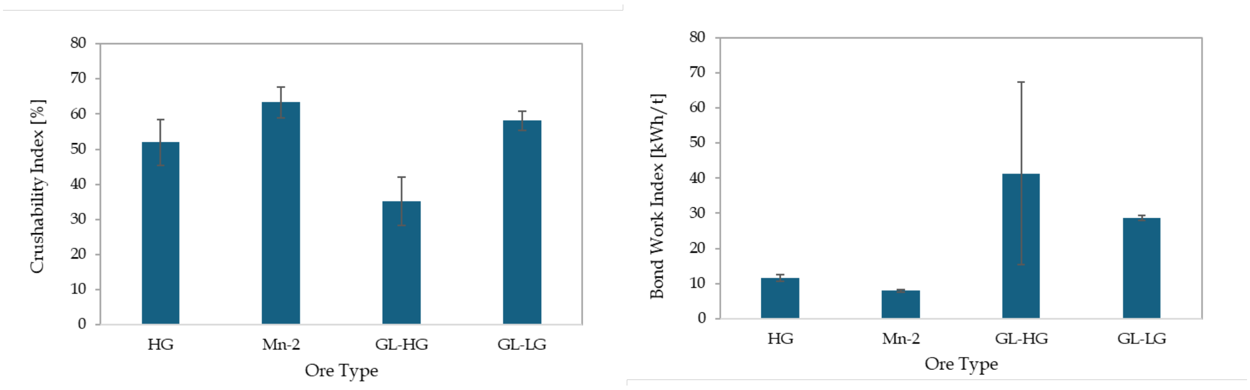

Figure 2. Crushability index (left) and Bond Work Index (right) for different ore types.

Comminution indices, including Crushability Index and BWI, varied across the ore types (Figure 2). The GL ore types consistently exhibited the highest resistance to breakage as per bond work index whilst the opposite what true for crushability. These trends appear, at first glance, to contradict expectations based solely on bulk mineralogy. For example, although HG and Mn-2 ores contain higher proportions of traditionally hard minerals like hausmannite and braunite, they were easier to grind than the gangue-rich GL ores.

The contradiction points to the potential influence of texture as a potentially dominant control on comminution behaviour. Fine-grained textures, characteristic of the Mamatwan-type GL ores, are known to increase hardness due to closely spaced grain boundaries that resist deformation and fracture (Moutinho et al., 2025). In contrast, the coarser crystalline textures of Wessels-type ores in HG and Mn-2 (Kleynstuber, 1984) may facilitate crack propagation and more efficient energy transfer during comminution (Moutinho et al., 2025). Nevertheless, to further explore the role of mineralogy, machine learning techniques were used to identify and rank mineralogical variables (mineral content) in an attempt to correlate the role specific minerals found in the different ores played on Bond Work Index. Figure 3, shows some scatter plots that indicate trends for BWI vs mineral content for specific minerals in the ores tested.

Samples with higher contents of manganite, hematite, and braunite 1 showed lower BWI values, suggesting that increase in these minerals due to their hardness or brittleness may enhance breakage. Conversely increasing content of minerals such as bixbyite, kutnohorite, calcite, and dolomite which are softer mineral was generally associated with increased grinding resistance. Again the contraindications point towards an alternate mechanism such as texture providing a notable control on breakage as has been indicated in the literature (Moutinho et al., 2025).

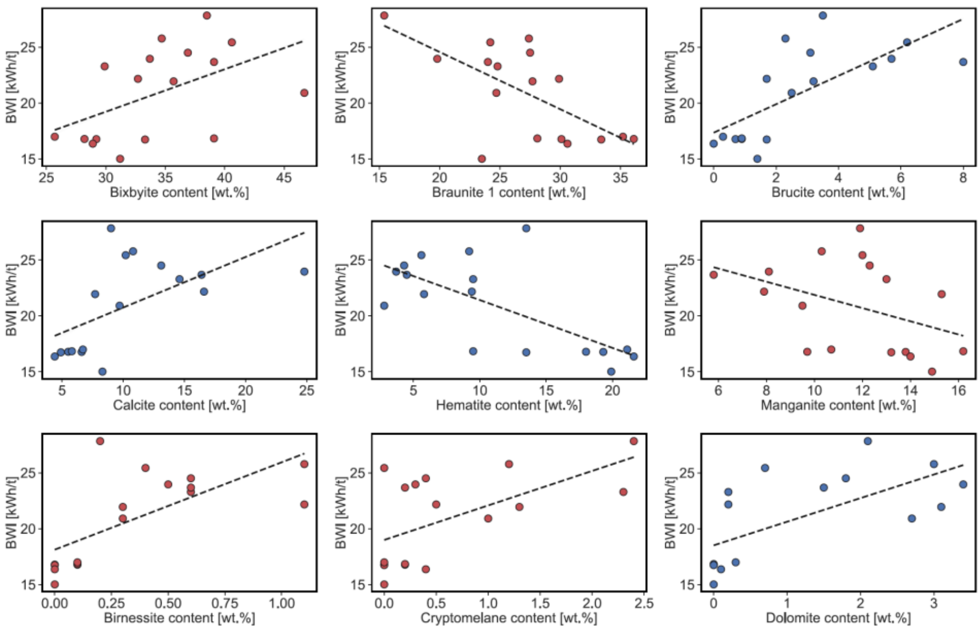

Figure 3. Bond work index vs mineral content for minerals indicating possible trends and effects of mineralogy

CONCLUSIONS

This work determined that comminution response in the Kalahari Manganese Field is possibly governed by a combination of bulk texture and mineralogical composition based on the mineralogical correlations not entirely describing the breakage characteristics. While fine-grained, gangue-rich Mamatwan-type ores are more resistant to breakage overall, machine learning analyses revealed consistent albeit moderate correlations between specific mineral phases and grindability. These findings support the feasibility of mineralogy-based predictive modelling, provided it is contextualised within a broader understanding of textural variability.

REFERENCES

Chetty D, (2008). A geometallurgical evaluation of the ores of the northern Kalahari Manganese Deposit, South Africa, PhD Thesis, University of Johannesburg

Gutzmer, J. & Beukes, N., 1996. Mineral paragenesis of the Kalahari manganese field, South Africa. Ore *Geology Reviews*, Volume 11, pp. 405-428.

Kleynstuber A.S.L. (1984). The Mineralogy of the manganese-bearing Hotazel Formation, of the Proterozoic Transvaal sequence in Griqualand west, South Africa, Trans. geol. Soc. S. Afr., 87 (1984), 257-272

Moutinho, V.F., Neumann, R. and Tavares, L.M., 2025. Influence of mineralogy and texture on the fragmentation behavior of iron ores. Proc Comminution'25, 1, pp.114-130.

Steenkamp, J. D. et al., 2020. From Ore Body to High Temperature Processing of Complex Ores; Manganese- A South African Perspective. *The Minerals, Metals & Materials Society*, 72(10), pp. 3422-3434.

von der Heyden, B.P., Tadie, M., Mathebula, P. and van Eeden, L., 2024. The role of mineralogy and texture in predicting comminution behaviour of manganese ores using machine learning. *Process Mineralogy* 2024, Minerals Engineering International, Extended Abstract.

Margreth Tadie

Co-Chair ARM Geometallurgical Research Chair
Stellenbosch University

Dr Margreth Tadie is the co-chair of the African Rainbow Minerals Research Chair in Geometallurgy at Stellenbosch University. A chemical engineer by training, she earned her PhD from the University of Cape Town with a specialization in froth flotation and has since built a research portfolio that integrates process mineralogy, process modelling, and the valorisation of tailings.

Her work bridges academic research and industrial application, with a focus on developing geometallurgical frameworks that enhance resource efficiency and support circular mining. Dr Tadie has collaborated with the PGM, gold, Iron and Manganese industries on flowsheet development and waste reprocessing and regularly consults on extractive metallurgy and geometallurgy projects.

She is a former Royal Society Future Leaders – African Independent Research (FLAIR) Fellow and a fellow of South Africa's Future Professors Programme. With over 38 peer-reviewed publications and leadership in interdisciplinary geometallurgical research, she is actively involved in shaping geometallurgy as a critical discipline for sustainable mining in Africa and beyond.

Understanding the economic importance and scientific significance of oceanic Fe-Mn crusts

A. Menzies[1], P. Josso[2]

[1]Bruker Nano Analytics GmbH, Germany
[2]British Geological Survey, U.K

INTRODUCTION

Fe-Mn crusts, or ferromanganese crusts, are marine sedimentary mineral deposits primarily composed of iron and manganese oxides. These crusts are of both scientific and economic interest due to their unique chemical composition, which includes valuable metals like cobalt, nickel, copper, titanium, platinum, tellurium and rare earth elements. They form as thin layers on rock surfaces in the deep ocean ranging from 500 to 7000 metres, particularly on seamounts, ridges, and plateaus, over millions of years through the direct precipitation of oxides from seawater and possible subsequent phosphatisation episodes.

Firstly, Fe-Mn crusts are valuable for scientific research, as they act as an historical record of past ocean conditions. Their slow growth rate and ability to accumulate elements over long periods make them ideal for studying changes in the marine environment and the Earth's climate.

Secondly, Fe-Mn crusts are of growing interest as a potential source of valuable metals, particularly nickel and cobalt, which are essential for emerging technologies. The high concentrations of various metals in Fe-Mn crusts, compared to land-based deposits, make them attractive for potential future mining operations. It should be noted that such potential, as described here, does not discuss the political nor environmental considerations, as this is a separate topic; albeit important and relevant.

Micro-XRF is the ideal analytical tool for characterising and understanding the formation and economic potential of Fe-Mn crusts as it requires minimal sample preparation, has a small spot size, and the technique is sensitive to base metal elements, even at trace concentrations. Hand specimens and thin sections of various sizes were analysed using the Bruker micro-XRF Tornado (enclosed source) and Jetstream (open source) systems. Samples from the following locations have been analysed: New England Seamount Chain, Hatton Bank, Walvis Ridge and the Sierra Leone Rise.

A cursory glance at the Figures 1 and 2 clearly highlight the range of elements present in these Fe-Mn crusts, especially the base metals. In particular, a large Fe-Mn Nodule is shown in Figure 1, which highlights the presence of these elements and the growth structures and banding therein. This specimen is approximately 15 cm in its longest dimension. Figure 2 shows a comparison between various Fe-Mn crusts from around the world; again, highlighting their variability and textures.

In summary, micro-XRF can provide detailed information at various scales very quickly, thus enabling an evaluation of ore characterisation during the early stages of exploration. In addition, such an ore characterisation will provide relevant information for understanding the geometallurgical requirements and implications for process planning, which ultimately has a significant impact on the feasibility of extracting any of these critical minerals.

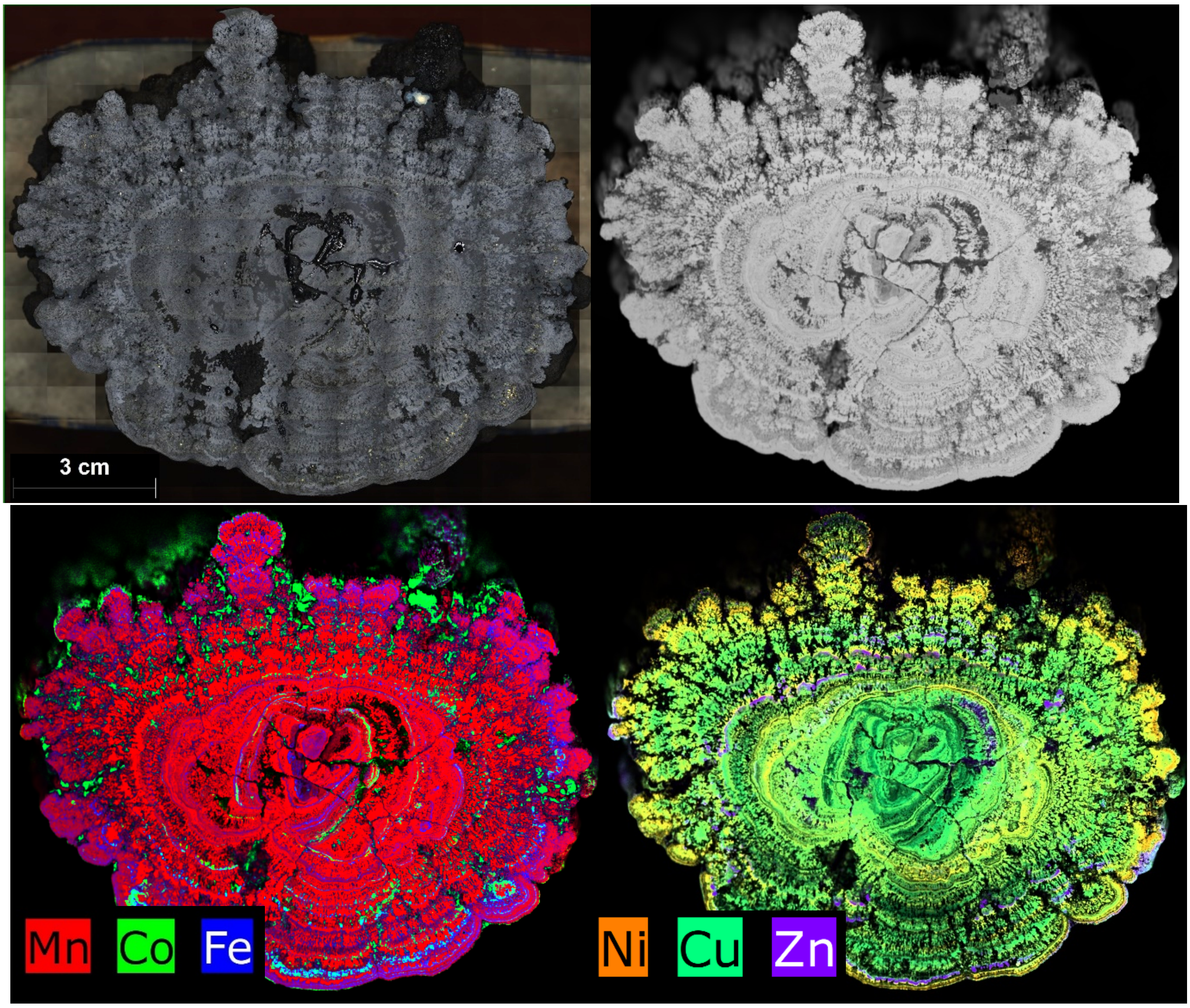

Figure 1. Large Fe-Mn Nodule analysed using the Bruker micro-XRF Tornado system. Clockwise from top left: Optical image; total X-ray intensity image; Ni, Cu and Zn overlaid elemental intensity image; Mn, Co, and Fe overlaid elemental intensity image.

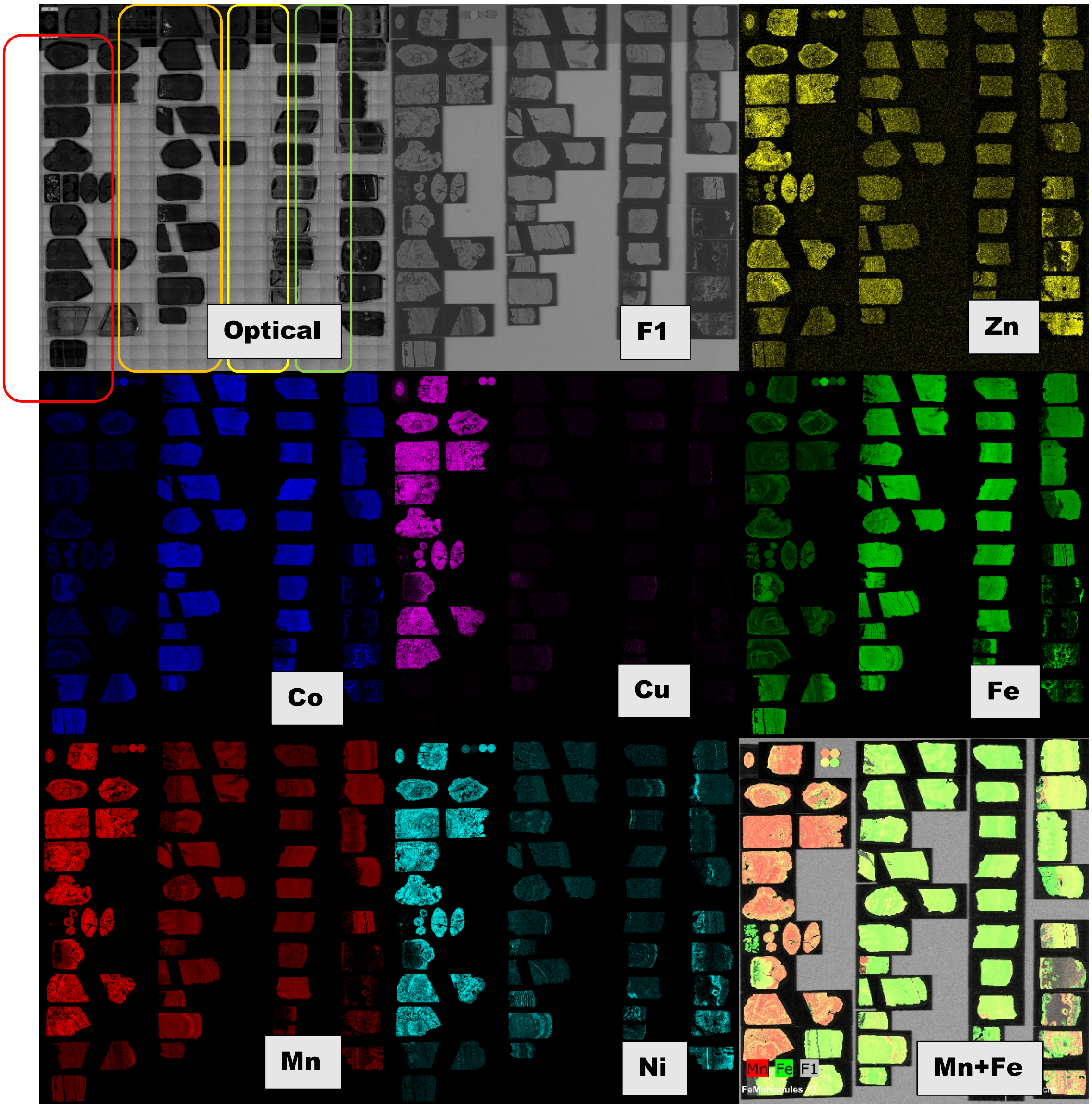

Figure 2. Thin sections analysed using the Bruker micro-XRF Jetstream system. Each column of thin sections is from an individual location. The four circular discs at the top of each image are in-house standards. Top Row: Optical image; total X-ray intensity image; Zn elemental intensity image; Middle Row: Co, Cu, and Fe elemental intensity images; Bottom Row: Mn, Ni, and Fe elemental intensity images.

Andrew Menzies

Senior Applications Scientist
Bruker Nano Analytics

Andrew Menzies holds a Doctorate of Geochemistry from University of Cape Town (South Africa) and a Bachelors of Science and Bachelors of Commerce from University of Auckland (New Zealand). He has over 25 years professional experience working as a geologist involved in numerous projects around the world ranging from grassroots exploration, follow-up reconnaissance exploration, target evaluation, laboratory analysis, and consulting and project management. During this time he has used various analytical techniques and managed analytical laboratories. He was an academic (geochemistry) at Universidad Católica del Norte, (Antofagasta, Chile) from 2011 to 2018 teaching Geochemistry, and supervised numerous doctorate and masters students, and is an active member in numerous geological societies. He is currently employed as a senior application scientist at Bruker Nano Analytics. Research interests include ore deposit mineralogy and mineral processing; mantle geochemistry and the origin of diamonds; automated mineralogical analysis and applications, especially using micro-XRF and AMICS, and analytical standards preparation and evaluation.

Textural implications on iron ore beneficiation outcomes based on jigging – A case study

K. Netshikulwe[1], E.R. Manjengwa[2], B.P. von der Heyden[2], M. Tadie[2]

1African Rainbow Minerals, South Africa
[2]Stellenbosch University, South Africa

BACKGROUND

Iron finds extensive use in the construction, automotive and military industries. It is projected that the current South African iron ore reserves, situated in the Northern Cape, are just under 700 million tonnes (as of June 2023), and at the current mining and processing rates are estimated to have a Life of Mine (LOM) of roughly 13 years. Alternative ore deposits may range from low-grade ores to fine-grained ores featuring complex mineralogy and ore textures (Netshikulwe, 2025). Low grade iron ore deposits with complex textures impose difficulties on the beneficiation process (Mijal *et al.,* 2020), meaning that understanding the mineralogical characteristics is essential to the geometallurgical program. According to literature the Blinkklip breccia has received little attention (Thokoa, 2020). The Breccia consists of a mixture of banded iron formations, and chert and fine-grained hematite (Gutzmer, 1996). Scope exists to exploit lower grade ore deposits to sustain the South African iron ore resource supply. Common iron ore beneficiation methods include gravity and magnetic separation methods that exploit the density and magnetic properties of the ore, respectively, to effect separation. Gravity separation methods include jigging, spiral concentrators, dense medium separation and shaking tables. Jigging can be used to beneficiate coarse iron ore particles (Umadevi *et al*., 2014; Will and Finch, 2016). The outcomes of jigging campaigns are influenced by the interaction of different factors that consider the mechanical, ore bed, bulk fluid and operational conditions. In a case study examining the beneficiation potential of low-grade iron ore deposits, gravity-based methods were examined. In this paper the influence of textural variations on the outcomes when using jigging as a beneficiation method was considered.

Objectives

- Examine the extent to which gravity-based separation methods could be used to beneficiate the Blinkklip breccia.
- Understand the implications of textural variations on concentrate grade.
- Assess whether the coarse particle jigging alone is sufficient to beneficiate the low grade Blinkklip breccia iron ore deposit.

Experimental Procedure

The approach that was applied to address the study objectives is presented in Figure 1.

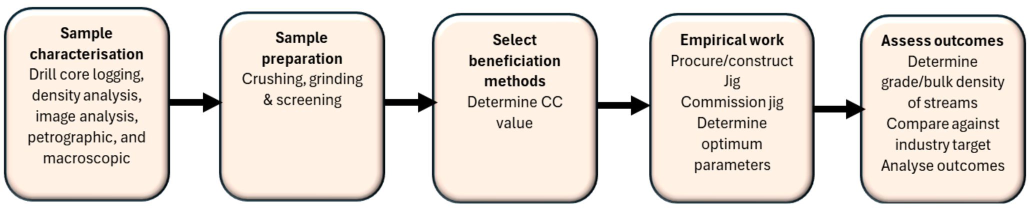

Figure 1: Framework used for the study.

Iron-ore samples used for the study were collected from Makganyene farm and subjected to detailed mineralogical characterisation. The characterisation work enabled the definition of four texture classes based on the mineralogical composition, namely, BK1 - clast supported hematite-rich type, BK2 - clast supported silica-rich type, BK3 - clast-supported hematite-silica mixture type, BK4 - matrix-supported hematite-silica mixture type.

A hydraulic jig concentrator was built, commissioned and used to examine the potential of beneficiating low grade iron deposits of the Northern Cape. Outcomes from the commissioning campaigns enabled the primary researcher to understand the operating capability of the equipment. For the study, two operating parameters were varied, namely stroke depth and speed. Optimisation tests were undertaken to select the best operating conditions for the jigging tests. The optimisation tests were conducted under four distinct operating conditions. Run A was conducted at a jigging speed of 320 rpm with a stroke depth of 3.2 cm. Run B was conducted at 280 rpm, maintaining the stroke depth of 3.2 cm. In Run C, the speed was set to 300 rpm with a reduced stroke depth of 2.7 cm, while Run D maintained a speed of 300 rpm with a stroke depth of 3.0 cm. Results from the optimisation tests revealed that a stroke depth of 2.8 cm and jig speed of 320 rpm was found to yield the best outcomes. Further tests were conducted on all four textures in triplicate. Additionally, two composite samples that aimed to simulate the actual ore body were used for the jigging tests. Batch tests were undertaken for a run time of four minutes. The concentrate and tailings streams were collected and dried overnight at 60°C. The product streams were screened, and bulk density measurements using the Archimedes principle were done for each particle size class.

RESULTS

Optimum runs

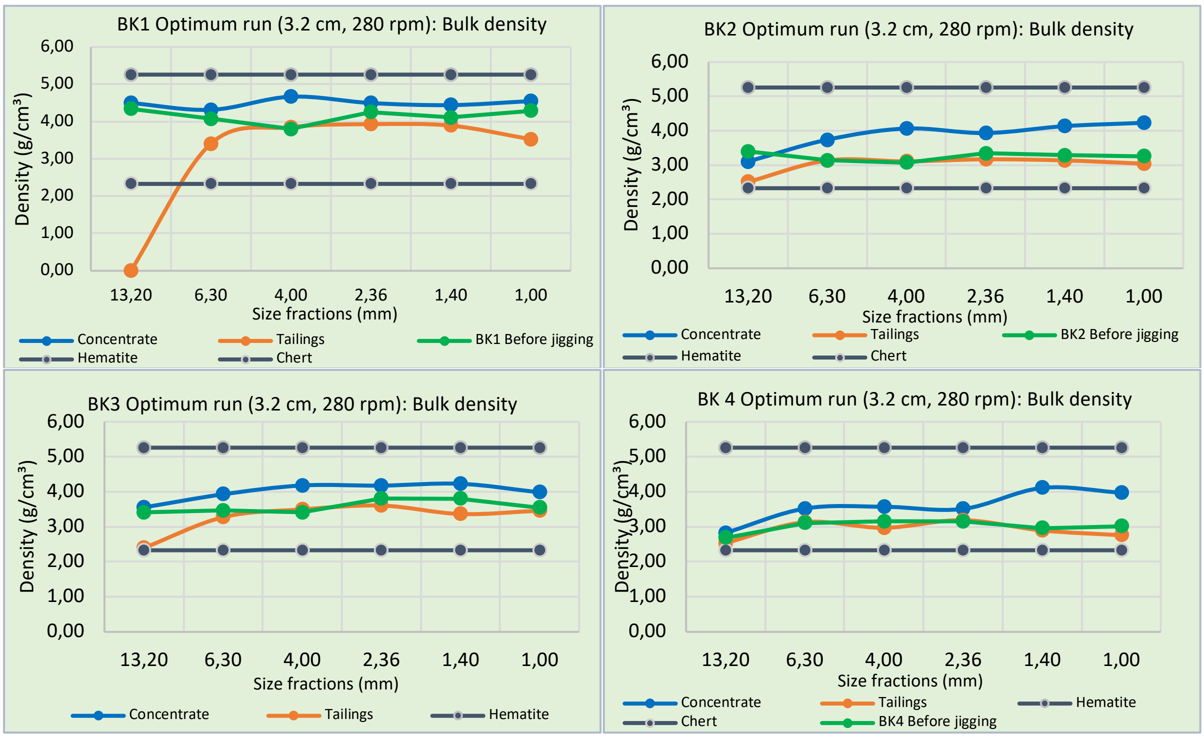

Figure 2: Jigging tests results for all four texture classes after running at the optimum conditions (stroke depth 3.2 cm and speed 280 rpm).

Jigging tests conducted at optimum operating settings (stroke depth = 3.2 cm, speed = 280 rpm) showed distinct performance differences across the four Blinkklip breccia ore textures. The clast-supported hematite-rich breccia (BK1) achieved the highest concentrate mass recovery of 71.6%, with concentrate bulk densities ranging from 4.32–4.67 g/cm^3 (Figure 4). The clast-supported hematite–silica mixed breccia (BK3) yielded an intermediate recovery of 40.9%, while the chert-rich breccia (BK2) produced a lower recovery of 28.8%. The matrix-supported hematite–silica breccia (BK4) recorded the poorest performance with a recovery of 19.7%, reflecting limited liberation of hematite at coarse size fractions. Across all textures, coarse (+6.3 mm) material was generally concentrated, while finer fractions were more prevalent in the tailings (Figure 2). The concentrate grade results also indicate a strong influence of texture on beneficiation performance. BK1 produced the highest grades in both size fractions (63.34% fines; 61.13% lumpy), reflecting its favourable response to jigging. BK2 (51.39% fines; 38.46% lumpy) and BK4 (42.71% fines; 35.64% lumpy) achieved higher grades in the finer fractions, suggesting improved liberation at smaller sizes. BK3, however, performed better in the lumpy fraction (45.79% vs 31.14% fines) indicating that hematite is more concentrated in lumpy fractions, while the fines are mostly gangue rich. These findings show that beneficiation efficiency is dependent on texture.

CONCLUSIONS

The extent to which gravity-based separation methods could be used to beneficiate the low-grade Blinkklip breccia deposit was examined. The results of empirical studies showed that jigging could be used to beneficiate the low-grade iron ore deposit from Makganyene farm. The study further examined the implications of textural variations on concentrate grade. The outcomes of the study revealed that textural variations do affect jigging outcomes. Mineral textures affect rock breakage patterns; therefore, textures inherently have an influence on the morphology of the particles formed, degree of liberation and the extent of segregation during jigging. However, other factors do come into play such as the operating conditions. Finally, the paper assessed whether coarse particle jigging alone is sufficient to beneficiate the low grade Blinkklip breccia iron ore deposit. The results revealed that recovery of particle size fractions >6.3 mm with an iron bulk density >4.0g/cm^3 (corresponds to an Fe Grade of roughly 39.88%) was not possible for textures BK2, BK3 and BK4 having low iron grades. The iron grade in the concentrate stream increased with decreasing particle sizes, suggesting that a single jigging cycle would be inadequate and further size reduction and beneficiation using other gravity methods would be required.

REFERENCES

Gutzmer J. (1996). Genesis and Alteration of the Kalahari and Postmasburg Manganese deposits, Griqualand West, South Africa. Thesis. University of Johannesburg.

Mijał, W., Baic, I. & Blaschke, W. (2020). Modern Methods of Dry Mineral Separation-Polish Experience. In Proceedings of the International Conference on Innovations for Sustainable and Responsible Mining: ISRM 2020-Volume 1 (pp. 407-425). Cham: Springer International Publishing.

Netshikulwe, K. (2025). The Mineralogy and Ore beneficiation characteristics of the Blinkklip Breccia mineralized zone, MSc Thesis, Stellenbosch University, Stellenbosch, South Africa

Thokoa, M. (2020). A comparative mineralogical and geochemical study of manganese deposits in the Postmasburg Manganese Field, South Africa.Gutzner, 1996

Umadevi., T., Abhishek, K., Singh, A. P., & Sah, R. (2014). Development of a process flowsheet for the beneficiation of low-grade iron ore fines from the Bellary-Hospet region of Karnataka, India. Mining, Metallurgy & Exploration, 31, 162-168.

Wills, B. A., & Finch, J. (2016). Wills' mineral processing technology: an introduction to the practical aspects of ore treatment and mineral recovery. Butterworth-heinemann.

Khuliso Netshikulwe

Geology graduate: Drilling Assistant
African rainbow Minerals

I am a dedicated Earth Sciences professional with a Master of Science in Earth Sciences (Cum Laude) from Stellenbosch University, completed under the African Rainbow Minerals Geometallurgy Research Chair. My research focused on the mineralogy and beneficiation characteristics of the Blinkklip Breccia mineralized zone, exploring its implications for the economic extraction of iron ore resources. I hold a Bachelor of Science in Mining and Environmental Geology from the University of Venda, where I was recognized as the Most Promising Geologist. I have developed strong skills in mineralogical analysis, including mineral characterization, and geometallurgical test work. I have skills in 3D geological modelling using Leapfrog Geo, data visualization, and multivariate geochemical analysis. I am currently working within the Exploration and New Business department at African Rainbow Minerals. I am passionate about uncovering the stories told by rocks and minerals, and I strive to apply scientific precision and creative problem-solving to support innovative and sustainable practices in the minerals and Geometallurgy sectors.

Geometallurgy learnings from First Quantum Minerals' Zambian operations

L. Little, A. Kottgen, M. Chibesa, P. Ogilvie

First Quantum Minerals Ltd., Zambia

INTRODUCTION

Within the North-Western Province of Zambia, First Quantum Minerals has two copper mines (Kansanshi and Sentinel) and a nickel mine (Enterprise). Although there are some similarities between these deposits, they each have different geometallurgical challenges. Kansanshi, operational since 2005, has well-established approaches to dealing with highly localised variability in copper grade and copper oxidation extent, with recovery optimised via a combination of flotation and leach processing plants. However, the 'well-established' understanding does have gaps to be filled. Sentinel, upon start-up in 2016, had unexpected, severe challenges with graphitic carbon that was brought under control with depressants. Both Kansanshi and Sentinel went through periods of throughput being impacted by hard ore in 2022 - 2023. Learning from these experiences, 'Geomet' for both Enterprise and the Kansanshi S3 project started before mining did.

At Enterprise, key ore types with various processing responses were modelled based on element-to-mineral conversion from the multi-element dataset. For Enterprise, the quantification of talc for determining the pre-flotation circuit configuration was a challenge, with a wide range of magnesium silicates present in the ore and quantities of talc ranging between 5% and 60% for different ore types. Similarly, nickel deportment to sulfides vs. silicates was a key variable impacting recovery that was a challenge to quantify. Operationally, with a relatively small team, daily production meetings were structured to align mining and processing targets, not just with each other, but to meet specific concentrate sales requirements.

For S3, an on-site Geomet program has comprised a small interdisciplinary team with one dedicated co-ordinator encouraging collaboration between specialists within different departments. Key objectives have included mine-to-mill fragmentation optimisation for different lithologies, and characterisation of ore hardness. For the latter, 1600 m of diamond drilling was performed, of which 870 m was subsampled in 3 m intervals for analysis. A combination of HiT, Geopyora and SMC was used for hardness characterisation, along with automated mineralogy using the TIMA and multi-element assays to assess potential hardness proxies. Among other learnings, this work has clarified that one key lithology is mostly very hard, which has been incorporated in a throughput model for long-term planning.

To date, despite various challenges and limitations, 'Geomet' at First Quantum is delivering value, and we look forward to continuously improving both the quality of our interdisciplinary working relationships, and the detail and level of confidence afforded by our models. Key site learnings will be carried forward to other First Quantum Greenfields projects.

Dr Lucy Jane Little

Superintendent, Process Mineralogy and Geometallurgy
First Quantum Minerals Ltd.

Lucy has worked at Kansanshi since 2017, gradually making minor steps towards geometallurgy while focusing on process mineralogy and various minerals processing projects. In the last two years, she has worked on more ambitious geometallurgical projects, attempting to characterise and effectively predict and communicate the likely impacts of key ore variables on production over the medium to long term.

Axel Kottgen
Assistant General Manager
First Quantum Minerals Ltd.

Axel moved to Kansanshi as the Assistant General Manager in 2024 after his success as project manager for the Enterprise Nickel Project over the preceding few years. Axel is passionate about geometallurgy and promotes and supports interdisciplinary collaboration in both technical and operational spaces. He values the information and understanding provided by geometallurgical work for strategic decision making.